Multidimensional fractionation of complex polymers by comprehensive online-coupled thermal field-flow fractionation and size exclusion chromatography.

by

Zanelle Viktor

This thesis is presented in partial fulfilment
of the requirements for the degree of

Doctor of Philosophy (Polymer Science)

at the
University of Stellenbosch

Supervisor: Prof Harald Pasch

Faculty of Science

Department of Chemistry and Polymer Science

December 2020

Declaration

By submitting this dissertation electronically, I declare that the entirety of the work contained therein is my own, original work, that I am the sole author thereof (save to the extent explicitly stated otherwise), that reproduction and publication thereof by Stellenbosch University will not infringe any third party rights and that I have not previously in its entirety or in part submitted it for obtaining any qualification.

Zanelle Viktor

December 2020

Declaration for Publication

For the manuscript included within this dissertation, the nature and the scope of the contribution made by the candidate was as follows:

Nature of Contributions	Extent of Contribution (%)
Experimental work, data analysis, manuscript preparation, addressing of reviewers' comments	90

The contribution of the co-author of the manuscript presented in the dissertation was as follows:

Name	Email address	Nature of Contribution	Extent of Contribution (%)
Harald Pasch	hpasch@sun.ac.za	Supervision and mentoring, Revision and correcting of manuscript for publication	10

Declaration by co-author

1. The declaration above accurately reflects the nature and extent of the contributions of the candidate and the co-author to the manuscripts in the dissertation.
2. In addition to the co-author specified above, no other authors contributed to the manuscripts in the dissertation.
3. Potential conflicts of interest have been disclosed to all parties and all parties consented to the inclusion of the results presented in the manuscripts into the dissertation.

December 2020

Abstract

The comprehensive characterization of complex polymeric materials remains a primary objective in research and industry. It is important to understand the molecular heterogeneity of complex polymeric materials and to establish correlations between the structure and the physical properties of a given polymeric material as it influences the end-use application thereof. Polymeric materials are distributed with regard to multiple molecular properties e.g. molecular mass, chemical composition and molecular topology (such as branching, microstructure and functionality). Due to the molecular complexity of polymeric materials, characterization and separation of the polymer with regard to its various distributions remains a major challenge for the analytical scientist. As a result, new analytical approaches have been developed over the years as well as advancing the capabilities of existing analytical techniques. In recent years, field-flow fractionation (FFF), a channel-based separation technique, has emerged as a suitable analytical method for the fractionation and characterization of complex polymers. FFF has been shown to be selective towards different molecular properties and is capable of providing comprehensive molecular distribution information. Thermal field-flow fractionation (ThFFF) and asymmetric flow field-flow fractionation (AsFlFFF) are two of the main sub-techniques of FFF used for polymer characterization. FFF is a well suited analytical technique to be used in either a multidetector hyphenation configuration or in a multidimensional configuration to address the characterization of the multiple molecular distributions present in a complex polymeric material. In the first part of the present research, a comprehensive online multidimensional analytical approach has been developed for the characterization of complex polymers. ThFFF, an analytical technique that has been shown to be sensitive towards chemical composition and topology, has been coupled to size exclusion chromatography (SEC), which separates based on the hydrodynamic size of the analyte molecules. To illustrate the capabilities of the developed ThFFF X SEC, poly(styrene)-***b***-poly(methyl methacrylate) block copolymers were separated and characterized. It was shown that in a single analysis, detailed molecular information (chemical composition and molecular mass distribution) as well thermal and translational diffusion information could be obtained. To further demonstrate the capabilities of the multidimensional method it was shown that in instances where separation is less than ideal, valuable information is still obtainable by hyphenation with information-rich detectors to ThFFF X SEC. In addition to the developed ThFFF X SEC technique, a method was developed that successfully separated poly(methyl methacrylate) (PMMA) according to tacticity using AsFlFFF. The solution behaviour of syndiotactic-, atactic- and isotactic PMMA with similar molecular masses was investigated in solvents with different thermodynamic properties. It was shown that by careful

selection of the carrier liquid and channel temperature, microstructure-based separation can be achieved in AsFlFFF.

Uittreksel

Die karakterisering van komplekse polimere bly ‘n primêre doel in die veld van navorsing asook in die nywerheid. Dit is van belang om die molekulêre heterogeniteit van komplekse polimere te verstaan en die korrelasie tussen die struktuur en die fisiese eienskappe van ‘n gegewe polimeermateriaal te bepaal, aangesien dit die eindtoepassing daarvan beïnvloed. Komplekse polimere het verspreidings in veelvuldige molekulêre eienskappe bv. molekulêre massa, chemiese samestelling en molekulêre topologie (soos vertakings, mikrostrutuur en funksionaliteit). As gevolg van die molekulêre kompleksiteit van polimeermateriale, bly die karakterisering en skeiding van die polimeermateriaal ten opsigte van sy verskillende verspreidings ‘n uitdaging. In ‘n poging om dié uitdaging aan te spreek, word óf nuwe analitiese metodes ontwikkel óf die vermoë van bestaande analitiese metodes word verbeter. ‘n Voorbeeld van ‘n nuwe analitiese metode wat in die afgelope jare ontwikkel is, is veldvloei-fraksionering (FFF). FFF is selektief vir die verskillende molekulêre eienskappe en is instaat daarvan om gedetailleerde inligting rakende die molekulêre verspeidings, wat teenwoordig is in polimeermateriale, the voorsien. FFF is ‘n gepaste analitiese tegniek wat die vermoë het om aan veelvoudige detektore gekoppel te kan word of dit kan selfs in ‘n multi-dimensionele konfigurasie gekoppel word met ander analitiese tegnieke om die molekulêre verdelings van polimeermateriale te karakteriseer.

In die eerste deel van die navorsing wat aangebied is, is 'n uitgebreide aanlyn multi-dimensionele analitiese protokol ontwikkel vir die karakterisering van komplekse polimere. Termiese veldvloei-fraktionering (ThFFF), wat sensitief is vir chemiese samestelling en topologie, is gekoppel aan grootte uistluitings chromatografie (SEC), wat die analietmolekules skei op grond van hulle hidrodinamiese grootte. Om die potensiaal van ThFFF X SEC te illustreer, is poli(stireen)-***b***-poli(metiel metakrilaat) blok-kopolimeer geskei en gekarakteriseer. Die resultate het getoon dat in 'n enkele analiese gedetailleerde molekulêre inligting (chemiese samestelling en molekulêre massa verspreiding) sowel as termiese en normale diffusie-inligting verkry kon word. Daarbenewens is aangetoon dat met selektiewe deteksie, waardevolle inligting steeds bekombaar is in die geval van onvoldoende skeiding van ‘n monster, deur inligtingryke detektore te koppel aan ThFFF X SEC. ‘n Voorbeeld van soos detektor is ultraviolet (UV).

In die tweede deel van die navorsing wat aangebied is, is die skeidingsvermoë en selektiwiteit van asimmetriese vloei veldvloei-fraktionering (AsFlFFF) gedemonstreer. Die retensie gedrag van sindiotaktiese, ataktiese en isotaktiese poli(metiel metakrilaat) van soortgelyke molekulêre massas in oplosmiddels met verskillende termodinamiese eienskappe is ondersoek. Daar is aangetoon dat deur die noukeurige seleksie van die dravloeistof en die temperatuur van die kanaal, mikrostruktuur-gebaseerde skeiding in AsFlFFF verkry kan word.

Acknowledgements

I wish to express my sincere gratitude and thanks to the following individuals and institutes for their contribution throughout this research endeavour:

Prof Harald Pasch, my supervisor, who gave me the opportunity to work with him and broaden my scientific knowledge. Thank you for your guidance, knowledge and efforts. I appreciate all the time you invested in me, bestowing upon me your insights and wisdom that I shall carry with me. Thank you for the funding and financial support.

Members and staff of the Polymer Science Division, for all the technical and administration assistance. Thank you for always going above and beyond to help and assist. I especially want to express my utmost gratitude and thanks to **Ms. Erinda Cooper** for her unwavering support.

Pasch Polymer Analytical Group (past and present), fellow students and researchers, for your advice, encouragement and assistance.

Justin, thank you for all your support, motivation, encouragement and love.

Friends and Family, a special thanks to my mother, brother and sister. Thank you for walking alongside me, encouraging me, guiding me and believing in me. Thank you for the sacrifices that you have made in order for me to achieve my dreams, I am eternally grateful.

Table of Contents

List of Figures

List of Tables

List of Abbreviations

2D-LC	Twodimensional liquid chromatography
ACN	Acetonitrile
AsFlFFF	Asymmetric flow field-flow fractionation
a-PMMA	Atactic poly(methyl methacrylate)
BuA	Poly(butyl methacrylate)
CC	Critical condition
$CHCl_3$	Chloroform
DLS	Dynamic light scattering
DMA	Dynamical mechanical analysis
dRI	Differential refractive index
DSC	Differential scanning calorimetry
ELSD	Evaporative light scattering detector
ESI-MS	Electrospray ionization mass spectrometry
FFF	Field-flow fractionation
FlFFF	Flow field-flow fractionation
FTIR	Fourier Transform Infrared spectroscopy
HDC	Hydrodynamic chromatography
HPLC	High performance liquid chromatography
^{1}H NMR	Proton nuclear magnetic resonance
IC	Interaction chromatography
IR	Infrared spectroscopy
i-PMMA	Isotactic poly(methyl methacrylate)
LAC	Liquid adsorption chromatography
LALLS	Low angle laser light scattering
LC	Liquid chromatography
NMR	Nuclear magnetic resonance
MALS	Multiangle light scattering
MALLS	Multiangle laser light scattering
MS	Mass spectrometry
MALDI-TOF MS	Matrix assisted laser desorption/ionization time-of-flight mass spectrometry
PB	Poly(butadiene)
PI	Poly(isoprene)
PMMA	Poly(methyl methacrylate)

PS	Poly(styrene)
PS-b-PMMA	Poly(styrene)-***b***-poly(methyl methacrylate) block copolymer
RI	Refractive index
SEC	Size exclusion chromatography
SEM	Scanning electron microscopy
s-PMMA	Syndiotactic poly(methyl methacrylate)
TEM	Transmission electron microscopy
TGA	Thermogravimetric analysis
ThFFF	Thermal field-flow fractionation
THF	Tetrahydrofuran
UV	Ultraviolet

List of Symbols

A_{acc}	Surface area of the accumulation wall
b_0	Breadth of the channel inlet
b_L	Breadth of the channel outlet
c_0	Concentration at the accumulation wall (x = 0)
$c(x)$	Concentration profile of analyte
Đ	Dispersity
D	Normal (translational) diffusion coefficient
D_h	Hydrodynamic diameter
d_n/d_c	Refractive index increment
D_T	Thermal diffusion coefficient
F	Applied force
f	Frictional force
ΔG	Change in Gibbs free energy
ΔH	Change in enthalpy
H	Plate height
H_d	Axial diffusion factor
H_i	Experimental factor
H_n	Non-equilibrium factor
H_p	High dispersity factor
k	Boltzmann's constant
L	Length of the channel
ℓ	Mean layer thickness
M_n	Number average molecular weight
M_w	Weight average molecular weight
N	Total number of theoretical plate heights
ŋ	Viscosity
S_T	Soret coefficient
ΔS	Change in entropy
R	Retention ratio
R_g	Radius of gyration
R_s	Resolution
τ	Relaxation time
T	Absolute temperature

ΔT	Applied temperature gradient
t_0	Retention time of unretained analyte
Δt_r	Difference in retention time
t_r	Retention time of retained analyte
U	Velocity
V_0	Void volume
V_c	Volumetric cross-flow rate
V_{in}	Volumetric flow rate of the channel inlet
V_{out}	Volumetric flow rate of the channel outlet
(x)	Average velocity of the carrier liquid
w	Channel thickness
x	Distance from the channel wall
y	Channel area excluded by a tapered inlet
z’	Distance from the channel inlet to the focusing point
λ	Retention parameter
$4\sigma_t$	Average standard deviation of two analyte peaks quantified in time
θ	Scattering angle

CHAPTER 1

INTRODUCTION AND OBJECTIVES

1.1. Introduction

Understanding the different distributed properties of polymer materials has been the primary objective of many research studies in academia and in the polymer industry. Polymeric materials are considered to be multiply distributed with respect to molecular mass, chemical composition and topology (e.g. branching, microstructure and functionality). There has been a long-standing interest from polymer scientists which focuses on acquiring essential detailed information on the above mentioned distributions due to their significant influence on the physical and physicochemical properties of the polymer and its subsequent application [1, 2].

New polymeric materials continue to emerge with tailored properties, either for the advancement of science or to improve technological processes. This is either achieved by novel synthesis or by modifying existing polymeric materials to improve properties i.e. physical, mechanical or biocompatibility for new applications. As a result, tailor-made polymeric materials become increasingly complex and heterogeneous. For instance, a 'single' polymeric material can have several molecular distributions that are interdependent and correlative [1-4]. Hence, for comprehensive characterization of complex polymeric materials either the development of new techniques or the advancement of existing analytical techniques is required [1, 2, 4].

To characterize the various molecular distributions present within a complex polymeric material, separation is necessary. Conventional spectroscopic techniques (IR, NMR and MS) will not be adequate. As stand-alone techniques, they can only offer average values of molecular parameters with no distribution information [1, 5]. For this reason, a variety of chromatographic and fractionation techniques have become the standard methods for polymer characterization and for obtaining information on the different molecular distributions. Each of these methods is based on a fundamentally different principle, which predominantly governs the separation mechanism. Accordingly, each individual method might relate to the selective separation according to only one molecular property. In order to address multiple molecular distributions present in a complex polymeric material, two techniques can be coupled to acquire the necessary information. Two approaches are usually considered in multidimensional analytical protocols. Firstly, a selective separation method can be coupled with information-rich spectroscopic techniques to provide information on chemical composition, microstructure or functionality. For example, it can be coupled to concentration-sensitive and molecular mass-sensitive detectors to obtain molecular mass information. The second approach is to couple two analytical separation methods, preferably with a large orthogonality, in a multidimensional configuration. In other words, one method provides a selective separation according to one distributed property while the second method separates

according to a different molecular property. As a result, detailed information about two different molecular property distributions can be obtained simultaneously [1-4, 6, 7]. Column-based chromatography has been the leading method in the analysis of polymers to address the characterization of the molecular heterogeneity of complex polymers and is predominately used in both these approaches. Separation in column-based chromatography, such as liquid adsorption chromatography (LAC) and size exclusion chromatography (SEC), is based on the interaction of the analyte with a given stationary phase and in the case of SEC, driven by the difference in hydrodynamic diameter of the analyte molecules. The various combinations of different modes of column-based techniques hyphenated to information-rich spectroscopic techniques or coupled in a two-dimensional liquid chromatography (2D-LC) set-up have been widely reviewed [1, 3, 8-12].

Field-flow fractionation (FFF), being a complementary analytical fractionation technique to column-based chromatography, has received far less attention for the characterization of synthetic and natural polymers. FFF is an empty-channel separation technique of which thermal field-flow fractionation (ThFFF) and asymmetrical flow field-flow fractionation (AsFlFFF) are considered to be two of the primary sub-techniques for polymer characterization [13, 14]. The physical simplicity alongside its many experimental advantages over traditional column-based chromatography techniques makes FFF an ideal analytical technique and addresses many of the limitations inherent to column-based techniques [13-15]. Column-based techniques have inherent disadvantages which include (1) possible shear degradation, (2) long experimental analysis times with excessive use of solvents, and (3) limited number of detectors that are compatible with the experimental setup e.g. gradient LC, and lastly, (4) limited range of molecular masses that can be separated. FFF is generally performed under isocratic solvent conditions and is capable of separating ultrahigh molecular mass polymers and particles that can range from nanometer to micrometer sizes, with a sufficient resolution and minimal sample loss. Generally, samples do not require filtering before analysis in a FFF channel, which minimizes sample loss and possible sample degradation [13-15]. Therefore, FFF is an ideally suited analytical technique for multidetector hyphenation and/or to be used in a multi-dimensional configuration. The coupling of various fractionation techniques either hyphenated with a spectroscopic technique such as Fourier Transform Infrared Spectroscopy (FTIR) in an online methodology, or in a multidimensional configuration, has been reported in a number of studies [13-20]. By coupling ThFFF comprehensively online with SEC, the two complementary separation methods can potentially be used to separate complex polymers according to chemical composition, while simultaneously determining size and molecular mass distribution.

FFF has been applied to the characterization of a variety of polymeric materials, including polymer blends, copolymers, polymer self-assemblies, aggregates, colloids, liposomes, proteins and nanoparticles [14, 21-26]. Both AsFlFFF and ThFFF can separate analytes according to their diffusion coefficient (D). ThFFF can additionally separate analytes according to chemical composition based on the Soret coefficient, which is determined by the interaction of the thermal diffusion and the normal diffusion. In the case of chemical composition separation, the Soret coefficient (S_T) is predominantly governed by changes in the thermal diffusion coefficient (D_T) of the analyte. At higher molecular masses D_T is independent of molecular mass for polymers with the same chemical structure. In ThFFF, analytes with the same Soret coefficient co-elute regardless of composition and hydrodynamic diameter [17, 27, 28]. Williams *et al.* proved that ThFFF is a powerful separation method for the chemical composition analysis of copolymers [29, 30]. The microstructure-based separation of poly(butadiene), poly(methyl methacrylate) and poly(isoprene) by ThFFF has been presented by Greyling *et al*. demonstrating the sensitivity of ThFFF towards composition [31-33].

AsFlFFF has been used in the investigation of structural parameters and the molecular mass determination of complex polymers [13-15, 34 - 37]. It is considered as a complementary molecular mass characterization technique to SEC, where separation is based on the difference in the hydrodynamic diameter. Different from SEC, the separation in AsFlFFF is based on the difference in diffusion coefficients and correlates to the hydrodynamic diameter, which is influenced by the thermodynamic quality of the solvent and temperature. The diffusion coefficient is a function of molecular parameters such as molecular mass, chemical composition and molecular topology [13-15]. Therefore, AsFlFFF can potentially be capable of microstructure-based separation of polymers with different tacticities and through the use of solvents of different thermodynamic qualities and viscosities at various channel temperatures, improve resolution.

1.2. Aims and objectives

One of the main aims of this research is to develop a comprehensive online multidimensional protocol for the coupling of a channel-based technique and a column-based technique. This aim is divided into two parts. The first part is to address the online coupling of ThFFF and SEC for the analysis of complex polymers and the optimization of the experimental conditions that are required for the coupling of the two techniques. Part two of the research is to validate and demonstrate the capabilities of the comprehensive online ThFFF x SEC protocol for the characterization of complex polymers, and to provide information on various molecular properties with a single analysis.

The main objectives of the present study are to:

(1) Develop a protocol for the comprehensive online coupling of ThFFF to SEC, which includes the optimization of the experimental conditions to couple two fundamentally different techniques. The experimental parameters investigated for the first dimension, ThFFF, include:
   (a) Analysis time by exploring different methods in which to apply different temperature gradient profiles.
   (b) Flow rate.
   (c) Sample concentration.
   (d) Temperature.
   (e) Relaxation time.

(2) Prepare a range of complex polymer samples which include:
   (a) Blends of different poly(styrene) homopolymers and blends of different poly(methyl methacrylate) homopolymers.
   (b) Blends of poly(styrene)-***b***-poly(methyl methacrylate) block copolymers with similar chemical compositions and different molecular masses.
   (c) Blends of poly(styrene)-***b***-poly(methyl methacrylate) block copolymers with similar molecular masses and different chemical compositions.
   (d) Blends of poly(styrene)-***b***-poly(methyl methacrylate) block copolymers with various poly(styrene) and poly(methyl methacrylate) homopolymers.

(3) Characterize the complex polymer samples by online ThFFF x SEC, hyphenated with a UV-detector and an evaporative light scattering detector (ELSD) as two complementary concentration-sensitive detectors, to illustrate:
   (a) The separation capabilities of the coupled technique.
   (b) The merits of using information-rich detectors to provide quantitative information.

The second aim presented in this dissertation, is to use AsFlFFF for the microstructure-based separation of polymers with different tacticities to determine the separation capabilities of the technique. As separation in AsFlFFF is based on normal diffusion, which relates to the hydrodynamic diameter of the analyte, the main objective was to investigate the solution behaviour of syndiotactic, atactic and isotactic poly(methyl methacrylate)s of similar molecular masses, in solvents of different thermodynamic properties. In addition to developing a separation method, the

objectives include investigating the effect of the solvent quality and channel temperature on the separation.

The main objectives for this study are to:

(1) Develop a separation method and optimize experimental parameters to achieve sufficient separation of syndiotactic, atactic and isotactic PMMA homopolymers by AsFlFFF.

(2) Investigate the solution behaviour of the various isomers of PMMA in solvents of different thermodynamic properties. The solvents include:
   (a) Tetrahydrofuran (THF), a thermodynamically good solvent and a strong stereocomplexing solvent for PMMA.
   (b) Chloroform ($CHCl_3$), a thermodynamically good solvent and a non-stereocomplexing solvent for PMMA.
   (c) Acetonitrile (ACN), a theta solvent and a strong stereocomplexing solvent for PMMA.

(3) Investigate the influence of temperature of the separation and solution behaviour of the various isomers of PMMA by analysing the PMMA samples at different channel temperatures.

1.3. Layout of dissertation

The dissertation consists of five chapters compiled to present the scope, purpose and outcome of the research achieved in a compendious manner. In **Chapter 1**, the importance of the research conducted is introduced in a brief overview leading to the formulation of the research aims and objectives.

The fundamental importance of polymer characterization is briefly discussed in **Chapter 2**. The key focus is on providing a concise discussion on the theoretical background and mechanism of the relevant analytical techniques and the information-rich detectors used in this study. Field-flow fractionation (FFF) and size exclusion chromatography (SEC) are the two primary analytical techniques used along with various detectors such as multiangle laser light scattering (MALLS), ultraviolet (UV), differential refractive index (dRI) and evaporative light scattering (ELS). The comprehensive online coupling of a channel-based technique with a column-based technique is discussed.

Chapter 3 focuses on the first aim of the dissertation, the comprehensive online coupling of a channel-based technique with a column-based technique, in a multidimensional configuration for

the analysis of complex polymers, such as poly(styrene)-***b***-poly(methyl methacrylate) (PS-b-PMMA) block copolymers. This chapter encompasses the approach taken for the coupling of ThFFF with SEC and the optimization of the experimental parameters required to couple the two techniques.

In **Chapter 4**, the second aim of the dissertation is discussed. It illustrates how the capabilities of existing analytical techniques such as AsFlFFF can be extended by exploiting experimental parameters such as the thermodynamic quality of the solvent and the analysis temperature. The method development and optimization of experimental parameters to achieve sufficient separation of syndiotactic- and isotactic PMMA homopolymers is presented.

Lastly, conclusions and recommendations with regard to the two main aims of the dissertation are summarized in **Chapter 5**.

References

[1] H. Pasch, Hyphenated separation techniques for complex polymers, Polym. Chem. 4 (2013) 2628–2650.

[2] H. Pasch, Advanced fractionation methods for the microstructure analysis of complex polymers, Polym. Adv. Technol. 26 (2015) 771–784.

[3] H. Pasch, B. Trathnigg, HPLC of Polymers, Springer-Verlag: Berlin, Germany, 1999.

[4] H. Pasch, B. Trathnigg, Multidimensional HPLC of Polymers, Springer-Verlag: Heidelberg, Germany, 2013.

[5] D. Held, P. Kilz, Characterization of polymers by liquid chromatography, Macromol. Symp. 231 (2006) 145–165.

[6] H. Pasch, Analysis of complex polymers by multidimensional techniques. Phys. Chem. Chem. Phys. 1 (1999) 3879–3890.

[7] I.A. Haidar Ahmad, A.M. Striegel, Determining the absolute, chemical-heterogeneity-corrected molar mass averages, distribution, and solution conformation of random copolymers, Anal. Bioanal. Chem. 396 (2010) 1589–1598.

[8] W. Radke, J. Falkenhagen, Liquid Interaction Chromatography, in: S. Fanali, P.R. Haddad, C.F. Poole, P. Schoenmakers, D. Lloyd (Eds.), Liquid chromatography, Elsevier: Amsterdam, The Netherlands; (2013) 93–129.

[9] W. Radke, Polymer separations by liquid interaction chromatography: Principles – prospects – limitations, J. Chromatogr. A. 1335 (2014) 62–79.

[10] P. Schoenmakers, P. Aarnoutse, Multidimensional separations of polymers, Anal. Chem. 86 (2014) 6172–6179.

[11] B.W.J. Pirok, A.F.G. Gargano, P.J. Schoenmakers, Optimizing separations in online comprehensive two-dimensional liquid chromatography, J. Sep. Sci. 41 (2018) 68–98.

[12] B. Trathnigg, S. Abrar, Characterization of complex copolymers by two-dimensional liquid chromatography, Procedia Chem. 2 (2010) 130–139.

[13] M.E. Schimpf, K. Caldwell, J.C. Giddings, Field-Flow Fractionation Handbook, John Wiley and Sons: New York, USA, 2000.

[14] F.A. Messaud, R.D. Sanderson, J.R. Runyon, T. Otte, H. Pasch, S.K.R. Williams, An overview on field-flow fractionation techniques and their applications in the separation and characterization of polymers, Prog. Polym. Sci. 34 (2009) 351–368.

[15] M.I. Malik, H. Pasch, Field-flow fractionation: New and exciting perspectives in polymer analysis, Prog. Polym. Sci. 63 (2016) 42–85.

[16] J.C. Giddings, Two-dimensional field-flow fractionation, J. Chromatogr. 504 (1990) 247–258.

[17] A.C. van Asten, R.J. van Dam, W. Th. Kok, R. Tijssen, H. Poppe, Determination of the compositional heterogeneity of polydisperse polymer samples by the coupling of size-exclusion chromatography and thermal field-flow fractionation, J. Chromatogr. A. 703 (1995) 245–263.

[18] E. Venema, P. de Leeuw, J.C. Kraak, H. Poppe, R. Tijssen, Polymer characterization using online coupling of thermal field-flow fractionation and hydrodynamic chromatography, J. Chromatogr. A. 765 (1997) 135–144.

[19] G. Yohannes, S.K. Wiedmer, J. Hiidenhovi, A. Hietanen, T. Hyötyläinen, Comprehensive two-dimensional field-flow fractionation-liquid chromatography in the analysis of large molecules, Anal. Chem. 79 (2007) 3091–3098.

[20] N. Radebe, T. Beskers, G. Greyling, H. Pasch, Online coupling of thermal field-flow fractionation and Fourier transform infrared spectroscopy as a powerful tool for polymer characterization, J. Chromatogr. A. 1587 (2019) 180–188.

[21] S.K.R. Williams, J.R. Runyon, A.A. Ashames, Field-Flow Fractionation: Addressing the nano challenge, Anal. Chem. 83 (2011) 634–642.

[22] C. van Batten, M. Hoyos, M. Martin, Thermal field-flow fractionation of colloidal materials: Methylmethacrylate-styrene linear di-block copolymers, Chromatographia. 45 (1997) 121–126.

[23] C.A. Ponyik, D.T. Wu, S.K.R. Williams, Separation and composition distribution determination of triblock copolymers by thermal field-flow fractionation, Anal. Bioanal. Chem. 405 (2013) 9033–9040.

[24] G. Greyling, H. Pasch, Characterisation of block copolymer self-assemblies by thermal field-flow fractionation, Polym. Int. 66 (2017) 745–751.

[25] U.L. Muza, G. Greyling, H. Pasch, Characterization of complex polymer self-assemblies and large aggregates by multidetector thermal field-flow fractionation, Anal. Chem. 89 (2017) 7216–7224.

[26] W. Hiller, W. van Aswegen, M. Hehn, H. Pasch, Online ThFFF–NMR: A novel tool for molar mass and chemical composition analysis of complex macromolecules, Macromolecules 46 (2013) 2544–2552.

[27] D. Melucci, C. Contado, I. Mingozzi, M. Hoyos, M. Martin, F. Dondi, Evaluation of the Soret coefficient for polystyrene in decalin by means of thermal field-flow fractionation, J. Liq. Chrom. & Rel. Technol. 23 (2000) 2067–2082.

[28] G. Greyling, H. Pasch, Thermal Field-Flow Fractionation of Polymers, Springer: Heidelberg, Germany, 2019.

[29] J.R. Runyon, S.K.R Williams, Composition and molecular weight analysis of styrene-acrylic copolymers using thermal field-flow fractionation. J. Chromatogr. A. 1218 (2011) 6774–6779.

[30] C.A. Ponyik, D.T. Wu, S.K.R Williams, Separation and composition distribution determination of triblock copolymers by thermal field-flow fractionation. Anal. Bioanal. Chem. 405 (2013) 9033–9040.

[31] G. Greyling, H. Pasch, Tacticity separation of poly(methyl methacrylate) by multidetector thermal field-flow fractionation. Anal. Chem. 87 (2015) 3011–3018.

[32] G. Greyling, H. Pasch, Multidetector thermal field-flow fractionation as a novel tool for the microstructure separation of polyisoprene and polybutadiene. Macromol. Rapid. Commun. 35 (2014) 1846–1851.

[33] G. Greyling, H. Pasch, Fractionation of poly(butyl methacrylate) by molecular topology using multidetector thermal field-flow fractionation. Macromol. Rapid. Commun. 36 (2015) 2143–2148.

[34] J. Ehrhart, A.-F. Mingotaud, F. Violleau, Asymmetrical flow field-flow fractionation with multi-angle light scattering and quasi elastic light scattering for characterization of poly(ethylene glycol-b-ε-caprolactone) block copolymer self-assemblies used as drug carriers for photodynamic therapy. J. Chromatogr. A. 1218:27 (2011) 4249–4256.

[35] H. Pasch, A.C. Makan, H. Chirowodza, N. Ngaza, W. Hiller, Analysis of complex polymers by field-flow fractionation. Anal. Bioanal. Chem. 406 (2014) 1585-1596.

[36] A.C. Makan, R.P. Williams, H. Pasch, Field-flow fractionation for the size, molar mass and gel content analysis of emulsion polymers of water-based coatings. Macromol. Chem. Phys. 217 (2016) 2027-2040.

[37] M. Wagner, C. Pietsch, L. Tauhardt, A. Schallon, U.S. Schubert, Characterization of cationic polymers by asymmetric flow field-flow fractionation and multi-angle light scattering - A comparison with traditional techniques. J. Chromatogr. A. 1325 (2014) 195-203.

CHAPTER 2

HISTORICAL AND THEORETICAL BACKGROUND

2.1. Polymer characterization

Characterization of polymers is key in the prediction and understanding of polymer properties and morphology. Complex polymers have multiple distributions in their physical and chemical properties [1, 3]. Therefore, fundamental knowledge is required about the chemical and physical properties of a polymeric material and the inherent property distributions, as the physical and chemical properties and end-use applications are interdependent [4-6].

Characterization of polymeric materials typically involves (1) molecular mass analysis, (2) molecular structure and/or chemical composition (architecture, microstructure, topology, branching) analysis, (3) spectroscopic studies for bulk characterization of repeat units or endgroup analysis, (4) thermal properties, (5) dynamics, mechanical, optical and physical properties and (6) morphology [3, 5, 6]. The analytical techniques and detectors generally utilized for the characterization of the various polymer properties are tabulated in **Table 2.1**.

Table 2.1 Characterization techniques for the analysis of polymer properties [1, 3, 5, 6]

Property	Technique
Molecular mass	Size exclusion chromatography (SEC), light scattering, osmometry and viscometry.
Molecular structure and/or chemical composition	Interaction chromatography (IC) such as solvent gradient IC, temperature gradient IC, liquid chromatography at critical condition (CC).
Bulk characterization of repeat units or endgroup analysis.	FTIR, NMR
Thermal properties	DSC, TGA
Dynamics, mechanical, and physical properties.	DMA
Morphology	SEM, TEM

Polymer characterization techniques such as spectroscopy and chromatography along with the synthesis of polymers have had continuous research and development over the years. The interdependency of polymer characterization and polymer synthesis in order to comprehensively

investigate the properties of a polymer have contributed to numerous new prospects in the field of polymer analytics. One such example of new analytical method development is field-flow fractionation (FFF), a family of channel-based analytical techniques.

2.2. Field-flow fractionation

2.2.1. Introduction

FFF was pioneered by the group of J. Calvin Giddings in 1966 and has been commercially available since the late 1980's to early 90's [7-10]. FFF techniques have not received as much attention as other fractionation techniques that were developed during the same time such as interaction chromatography (IC), which has experienced significant development and is now a well-established and understood analytical technique for polymer characterization [2, 3, 11-13] In recent years, however, FFF has emerged as a powerful technique for the characterization of natural and synthetic polymers. FFF makes use of an empty channel, with no stationary phase, contrary to IC which entails the use of a stationary phase to achieve separation that is based on adsorption or partitioning of analytes between the stationary phase and the mobile phase [8, 9, 11, 12]. The scheme of a typical FFF channel is given in **Fig. 2.1**.

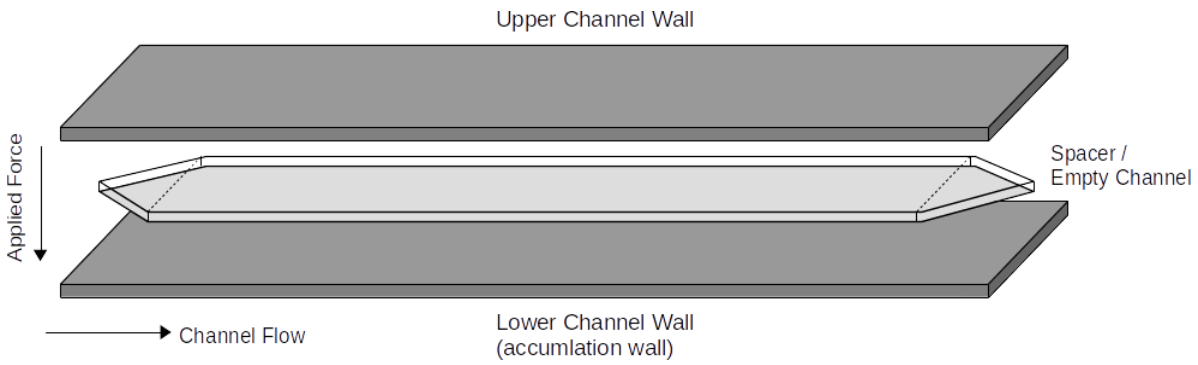

Figure 2.1 Schematic representation of a typical FFF channel.

In FFF, the separation mechanism depends upon an externally applied force field that is perpendicular to the parabolic flow velocity profile of the channel. The interaction and/or response of the analyte to a given applied force bring about analyte separation. The empty-channel system creates a favourable environment for polymer separation as it reduces shear degradation and the shear forces experienced by the analyte at the channel walls are at a minimum [14]. Hence, FFF is a suitable technique for the separation of high molecular mass polymers and polymeric materials that

are susceptible to shear degradation such as micelles, aggregates, colloids, liposomes, proteins and nanoparticles.

FFF has the capability to separate ultrahigh molecular mass polymers and particles which can range from nanometer to micrometer in size, with a sufficient resolution and minimal sample loss [15-20]. Depending on the characteristics of the analyte e.g. molecular mass, density, charge or chemical composition, different types of force fields can be applied to achieve separation. The various types of applied force fields have given rise to several sub-techniques within the FFF family of which thermal FFF (ThFFF) and flow-FFF (FlFFF) are the most referred to. The type of field applied determines the mode of operation that in return determines the elution order [7-9, 14]. The three modes possible in FFF are the normal (Brownian) mode, the steric mode and the hyper-layer mode [7-9, 14]. The normal Brownian mode of operation is the most implemented and is used to fractionate polymers less than 1 µm in diameter. The order of elution in normal mode is that the smaller size analytes will elute first followed by the analytes larger in size. The smaller analytes are able to migrate towards the channel centre and experience a faster flow velocity within the parabolic flow profile of the channel [8, 9, 14, 21-23].

The various FFF sub-techniques are acknowledged for their physical simplicity, easily adjustable experimental conditions and versatility. Nevertheless, novice users still consider FFF a complex analytical technique, because the establishment of a new separation protocol requires a good understanding of the principles of each of the sub-techniques and the experimental parameters associated with them. The sections to follow contain the essential facts of FFF with relevance to the research studies undertaken herein. For a more comprehensive read into the various sub-techniques and modes of operation refer to the Field-Flow Fractionation Handbook [14].

2.2.2. General principles and theoretical background

The key feature of the flow-based FFF techniques is the thin and empty channel constructed by clamping two plates (otherwise known as walls) together with a spacer in between. The spacer is usually clamped between two surfaces parallel to each other, through which the carrier liquid flows. A schematic illustration of a typical FFF channel and the general separation mechanism is given in **Fig.2.2**. The general principle and theoretical background has been described well in publications and were referenced to provide a concise overview of the theory presented in this section [7-10, 14, 21-24].

The flow in the FFF channel is classified as laminar flow and exhibits a near parabolic flow profile. As a result, different flow velocity streams are present within the channel. The flow stream closest to the channel wall is near zero velocity, while the flow streams nearing the centre of the channel increase in velocity, with the maximum velocity at the channel centre which decreases as it nears the opposite channel wall. It is important to note that at the channel wall the frictional drag is at its highest and hence the near-zero velocity of the carrier liquid. The frictional drag decreases towards the centre of the channel resulting in an increase in the carrier flow velocity, producing the parabolic flow profile. The parabolic flow profile is defined by the Navier-Stokes equation for fluid flow as follows:

$$v(x) = 6 < v > [(\frac{x}{w}) - (\frac{x}{w})^2)] \quad (2.1)$$

where $v(x)$ is the average velocity of the carrier liquid throughout the channel, w is the channel thickness and x is the distance from the channel wall (x = 0 at the accumulation wall). Perpendicular to the flow stream, an external force field is applied to achieve retention and subsequently separation in a thin flow channel. Upon injection, a sample is forced to migrate towards the accumulation wall at a velocity U, based on its interaction with the applied field (F), where it concentrates. The velocity U is influenced by the frictional drag and the magnitude of the applied force as shown:

$$U = \frac{F}{f} \quad (2.2)$$

The frictional force is characterized by the frictional coefficient that is described by Stokes equation for non-spherical analytes:

$$f = 3\pi\eta d_h \quad (2.3)$$

where d_H is the size of the analyte in a given solution (more commonly referred to as the hydrodynamic diameter) and η denotes the viscosity of the solution.

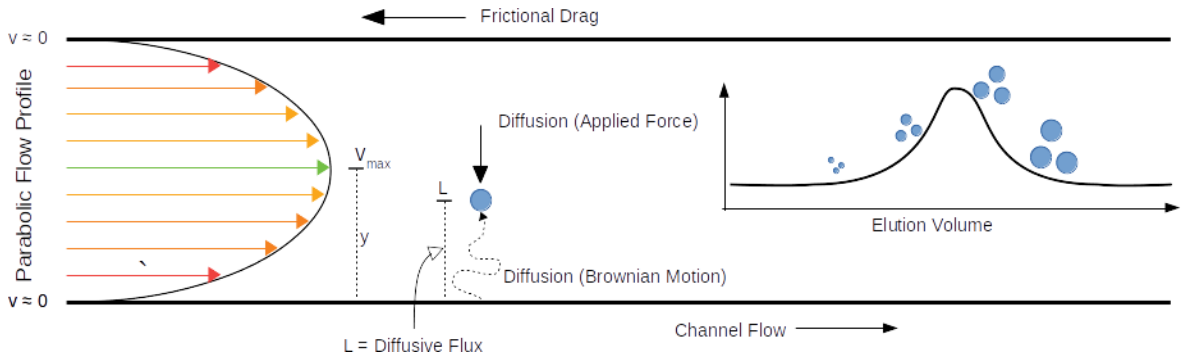

Figure 2.2 Schematic illustration of the parabolic flow profile, the diffusion of analytes, the migration forces and mean layer thickness as it exists within a typical FFF channel.

A concentration build-up of analyte molecules arises at the accumulation wall due to the applied force. In order to prevent the concentration build-up, analytes oppose the applied force by migrating back into the channel according to Fick's Law of diffusion i.e. the random movement of analytes influenced by a concentration gradient. The diffusion of analytes across the channel is affected by the frictional drag it experiences and is expressed by the Nernst-Einstein equation:

$$D = \frac{k\mathrm{T}}{f} \tag{2.4}$$

where D is the normal diffusion coefficient, k is Boltzmann's constant and T is the absolute temperature. By substituting equation (**2.2**) into equation (**2.4**), the diffusion coefficient can be written as:

$$D = \frac{kT}{(\frac{U}{F})} \tag{2.5}$$

Alternatively, by substituting equation (**2.3**) into equation (**2.4**), the diffusion coefficient can be determined by die Stokes-Einstein equation:

$$D = \frac{kT}{3\pi\eta d_h} \tag{2.6}$$

As a result of the diffusive force, different analytes form thin clouds or layers of different thicknesses at various distances from the accumulation wall. Accordingly, the different analyte clouds occupy different flow velocity streams. The distance that the analytes diffuse from the accumulation wall into separate thin clouds of analytes is defined as the mean layer thickness (ℓ):

$$\ell = \frac{kT}{F} = \frac{D}{U} \tag{2.7}$$

When the two opposing migration forces balance, the cloud of analytes reaches an equilibrium distribution across the channel velocity streams. This generates an exponential concentration profile that is a function of the mean layer thickness as expressed:

$$c(x) = c_0 \, exp\,(-\frac{x}{\ell}) \tag{2.8}$$

The concentration profile caused by the applied force field is denoted as c(x) and c_0 represents the concentration at the accumulation wall (x = 0). In effect, the concentration profile governs the retention of analytes in FFF and correlates to the physicochemical properties of the analytes. The degree of retention in FFF is based on the interaction between the analyte molecules and the applied field, and the concentration profile as a result thereof. The interaction is different for each analyte as it is influenced by the intrinsic properties of the analyte, the mobility parameters associated with the carrier liquid and the strength of the applied force field. The extent of the interaction is measured by the dimensionless retention parameter (λ) and is given by:

$$\lambda = \frac{\ell}{w} = \frac{kT}{wF} = \frac{D}{Uw} \tag{2.9}$$

It is important to note that equation (**2.9**) is only a basic expression for FFF as the retention parameter and the applied force field is different for each sub-technique of FFF. The retention parameter is significant as it (1) defines the distance of the analyte cloud from the accumulation wall relative to the channel thickness, (2) relates to the force applied on the analyte, (3) correlates the interaction of the analyte with force field to the physicochemical properties of the retained analyte and, (4) describes the retention of various analyte clouds which are restricted to different flow velocity streams which are slower than the carrier liquid velocity. Analyte retention is, thus, defined by the retention ratio and is expressed by the concentration profile and the carrier flow velocity as follows:

$$R = \frac{<c(x)v(x)>}{<c(x)><v(x)>} \tag{2.10}$$

By substitution of equation (**2.1**) and equation (**2.8**) into equation (**2.10**) and subsequently rearranging equation (**2.9**) to ℓ = λ w, and substituting it into equation (**2.8**), the retention can be expressed in terms of the retention parameter:

$$R = 6\lambda \,(coth(\frac{1}{2}\lambda - 2\lambda)) \tag{2.11}$$

The retention ratio can alternatively be determined empirically and is described in terms of retention time:

$$R = \frac{t_0}{t_t} \tag{2.12}$$

Where t_0 is the peak maximum retention time of an unretained analyte and t_r is the peak maximum retention time of a retained analyte. The theoretical parameters can be correlated to the empirical parameter through the retention ratio and/or retention time by the approximation as shown in equation (**2.13**). However, this is at best accurate within 5 % error and only if λ is smaller than 0.2 [14].

$$R = \frac{t_0}{t_r} = 6\lambda \tag{2.13}$$

The empirical retention time is imperative in determining the resolution (R_s) capabilities of a specific system under well-defined conditions. Note that in FFF the resolution is often termed as the fractionation power. The resolution of a system is evaluated by the degree to which two neighbouring analyte peaks separate. This is measured by the difference in the retention time at peak height of the analytes and is defined by:

$$Rs = \frac{\Delta t_r}{4\sigma_t} \tag{2.14}$$

Δt_r represents the difference in the retention time of two analytes and $4\sigma_t$ is the average standard deviation of two analyte peaks quantified in time. The resolution depends on a number of experimental parameters including the retention parameter, the channel thickness and length, the selectivity and the plate height.

The plate height (H) is a theoretical expression for the separation efficiency of a FFF technique and is defined by:

$$H = \frac{L}{N} \tag{2.15}$$

where L is the length of the channel and N the total number of theoretical plates. The efficiency is dependent on the peak broadening that occurs based on the dispersion of the analyte cloud and the time that the analytes spend in the channel. Thus, a smaller plate height value means less peak broadening occurs and as a result the technique is more efficient. The plate height is defined in FFF by the summation of four peak broadening factors. The first factor is the axial diffusion (H_d) of the analyte along the axial flow direction in reaction to the axial concentration gradient. The second factor is the non-equilibrium (H_n), which is the principal contributor to peak broadening in FFF. H_n describes the phenomenon where analytes within a distinct analyte cloud are at slightly different

flow velocity streams and thus migrate through the channel at different rates in the axial flow direction and thus produce peak broadening. A sample that has a high dispersity (H_p) can cause peak broadening as it is able to generate a continuous extended concentration profile across the channel. This reduces the ability of the FFF technique to separate the analytes into distinct peaks. The last contributing factor is the instrumental and experimental factor (H_i). The plate height value can be represented as follows:

$$H = H_d + H_n + H_p + H_i \quad (2.16)$$

The theory of FFF has been developed based on a number of assumptions and approximations, for instance that the parabolic flow is uniform across the channel; the exponential concentration profile is based on a uniformly applied force field, that there is no analyte-analyte interaction or analyte-wall interaction. For this reason, a significant deviation does exist between the value determined by the theoretical approach and obtained by the experiment.

2.2.3. Thermal field-flow fractionation

The theoretical background with regard to ThFFF has been well-established and described in literature, and was referenced to summarize the theory of ThFFF as discussed below [8,9 14,24-29]. In ThFFF, an external temperature gradient is generated between the two channel walls by heating the upper wall and cooling the lower wall. The temperature gradient (ΔT) is thus the driving force in ThFFF and is applied perpendicular to the axial flow direction of the channel to achieve retention and separation of analytes as shown in **Fig. 2.3.** The applied temperature gradient force is expressed by:

$$F = kT\left(\frac{D_T}{D}\right)\Delta T \quad (2.17)$$

where k is Boltzmann's constant, T is the absolute temperature, D_T is the thermal diffusion coefficient, and D is the normal diffusion coefficient. ΔT is the applied temperature gradient across the channel.

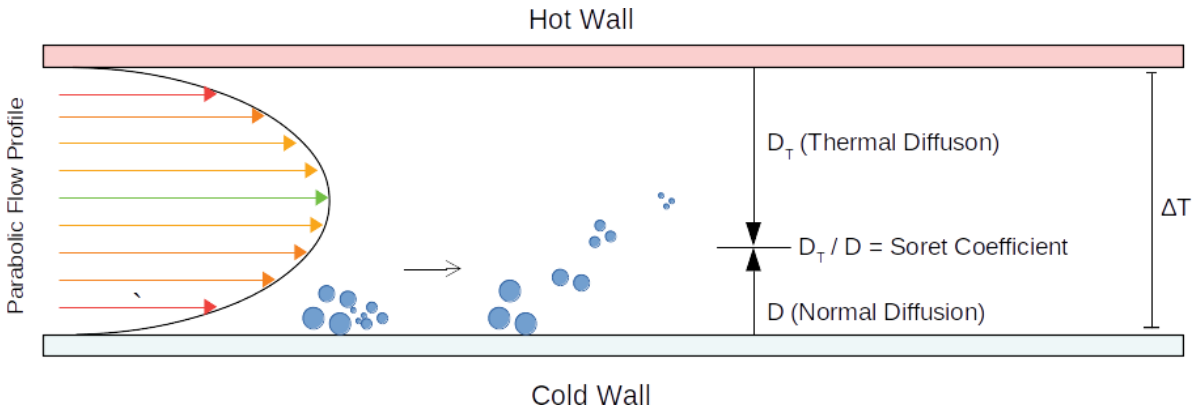

Figure 2.3 Schematic representation of a ThFFF channel and its separation mechanism.

When a sample is injected into the ThFFF channel, analyte molecules migrate from the hot wall towards the cold wall (accumulation wall) where they concentrate. This migration is termed the thermal diffusion and is quantified by the thermal diffusion coefficient, D_T. In order to counteract the concentration build-up, analyte molecules migrate from the cold wall towards the centre of the channel by means of normal diffusion. As a result, the different analyte molecules will reside at various mean layer thicknesses from the cold wall and subsequently occupy different flow velocity streams in the parabolic flow stream of the channel. The distance of the analyte molecules extending from the cold wall towards the channel centre is determined by the interaction between the two diffusive forces. This interaction is quantified by the ratio of the thermal diffusion coefficient to the normal diffusion coefficient and is denoted by the Soret coefficient (S_T).

$$S_T = \frac{D_T}{D} \tag{2.18}$$

The Soret coefficient can either be dominated by D or D_T, depending on the analyte and experimental parameters. D_T is determined by the chemical composition of the analyte and the nature of the solvent used for both dissolution and the carrier liquid. D is a function of the hydrodynamic diameter of the analyte in the solvent and can be determined by the Stokes-Einstein equation as expressed by equation (**2.6**). Alternatively, D can be determined experimentally by various methods, such as dynamic light scattering (DLS), SEC or dispersion measurements. This indicates that ThFFF has the ability to provide information on both the chemical composition and/or the molecular mass of an analyte.

The Soret coefficient governs the retention and subsequent separation of analytes in the ThFFF channel. Separation of analytes is achieved when there is a difference in the Soret coefficients. Retention of analytes is based on the field strength and the Soret coefficient. The interaction of the analyte with the applied temperature force in ThFFF, expressed by λ, is associated with the

temperature difference. Based on the assumptions that (1) the applied temperature gradient is constant across the channel and (2) the thermal conductivity dependency of the carrier liquid is neglected, the retention parameter in ThFFF can be expressed as:

$$\lambda = \frac{D}{D_T}\Delta T \tag{2.19}$$

The flow profile in the ThFFF channel is not an absolute parabolic profile, as a change in temperature across the channel influences the temperature dependent parameters of the carrier liquid such as viscosity and thermal conductivity. Correspondingly, the concentration profile and carrier liquid velocity change in accordance with temperature changes. Hence, equation (**2.10**) is modified to account for these experimental variances and related to the retention parameter as given:

$$R = 6\lambda\,[v + (1 - 6\lambda v)\,[coth\,(\frac{1}{2}\lambda - 2\lambda)] \tag{2.20}$$

The retention in ThFFF can also be determined empirically from the void time (t_0), the time required for an unretained analyte to elute from the channel, and the retention time at peak maximum (t_r):

$$R = \frac{t_r}{t_0} = \frac{D_T\,\Delta T}{6D} \tag{2.21}$$

An alternative approach is to calculate D_T experimentally from the retention time at peak maximum of the eluting peak.

$$D_T = \frac{6D\,t_r}{\Delta T\,t_0} \tag{2.22}$$

The resolution and efficiency in ThFFF is influenced by the applied temperature gradient as well as the relaxation step. Relaxation step refers to the relaxation time (τ) required for analytes to reach an equilibrium distribution across the channel velocity streams i.e. a steady-state concentration profile. The resolution can be enhanced as the dispersion of the analyte cloud can be kept to a minimum, reducing the degree of peak broadening in the channel. During the relaxation time, the channel flow is redirected round the channel and thus depends on experimental parameters such as the channel thickness (w), the applied temperature gradient and the thermal diffusion coefficient of the analyte:

$$\tau = \frac{w^2}{D_T\Delta T} \tag{2.23}$$

ThFFF has been proven to be a powerful technique for the separation and characterization of a range of polymers, particles and aggregates. As separation is govern by S_T, which correlates to the chemical composition, ThFFF has successfully been able to characterize homopolymers, block

copolymers and micelles based not only on its chemical composition, but was also shown to be capable of microstructure-based separation [27, 30-40]

2.2.4. Asymmetric flow field-flow fractionation

The theory of flow field-flow fractionation (FlFFF) has been well-described in literature and were referred to, to provide a brief theoretical background of FlFFF and its sub-techniques [7, 14 , 41-43]. In FlFFF the externally applied field is known as the cross flow. The cross flow is generated perpendicular to the parabolic flow streams between two channel walls to achieve separation and retention of analytes. Based on the manner in which the cross flow is generated, FlFFF is divided into two techniques, (1) symmetrical FlFFF and (2) asymmetrical FlFFF. The difference in the two techniques is related to the way the cross flow is generated and the configuration of the channel walls. Symmetrical FlFFF has two permeable porous frits as the channel walls. In order to generate the cross flow, the carrier liquid is pumped through the upper channel wall frit and leaves the channel through the lower permeable porous frit channel wall.

Asymmetric FlFFF (AsFlFFF) consists of a solid impermeable upper channel wall and a lower semi-permeable frit channel wall. The single channel inlet flow diverges into the axial flow and the cross flow, which is generated by using a semi-permeable frit as one of the channel walls. To prevent the loss of analyte molecules with the cross flow, an ultrafiltration membrane with a specific molecular mass cut-off is placed on top the frit. A schematic representation of the AsFlFFF technique is shown in **Fig. 2.4**.

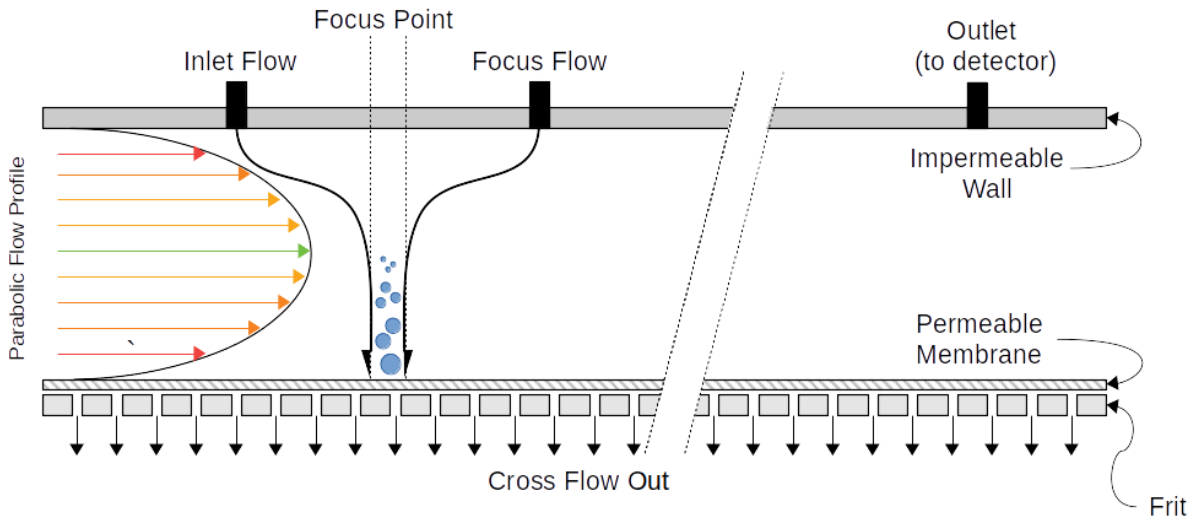

Figure 2.4 Schematic illustration of an AsFlFFF channel and its separation mechanism.

Upon injecting a sample into the AsFlFFF channel, the analyte molecules are forced in the direction of the accumulation wall by the cross flow at a velocity, U, where the analytes concentrate. The velocity and the force (F) of the cross flow generated are expressed by equation (**2.24**) and (**2.25**), respectively:

$$U = \frac{V_c}{A_{acc}} \tag{2.24}$$

$$F = \frac{V_c w k T}{V_0 D} \tag{2.25}$$

where V_c is the volumetric cross-flow rate, A_{acc} is the surface area of the accumulation wall, w is the channel thickness, is k Boltzmann's constant, T the absolute temperature, V_0 is the void volume and D the normal diffusion coefficient. In order to oppose the concentration build-up, the analyte molecules migrate via Brownian motion into the channel over the height and length of the channel to different flow velocity streams within the parabolic flow. The migration is known as normal diffusion and denoted by the diffusion coefficient D. Smaller analyte molecules diffuse faster from the accumulation wall towards the channel centre than larger analyte molecules since they have larger diffusion coefficients and thus reside at various mean layer thicknesses (ℓ). The distance the analytes diffuse from the accumulation wall is based on the interaction of the analyte with the cross-flow field. Additionally, the magnitude of the cross-flow force influences the time required for the analyte molecules to reach a steady-state concentration profile across the channel.

The D is the driving force for retention and resultant separation in AsFlFFF and is associated with the hydrodynamic diameter (d_h) of the analyte in a given solvent by the Stokes-Einstein equation (**eq. 2.6**). Thus, AsFlFFF can determine the molecular mass and molecular mass distribution of a polymeric sample with the aid of suitable mass-sensitive detectors e.g. MALS and viscometer [44, 45]. Analytes with different diffusion coefficients will be retained to a different degree ensuring separation. Retention of the analyte is based on the rate of the cross-flow and the D. The interaction of the analyte with the cross-flow force, i.e. the retention parameter (λ), is described by:

$$\lambda = \frac{D V_0}{V_c w^2} \tag{2.26}$$

To account for the lack of cross flow at the upper solid wall, due to the inlet flow being diversed into the axial flow and the cross-flow, the calculation of the retention in AsFlFFF is an approximation. The retention time in AsFlFFF can be calculated by the simplified equation given:

$$t_r = \frac{w^2}{6D} ln(1 + \frac{V_c}{V_{out}}) \tag{2.27}$$

where V_{out} is the volumetric flow rate of the channel outlet. This is calculated by subtracting the volumetric flow rate of the cross flow from the volumetric flow rate of the channel inlet (V_{In}). Using the retention times obtained experimentally, the diffusion coefficient can be determined:

$$D = \frac{t_0 w^2 V_c}{6 t_r V_0} \tag{2.28}$$

where t_0 is the void time, w is the channel thickness and V_0 the void volume of the channel. In AsFlFFF, the void time is expressed as:

$$t_0 = \frac{V_0}{V_c} ln\{1 + \frac{V_c}{V_{out}} [1 - w \frac{b_o z' - b_o - \frac{b_L}{2L} z'^2 - y}{V_0}]\} \tag{2.29}$$

where b_0 is the breadth of the channel inlet, b_L is the breath of the channel outlet, z' is the distance from the channel inlet to the focusing point, y is the channel area excluded by a tapered inlet and L is the length of the channel.

By substituting the Stokes-Einstein diffusion coefficient equation ($D = \frac{kT}{3\pi\eta d_h}$) into equation (**2.28**), the hydrodynamic diameter (d_h) of comparable spherical analytes can be obtained. The retention equation can be used to determine the d_h directly from the retention time, t_r:

$$d_h = \left(\frac{2kTV_0}{\pi\eta V_c w^2 t_0}\right) t_r \tag{2.30}$$

In AsFlFFF, the resolution and efficiency in separation can be advanced by incorporating a focussing step upon injecting a sample into the channel. The focussing step is when the carrier liquid is pumped in near the channel outlet, in the opposite direction than the axial flow stream of the channel. The point where the two opposing flow streams meet is known as the focusing point. This step prevents the analytes from diffusing along the length of the channel and allows sufficient time for the analyte clouds to reach different steady states. This is termed relaxation. The focussing step/relaxation of the analytes aids in improving the resolution and reducing the degree of peak broadening.

AsFlFFF has been used in the characterization of complex polymers with regard to molecular mass and structural parameters [18, 20, 41-49]. As the separation in AsFlFFF is predominantly governed by D, it can potentially be capable of separating polymers that differ with regard to tacticity through the use of solvents of different thermodynamic qualities and viscosities at various channel temperatures.

2.3. Multidimensional analytical techniques

For the comprehensive characterization of well-defined polymers with one molecular property distribution, one-dimensional analytical techniques have proven to be successful in providing information on a selected single property such as molecular mass or chemical composition or functionality. However, one-dimensional techniques are not efficient for the characterization of complex polymers having two or more distributions in molecular properties. Complex polymers consist of various properties with distributions (functionality type, chemical composition, microstructure, topology and/or molecular mass) that coincide and are interdependent. The molecular heterogeneity of complex polymers, thus, requires a multidimensional characterization approach to characterize each molecular property separately [50-52].

A multidimensional protocol is a systematic approach to maximize the information obtained from the combination of one-dimensional analytical techniques as information on several distributed properties and their respective correlation can be acquired in (possibly) a single analysis. The protocol is based on the concept of orthogonality and the maximization thereof. This protocol has been successfully applied to 'orthogonal' chromatographic separations. Conventionally, the separation mechanisms of the techniques used in each direction are fundamentally different. Each technique has a distinct selectivity towards one of the distributed properties, while simultaneously being non-selective towards another property. The advantages of such a protocol are the optimization of the resolving power, the reproducibility and the efficiency in characterization. Over the years, multidimensional techniques hyphenated with information-rich detectors have become a routine approach for the separation and characterization of the molecular heterogeneity of complex polymers [53-56].

In a multidimensional chromatographic analysis, a sample will be subjected to one separation mechanism sensitive to either chemical or structural differences, and the subsequently collected fractions will then be subjected to the next separation mechanism, before detection. The fractions are generally collected in storage loops attached to an electronically controlled switching valve that transfers the fractions in continuous sequential manner to the next analytical step [50, 52, 55]. Several variations of multidimensional configurations have been selectively combined to obtain valuable information in respect to the distributed properties of complex polymers. Ample reviews dedicated to the different multidimensional approaches that have been used for polymer characterization over the years have been published [51-56]. A schematic of a typical multidimensional system configuration is shown in **Fig. 2.5**.

One of the primary configurations for multidimensional analysis of polymers is the coupling of two column-based liquid chromatography (LC) techniques such as liquid interaction chromatography (IC) and SEC. IC has been the customary method used for the chemical composition characterization of polymers and uses a stationary phase to achieve separation. Separation in IC is based on adsorption or partitioning of analytes between the stationary phase and the mobile phase. SEC is the standard method for the molecular mass and molecular mass distribution characterization of polymers [50, 55].

Separation in SEC is achieved on a stationary phase with a given pore size distribution. Generally, the mobile phase will be a thermodynamically good solvent for the analyte. Separation of the analyte is based on the interaction of the analyte with the given stationary phase and is influenced by the random coil conformation that the analyte molecules adopt based on the interaction with the given solvent at a given temperature (T) [57, 58]. This process is described by the Gibbs free energy G:

$$\Delta G = \Delta H - T\Delta S \tag{2.31}$$

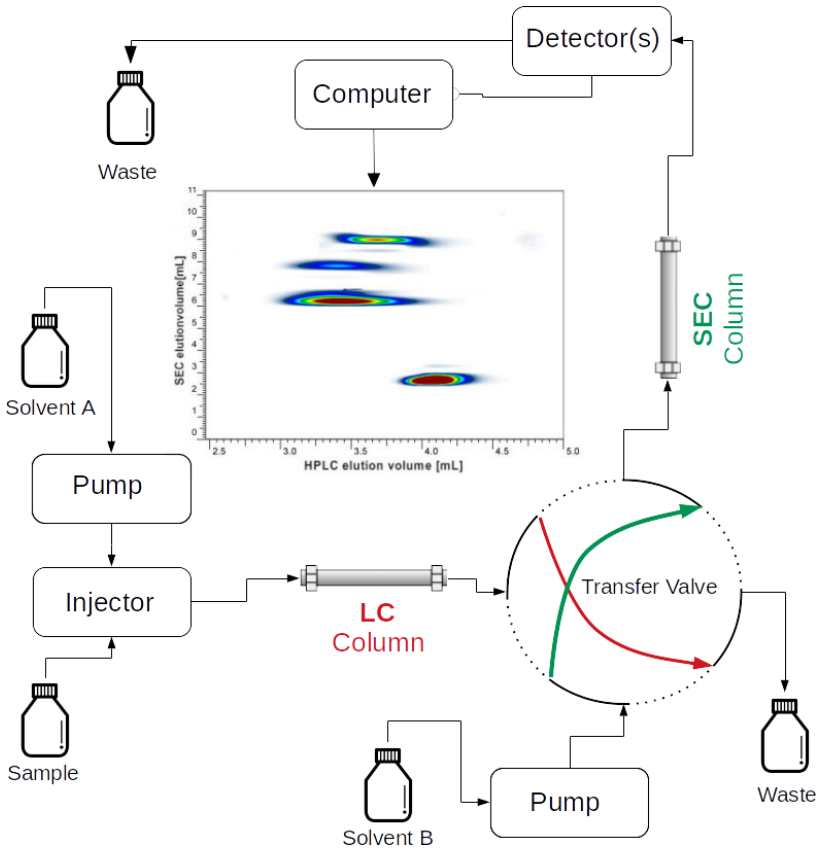

Figure 2.5 Schematic representation of a multidimensional configuration for the separation and characterization of complex polymers.

Thus, separation in SEC is predominantly entropy (ΔS) driven and is based on the conformational changes of the polymer analyte when penetrating the pores of the stationary phase. The conformational change of a polymer is generally referred to as the hydrodynamic volume (size) of a polymer, which is primarily determined by the polymer chain length [58, 59]. The hydrodynamic size of the polymer in a given solution is related to the molecular diffusion coefficient of the polymer and can be determined by the Stokes-Einstein equation (**eq. 2.6**). As separation is achieved based on the distribution of the analytes between the stationary phase and the mobile phase, chemical interaction of the analyte with the stationary phase are to be expected i.e. enthalpic effect (ΔH). As such, the separation is not purely sized-based. As a general rule, the stationary phase - analyte interaction is considered negligible in a thermodynamically good solvent. Therefore, the change in enthalpy is near zero ($\Delta H \cong 0$) [57, 60]. For this reason, elution in SEC is merely based on the hydrodynamic volume of the analyte, meaning that regardless of chemical composition, analytes with the same hydrodynamic volume shall elute at the same time from the column. The elution order in SEC is that larger analytes elute first followed by the smaller analytes. The larger analytes are excluded from the packing material because unlike smaller analytes, they cannot enter the pores [57, 60, 61].

SEC is classified as a relative method for the determination of molecular mass and molecular mass distribution of polymers. This means that a calibration of the column is required to which the molecular mass and molecular mass distribution of the analysed polymer is related to. The calibration and resultant calibration curve is constructed with a range of narrowly distributed polymeric standards of known molecular mass and chemical composition. The necessity of calibrating the column is an inherent limitation of SEC as it can result in the misrepresentation of the molecular mass properties [57, 58, 60]. In addition, the molecular mass characterization of complex polymers, with different architectures and functionalities, is a challenge as they have a different chemical composition to that of the calibration standards. However, the coupling of SEC with molecular mass-sensitive detectors, such as MALS and viscometer, assists in acquiring distribution information e.g. branching, radius of gyration and number average molecular mass [58, 60, 61]. By coupling SEC in a multi-dimensional configuration to a complementary method that separates according to chemical composition, detailed information about two different distribution properties e.g. chemical composition and molecular mass can be obtained simultaneously.

Alternatives to column-based interaction chromatography methods are channel-based fractionation techniques, which have been successfully applied for characterization of complex polymers such as block copolymers, particles, micelles and aggregates. Despite the robustness, numerous

experimental advantages (large range of solvent choices, low solvent consumption, short analysis time and multiple detector hyphenation capabilities) and low shear degradation, FFF as an analytical technique in multidimensional fractionation protocols has not received much attention.

To date, a limited amount of research has been published on the coupling of channel-based fractionation techniques in a multidimensional configuration with column-based chromatography techniques. The theoretical potential of coupling various FFF techniques to chromatographic techniques was first discussed by Calvin Giddings, the pioneer of FFF [62]. The first attempt to support Giddings' theory was the off-line coupling of SEC and ThFFF by van *Asten et al*. [63]. The study demonstrated that the off-line multidimensional technique developed, could successfully determine the chemical composition as a function of molecular mass of copolymers of butadiene-methyl methacrylate and styrene-methyl methacrylate and polymer blends of poly(styrene) blended with poly(butadiene) and poly(tetrahydrofuran). *Van Asten et al.* proposed that either FlFFF or hydrodynamic chromatography (HDC) could be used as an alternative method to SEC in this off-line technique. This statement of van *Asten et al.* was confirmed by *Venema et al.* [64] who successfully performed online coupling of ThFFF and HDC to characterize poly(isoprene) homopolymers and styrene-acrylonitrile copolymers. ThFFF was used as the first dimension and HDC was used in the second dimension to characterize the polymer fractions according to hydrodynamic size. The fractions subjected to the second dimension were obtained via the 'heart-cutting' fractionation method. This means that only a small portion of the total eluate was transferred to the second dimension. The study showed that the online coupling of ThFFF to HDC in a multidimensional configuration could be effective for the characterization of complex polymers. To our knowledge, the latest advancement in coupling of column- and channel-based techniques is the online coupling of AsFlFFF to reversed-phase liquid chromatography (RP-LC) in a comprehensive multidimensional configuration by *Yohannes et al.* [65]. It was shown that online AsFlFFF x RP-LC could characterize biopolymers such as egg white protein. The multidimensional technique was concluded to be robust, simple and easy to use for the comprehensive characterization of the protein with regard to physicochemical characteristics such as hydrophobicity and size.

Despite the advancement made in polymer characterization techniques, the characterization of complex polymers remains a challenge due to the interdependence of the various molecular property distributions. Therefore, one of the key aims of the work presented herein was to couple ThFFF to a chromatographic separation technique such as SEC in a comprehensive online multidimensional configuration as illustrated in **Fig. 2.6**. By coupling the two complementary separation techniques, compositional and molecular size information can be obtained at the same

time with the aid of information-rich detectors. The coupling of ThFFF, in which separation is driven by the translational and thermal diffusion coefficients, with SEC, in which separation is governed by the hydrodynamic size, makes this multidimensional analytical technique ideally suited for the characterization of complex polymer assemblies such as block copolymers and micelles [24, 58].

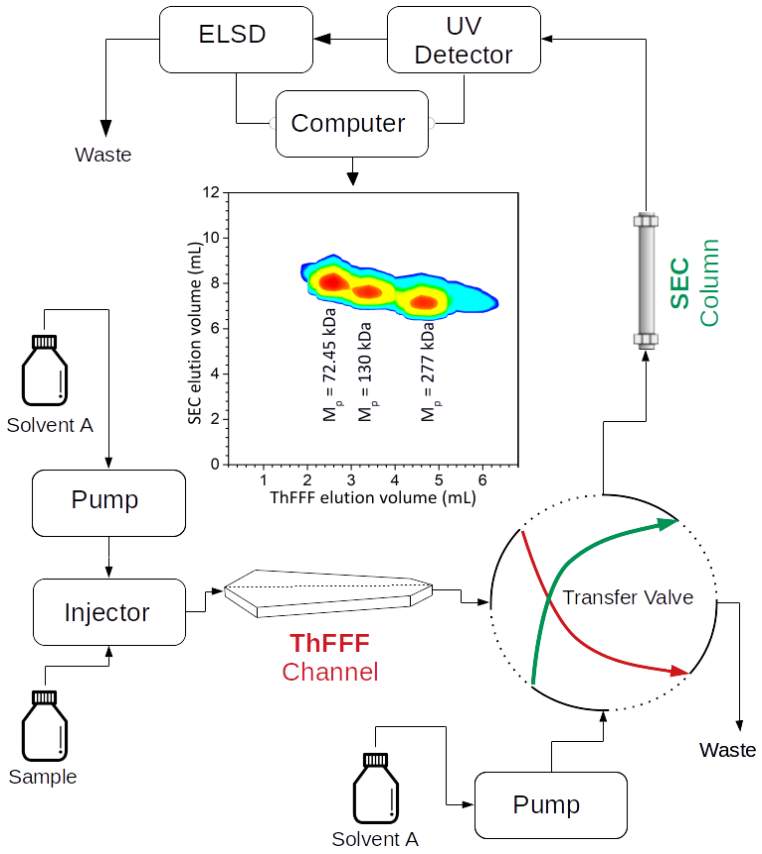

Figure 2.6 Schematic illustration of the comprehensive online coupling of ThFFF with SEC in a multidimensional configuration.

2.4. Detection methods

The aim of any analysis is to identify, verify and attain quantitative and/or graphical presentation of the molecular heterogeneity of a complex polymer, which can only be acquired with the aid of a proper detection approach. The detection of an analyte (solute) after being subjected to a separation technique is as important as deciding which selective type of separation method to use for analysis. A multiple detection approach is required to characterize complex polymers that exhibit various distributed properties as it can provide valuable information on the concentration, chemical composition and molecular mass of the analyte. This approach has become the general practice as information on the different molecular heterogeneities of the polymeric sample can be attained in a single analysis [1, 3, 6]. Detectors are required to be sensitive, selective, specific to a specific

property or parameter, and are in some cases non-destructive to the analyte, especially in a multiple detection configuration. The detectors and the sophisticated software required to record the detector signal produced are in many cases considered the most expensive and valued components of the analytical system configuration.

Detectors can be divided into selective, universal and molecular mass detectors (refer to **Table 2.2**). Generally, for the characterization of complex polymers a multiple detection approach is used i.e. selective detectors are coupled with universal detectors and in some cases in conjunction with molecular mass-sensitive detectors, or concentration detectors with molecular mass detectors [1, 3,6]. Two typical combinations for detector coupling to an analytical separation technique are, (1) a selective detector with a universal detector e.g. ultraviolet (UV) detector and differential refractive index (dRI) detector and, (2) a concentration detector with a molecular mass-sensitive detector such as light scattering detector for instance dRI and multiangle laser light scattering (MALLS). Molecular mass-sensitive detectors such as MALLS, dynamic light scattering (DLS) and viscometers, are capable of determining branching, molecular size, and confirmation as a function of molecular mass in a single analysis [1]. An alternative detection approach is the hyphenation of spectroscopic methods (NMR, Quadruple MS, MALDI-TOF MS, FTIR) to the column- and channel-based analytical technique for more advanced characterization of polymeric materials.

Table 2.2 Classification of detectors

Selective Detectors	**Universal Detectors**	**Molecular Mass Detectors**
Ultraviolet (UV) detector	Refractive index (RI) detector	Viscometry detectors - single capillary, differential
Infrared detector (FTIR)	Evaporative light scattering detector (ELSD)	Light scattering detectors - LALLS, MALLS
Nuclear Magnetic Resonance (NMR)	Density detector	Mass spectrometry - MALDI-TOF MS, ESI-MS
Fluorescence detector	Conductivity detector	
Electrochemical detector		

2.4.1. Differential refractive index detector

The operating principle of a dRI detector is based on the phenomenon that a solute will alter the refractive index of a solvent based on the solute's concentration and the solute's own refractive index [66, 67]. The following is a summarization of the basic operating condition of a dRI detector. Firstly, during operation, eluent passes through the reference flow cell continuously which serves as the baseline to which the detector flow cell is compared. Once the analyte elutes, it flows through the detector flow cell, altering the refractive index of the carrier liquid in which it is present. The difference in refractive indices between the reference cell and the detector flow cell is what constitutes the detection signal. The degree to which the refractive index is altered by the analyte is governed by a multitude of factors such as the chemical nature of the analyte, the analyte concentrations and the optical nature of analyte [66, 67]. Although the optical interactions that an analyte may have with a solvent are complex, dRI remains an important detector available to separation techniques with the only drawback being the limited sensitivity [66, 67]. The dRI detector is a good alternative concentration detector for polymeric samples that do not contain UV-active chromophores.

2.4.2. Ultraviolet detector

The detection principle of a UV detector is based on measuring the transmittance and/or absorbance at a given wavelength as a result of specific chromophore species of the analyte [66, 67]. An UV detector is an effective method for the determination of the concentration of a solute, since the Beer-Lambert law correlates the attenuation of the light to the concentration [66, 67]. Although a UV detector is considered versatile and efficient, it has a limited scope of use as it can only be used for polymers that contain a UV-active chromophore (at a given detector wavelength).

2.4.3. Evaporative light scattering detector

ELSD is a suitable universal concentration detector that operates irrespective of the chemical composition of the analyte or solvent and is a very sensitive detection method. ELSD is based on the principle that when an analyte of a given size passes through a light beam, it will scatter light [66, 68]. To summarize the basic operating condition of an ELSD, the eluent containing the analyte flows into a nebulizer chamber and is finely dispersed into droplets. The droplets travel along a drift-tube, which is heated above the boiling point of the carrier liquid. Once exposed to the heated drift-tube, the volatile carrier liquid evaporates while the non-volatile analyte species remain and form particles. The analyte particles move through a light beam and the scattered light from the analyte

particles is detected as a signal [66,68]. ELSD is a well suited detection method for multidimensional analysis as it can be used for both isocratic and gradient elution analysis in HPLC. However, the major drawback of an ELSD is that it is a destructive analysis method from which the sample cannot be recovered.

2.4.4. Multiangle laser light scattering

A MALLS detector is classified as an absolute detector that can directly determine molecular mass and radius of gyration (R_g) without the need of calibration relative to polymer standards when coupled with a concentration detector. The basic principle of a MALLS detector is based on the measuring of the average intensity fluctuations of the scattered light as a function of time. When the eluent containing the analyte passes through the beam, the analyte scatters light in reference to the incident light, which is the measured at multiple scattering angles (θ). Thus, a MALLS detector measures the angular dependency of the scattered light intensity [66, 69]. With the aid of a concentration detector the refractive index increments with concentration ($\frac{d_n}{d_c}$) can be acquired. The data obtained from both the light scattering detector and the concentration detector are processed by using either the Debye or Zimm model to plot the angular dependence of the scattered light to calculate the R_g value and molecular mass [66, 69].

2.4.5. Dynamic light scattering

DLS is a fast method to determine the average size of the bulk of a polymer sample in solution. The measurements are conducted at one detector angle (backscattering angle of 173°) and provide the z-average size of the polymer in solution. DLS is based on the principle of measuring the diffusion rate of an analyte in solution due to Brownian motion [70]. Brownian motion causes a fluctuation in the intensity of the scattered light, which is then measured. The size of the polymer in solution is then calculated using the Stokes-Einstein equation (**eq. 2.6**) which correlates the diffusion coefficient to the hydrodynamic diameter. As DLS only provides the average fluctuations of the scattered light intensity of the bulk of the polymer sample, information regarding the size distribution cannot be obtained. Additionally, information can be lost with regard to smaller molecules present in the sample [70]. DLS can be coupled online to a separation technique as a detector or can be used off-line as a stand-alone instrument.

References

[1] H. Pasch, Hyphenated separation techniques for complex polymers, Polym. Chem. 4 (2013) 2628–2650.

[2] H. Pasch, B. Trathnigg, HPLC of Polymers, Springer-Verlag: Berlin, Germany, 1999.

[3] G. Glöckner, Polymer Characterization by Liquid Chromatography, Elsevier Science Publisher, Amsterdam, The Netherlands, 1987.

[4] H. Pasch, Advanced fractionation methods for the microstructure analysis of complex polymers, Polym. Adv. Technol. 26 (2015) 771–784.

[5] J.M. Chalmers, R.J. Meier, (Ed) Comprehensive Analytical Chemistry - Molecular Characterization and Analysis of Polymers, Elsevier, Amsterdam, The Netherlands, 2008.

[6] D. Campbell, R.A. Pethrick, J.R. White, Polymer Characterization: Physical Techniques, Stanley Thornes (Publishers) Ltd, United Kingdom, 2000.

[7] J.C Giddings, F.J.F. Yang, M.N Myers, Flow field-flow fractionation: A versatile new separation method. Science. 193 (1976) 1244-1245.

[8] F.A. Messaud, R.D. Sanderson, J.R. Runyon, T. Otte, H. Pasch, S.K.R. Williams, An overview on field-flow fractionation techniques and their applications in the separation and characterization of polymers, Prog. Polym. Sci. 34 (2009) 351–368.

[9] M.I. Malik, H. Pasch, Field-flow fractionation: New and exciting perspectives in polymer analysis, Prog. Polym. Sci. 63 (2016) 42–85.

[10] J.C. Giddings, Field-flow fractionation: analysis of macromolecular, colloidal, and particulate materials, Science. 260 (1993) 1456–1465.

[11] W. Radke, J. Falkenhagen, Liquid Interaction Chromatography, in: S. Fanali, P.R. Haddad, C.F. Poole, P. Schoenmakers, D. Lloyd (Eds.), Liquid chromatography, Elsevier: Amsterdam, The Netherlands; (2013) 93–129.

[12] W. Radke, Polymer separations by liquid interaction chromatography: Principles – prospects – limitations, J. Chromatogr. A. 1335 (2014) 62–79.

[13] D. Held, P. Kilz, Characterization of polymers by liquid chromatography, Macromol. Symp. 231 (2006) 145–165.

[14] M.E. Schimpf, K. Caldwell, J.C. Giddings, Field-Flow Fractionation Handbook, John Wiley and Sons: New York, USA, 2000.

[15] Y.S. Gao, K.D. Caldwell, M.N. Myers, J.C. Giddings, Extension of thermal field-flow fractionation to ultra-high (20 x 106) molecular weight polystyrenes. Macromolecules. 18:6 (1985) 1272–1277.

[16] S.K.R. Williams, J.R. Runyon, A.A. Ashames, Field-Flow Fractionation: Addressing the Nano Challenge, Anal. Chem. 83 (2011) 634–642.

[17] M.H. Moon, J.C. Giddings, Size distribution of liposomes by flow field-flow fractionation. J. Pharmaceut. Biomed. 11 (1993) 911-920.

[18] M. Baalousha, B. Stolpe, J.R. Lead, Flow field-flow fractionation for the analysis and characterization of natural colloids and manufactured nanoparticles in environmental systems: A critical review, J. Chromatogr. A. 1218 (2011) 4078-4103.

[19] P. Reschiglian, A. Zattoni, B. Roda, E. Michelini, A. Roda, Field-flow fractionation and biotechnology, Trends Biotechnol. 23, 475 (2005).

[20] S.K.R. Willliams, D. Lee, Field-flow fractionation of proteins, polysaccharides, synthetic polymers, and supramolecular assemblies, J. Sep. Sci., 29 (2006) 1720.

[21] K.-G. Wahlund, Flow field-flow fractionation: Critical overview, J. Chromatogr. A, 1287 (2013) 97-112.

[22] T. Kowalkowski, B. Buszewski, C. Cantado, F. Dondi, Field-flow fractionation: theory, techniques, applications and the challenges, Crit. Rev. Anal. Chem., 36 (2006), 129-135

[23] W. Fraunhofer, G. Winter, The use of asymmetrical flow field-flow fractionation in pharmaceutics and biopharmaceutics, Eur. J. Pharm. Biopharm. 58, 369 (2004).

[24] G. Greyling, H. Pasch, Thermal Field-Flow Fractionation of Polymers, Springer-Verlag: Heidelberg, Germany, 2019.

[25] J.J. Gunderson, K.D. Caldwell, J.C. Giddings, Influence of temperature gradients on velocity profiles and separation parameters in thermal field-flow fractionation. Sep. Sci Technol, 19:10 (1984) 667-683.

[26] M.E. Schimpf, J.C. Giddings, Characterization of thermal diffusion of copolymers in solution by thermal field-flow fractionation, J. Polym. Sci. Part B Polym. Phys. 28 (1990) 2673–2680.

[27] J.J. Gunderson, J.C. Giddings, Chemical composition and molecular-size factors in polymer analysis by thermal field-flow fractionation and size exclusion chromatography, Macromolecules. 19 (1986) 2618–2621.

[28] D. Melucci, C. Contado, I. Mingozzi, M. Hoyos, M. Martin, F. Dondi, Evaluation of the Soret coefficient for polystyrene in decalin by means of thermal field-flow fractionation, J. Liq. Chrom. & Rel. Technol. 23 (2000) 2067–2082.

[29] E.P.C. Mes, W. Th. Kok, R. Tijssen, Prediction of polymer thermal diffusion coefficients from polymer-solvent interaction parameters: comparison with thermal field flow fractionation and thermal diffusion forced rayleigh scattering experiments, Int. J. Polym. Anal. Charact. 8 (2003) 133–153.

[30] C. van Batten, M. Hoyos, M. Martin, Thermal Field-Flow Fractionation of Colloidal Materials: Methylmethacrylate-Styrene Linear Di-Block Copolymers, Chromatographia. 45 (1997) 121–126.

[31] C.A. Ponyik, D.T. Wu, S.K.R. Williams, Separation and composition distribution determination of triblock copolymers by thermal field-flow fractionation, Anal. Bioanal. Chem. 405 (2013) 9033–9040.

[32] G. Greyling, H. Pasch, Characterisation of block copolymer self-assemblies by thermal field-flow fractionation, Polym. Int. 66 (2017) 745–751.

[33] U.L. Muza, G. Greyling, H. Pasch, Characterization of complex polymer self-assemblies and large aggregates by multidetector thermal field-flow fractionation, Anal. Chem. 89 (2017) 7216–7224.

[34] U.L. Muza, G. Greyling, H. Pasch, Core microstructure, morphology and chain arrangement of block copolymer self-assemblies as investigated by thermal field-flow fractionation. J. Chromatogr. A. 1562 (2018) 87–95.

[35] G. Greyling, H. Pasch, Multidetector thermal field-flow fractionation as a unique tool for the tacticity-based separation of poly(methyl methacrylate)-polystyrene block copolymer micelles. J. Chromatogr. A. 1414 (2015) 163–172.

[36] G. Greyling, H. Pasch, Multidetector thermal field-flow fractionation: a unique tool for monitoring the structure and dynamics of block copolymer micelles. Macromolecules. 49 (2016) 1882–1889.

[37] G. Greyling, H. Pasch, Tacticity separation of poly(methyl methacrylate) by multidetector thermal field-flow fractionation. Anal. Chem. 87 (2015) 3011–3018.

[38] G. Greyling, H. Pasch, Multidetector thermal field-flow fractionation as a novel tool for the microstructure separation of polyisoprene and polybutadiene. Macromol. Rapid. Commun. 35 (2014) 1846–1851.

[39] G. Greyling, H. Pasch, Fractionation of poly(butyl methacrylate) by molecular topology using multidetector thermal field-flow fractionation. Macromol. Rapid. Commun. 36 (2015) 2143–2148.

[40] W. Hiller, W. van Aswegen, M. Hehn, H. Pasch, Online ThFFF–NMR: A Novel tool for molar mass and chemical composition analysis of complex macromolecules, Macromolecules 46 (2013) 2544–2552.

[41] G. Yohannes, M. Jussila, K. Hartonen, M.-L., Riekkola, Asymmetrical flow field-flow fractionation technique for separation and characterization of biopolymers and bioparticles, J. Chromatogr. A. 1218 (2011) 4104-4116.

[42] K.-G, Wahlund, J.C. Giddings, Properties of an asymmetrical flow field-flow fractionation channel having a permeable wall. Anal. Chem. 59 (1987) 1332-1339.

[43] H. Cölfen, M. Antonietti, Field-flow fractionation techniques for polymer and colloid analysis. In: Schmidt M. (eds) New Developments in Polymer Analytics I. Advances in Polymer Science (150), Springer, Berlin, Heidelberg, 2000.

[44] M. Wagner, C. Pietsch, L. Tauhardt, A. Schallon, U.S. Schubert, Characterization of cationic polymers by asymmetric flow field-flow fractionation and multi-angle light scattering - A comparison with traditional techniques. J. Chromatogr. A. 1325 (2014) 195-203.

[45] J. Ehrhart, A.-F. Mingotaud, F. Violleau, Asymmetrical flow field-flow fractionation with multi-angle light scattering and quasi elastic light scattering for characterization of poly(ethylene glycol-b-ε-caprolactone) block copolymer self-assemblies used as drug carriers for photodynamic therapy. J. Chromatogr. A. 1218:27 (2011) 4249–4256.

[46] J. Otte, H. Pasch, T. Macko, R. Brüll, F.J. Stadler, J. Kaschta, F. Becker, M. Buback, Characterization of branched ultrahigh molar mass polymers by asymmetrical flow field-flow fractionation and size exclusion chromatography. J. Chromatogr. A. 1218:27 (2011) 4257-4267.

[47] C. Zielke, C. Fuentes, L. Piculell, L. Nilsson, Co-elution phenomena in polymer mixtures studied by asymmetric flow field-flow fractionation. J. of Chromatogr. A. 1532 (2018) 251-256.

[48] H. Pasch, A.C. Makan, H. Chirowodza, N. Ngaza, W. Hiller, Analysis of complex polymers by field-flow fractionation. Anal. Bioanal. Chem. 406 (2014) 1585-1596

[49] A.C. Makan, R.P. Williams, H. Pasch, Field flow fractionation for the size, molar mass and gel content analysis of emulsion polymers for water-based coatings. Macromol. Chem. Phys. 217 (2016) 2027-2040.

[50] H. Pasch, B. Trathnigg, Multidimensional HPLC of Polymers, Springer-Verlag: Heidelberg, Germany, 2013.

[51] A. van der Horst, P.J. Schoenmakers, Comprehensive two-dimensional liquid chromatography of polymers. J. of Chromatogr. A, 1000(1-2) (2003) 693-709.

[52] D. Berek, Strategies in two-dimensional liquid chromatographic separation of complex polymer systems. Macromol. Symp. 174 (2001) 413-434.

[53] B.W.J. Pirok, A.F.G. Gargano, P.J. Schoenmakers, Optimizing separations in online comprehensive two-dimensional liquid chromatography, J. Sep. Sci. 41 (2018) 68–98.

[54] B. Trathnigg, S. Abrar, Characterization of complex copolymers by two-dimensional liquid chromatography, Procedia Chem. 2 (2010) 130–139.

[55] I. François, K. Sandra, P. Sandra, Comprehensive liquid chromatography: Fundamental aspects and practical considerations – A review, Anal. Chim. Acta. 641 (2009) 14–31.

[56] D. Berek, Two-dimensional liquid chromatography of synthetic polymers. Anal. Bioanal. Chem. 396 (2010) 421-441.

[57] I. Teraoka, Calibration of retention volume in size exclusion chromatography by hydrodynamic radius. Macromolecules. 37:17 (2004) 6632-6639.

[58] Chi-San Wu, ed. Handbook Of Size Exclusion Chromatography And Related Techniques: Revised And Expanded, Marcel Dekker, Inc., New York, 2003.

[59] A.M. Striegel, J.J. Kirkland, W.W. Yau, D.D. Bly, Modern Size Exclusion Chromatography. Practice of Gel Permeation and Gel Filtration Chromatography, Wiley, New York, 2009.

[60] Y.-C. Guillaume, J.-F. Robert, C. Guinchard, A mathematical model for hydrodynamic and size exclusion chromatography of polymers on porous particles. Anal. Chem. 73 (2001) 3059-3064.

[61] S. Mori, H.G. Barth, Size exclusion chromatography. Springer-Verlag, Berlin, Heidelberg, 1999.

[62] J.C. Giddings, Two-dimensional field-flow fractionation, J. Chromatogr. 504 (1990) 247–258.

[63] A.C. van Asten, R.J. van Dam, W. Th. Kok, R. Tijssen, H. Poppe, Determination of the compositional heterogeneity of polydisperse polymer samples by the coupling of size-exclusion chromatography and thermal field-flow fractionation, J. Chromatogr. A. 703 (1995) 245–263.

[64] E. Venema, P. de Leeuw, J.C. Kraak, H. Poppe, R. Tijssen, Polymer characterization using online coupling of thermal field-flow fractionation and hydrodynamic chromatography, J. Chromatogr. A. 765 (1997) 135–144.

[65] G. Yohannes, S.K. Wiedmer, J. Hiidenhovi, A. Hietanen, T. Hyötyläinen, Comprehensive two-dimensional field-flow fractionation-liquid chromatography in the analysis of large molecules, Anal. Chem. 79 (2007) 3091–3098.

[66] M. Swartz, HPLC Detectors: A brief review, J. Liq. Chromatogr. R.T. 33 (2010) 1130-1150.

[67] A.D. Williams, UV and dRI detectors in liquid chromatography: The workhorse detectors, J. Chromatogr. Sci. 24 (1986) 495-498.

[68] N.C. Megoulas, A.M. Koupparis, Twenty years of evaporative light scattering detection, Crit. Rev. Anal. Chem. 35:4 (2005) 301-306.

[69] A. Olivia, M. Llabrés, J.B. Farina, Application of multi-angle laser light-scattering detection in the analysis of peptides and proteins. Curr. Drug Discov. Technol. 1:3 (2004) 229-242.

[70] B.J. Berne, R. Pecora, Dynamic Light Scattering: With Applications to Chemistry, Biology, and Physics, Dover Publications, Inc. New York, 2000

CHAPTER 3

TWO-DIMENSIONAL FRACTIONATION OF COMPLEX POLYMERS BY COMPREHENSIVE ONLINE-COUPLED THERMAL FIELD-FLOW FRACTIONATION AND SIZE EXCLUSION CHROMATOGRAPHY

3.1. Introduction

The concept of comprehensive online coupling of thermal field-flow fractionation (ThFFF) with size exclusion chromatography (SEC), including the fractionation and characterization of PS-***b***-PMMA block copolymers to illustrate the capabilities of this multidimensional separation approach, was published recently (Analytica Chimica Acta, 1107 (2020), 225-232) as enclosed. The purpose of the study, alongside the key points, results and conclusions are highlighted in the following overview summary:

Complex polymers are viewed as heterogeneous with regard to their molecular properties (e.g. molecular mass, chemical composition, functionality and topology), which are typically broadly distributed. The various molecular distributions are interrelated and influence the structural and physical properties of the given polymeric material and, hence, the end-use applications. To this end, advanced characterization tools have been developed over the years, in particular multidimensional analytical techniques. The coupling of two separation techniques in a multidimensional configuration, allows for the efficient and comprehensive characterization of complex polymers with regard to their different molecular distributions and their correlations.

The focus of the present study was to explore and introduce the concept of comprehensive online coupling of a channel-based fractionation technique, such as ThFFF, with a column-based technique, such as SEC, in a multidimensional configuration. ThFFF separating based on the interaction between thermal (D_T) and translational diffusion (D), which relates to the chemical composition of the analyte, was used in the first dimension. SEC was used in the second dimension, which separated the fractions that were comprehensively transferred from the first dimension, according to hydrodynamic diameter. From a hardware and configuration perspective, the set-up is quite simple, requiring only the coupling of two analytical instruments via an electronically controlled device, such as a switching valve. Even though a multidimensional analysis can yield a wealth of information, the result analysis remains inherently complicated. In comprehensive multidimensional analysis, the experimental parameters are interrelated i.e. the flow rate of the second dimension determines the flow rate of the first dimension, the rate and time at which the fractions are collected from the first dimension, transferred and fractionated in the second dimension. Hence, the online coupling of two fundamentally different techniques requires the optimization of the experimental conditions used in each separation dimension as well as when coupled together online. Optimization of the coupled system is especially important when comprehensive analysis is carried out i.e. when the entirety of the collected fractions in the first dimension is transferred to the second dimension. Thus, from an

experimental point of view, the coupling of two techniques in comprehensive online configuration requires a thorough and systematic approach.

The first step was to investigate and optimize the experimental parameters that included (1) analysis time, (2) flow rate, (3) applied temperature gradient, (4) analyte concentration to ensure sufficient detection after the second dimension, (5) compatibility of the carrier liquid used in both separation dimensions and (6) appropriate selection of detectors. In order to establish the experimental conditions that were required for the coupling of the two methods and providing evidence for the versatility of the comprehensive online ThFFF X SEC protocol, a range of well-defined poly(styrene) (PS) and poly(methyl methacrylate) (PMMA) homopolymer standards, in combination with poly(styrene)-***b***-poly(methyl methacrylate) (PS-***b***-PMMA) block copolymer standards, were fractionated and analysed. THF was used as the carrier liquid in both dimensions.

One of the primary experimental parameters that needed to be optimized was the analysis time. As ThFFF was used in the first dimension, a practical approach to minimize the analysis time is the way in which the temperature gradient is applied across the ThFFF channel. It was found that when an exponential decay temperature gradient is applied across the channel instead of a constant temperature profile, the analysis time decreased. However, the limitation of this optimization step was that the calculation of the thermal diffusion coefficient becomes complex, as D_T depends on the viscosity and thermal conductivity of the solvent is temperature dependent. Hence, as the applied temperature gradient changes across the channel, the solvent parameters change accordingly. As information regarding the chemical composition was required (that is obtained from D_T) a constant temperature gradient was used. Another key experimental parameter that needed to be addressed was the analyte concentration to ensure a strong detection signal after the second dimension to yield a suitable chromatogram. It was found that channel overloading occurred at a sample concentration of 1.5 $mg.mL^{-1}$ and higher. This was indicated by the peak tailing and unexpected bimodality that were observed in the fractograms of the samples at these concentrations. To eliminate the effects of channel overloading, a sample concentration of 0.5 $mg.mL^{-1}$ for both the homopolymers and block copolymers was used.

To illustrate the capabilities of ThFFF x SEC for the fractionation of complex polymer mixtures, various blends of either PS or PMMA with PS-***b***-PMMA block copolymers were investigated. The first blend investigated consisted of PS (33 $kg.mol^{-1}$) and PS-***b***-PMMA (81 $kg.mol^{-1}$, 33% PS) in order to mimic a reaction mixture that is commonly obtained during the synthesis of a block copolymer by controlled radical polymerization, where small traces of the first block are still present. The results showed that the sample blend could be fractionated by ThFFF. The separation was based on

chemical composition (via D_T) and molecular mass (D) in the first dimension. Thus, by being coupled to SEC, the quality of the results with regard to the molecular mass separation was enhanced due to the synergistic effects of the different fractionation principles. As good separation of the two components was obtained, the concentration of PS could be directly quantified from the ELSD signal. However, this was not the case for the block copolymer as the ELSD trace depends on chemical composition. With SEC used in the second dimension, both the components could be characterized with regard to their molecular mass distributions as separation is based on the hydrodynamic size, which in return correlates to the molecular mass. The second blend investigated was PMMA (60.5 $kg.mol^{-1}$) and PS-***b***-PMMA (124 $kg.mol^{-1}$, 50% PS). The first dimension separation of the two components was insufficient; however with the aid of a dual concentration detector set-up (UV-detector and ELSD), and the use of SEC in the second dimension, it was still possible to characterize the block copolymer with regard to its molecular mass. In the case of inadequate separation, one signal will be observed using the ELS detector that corresponds to both components. However, the UV-detector signal is based on the detection of UV-active chromophores. In this case, PMMA is considered to be optically transparent at the set wavelength of 270 nm and therefore the block copolymer was detected selectively.

It was concluded that the coupled technique has the ability to provide detailed molecular information e.g. chemical composition and molecular mass distribution, as well thermal and translational diffusion information in a single analysis. The study also demonstrated the benefit of hyphenating information-rich detectors, such as a UV-detector and an evaporative light scattering detector (ELSD), to the online ThFFF X SEC technique. In future work, the capabilities of the ThFFF X SEC technique hyphenated with a multidetector set-up will be explored in more detail for the characterization of complex polymers such as polymer self-assemblies.

3.2. Experimental

3.2.1 Materials

Samples of homopolymers and block copolymers were used as received from manufacturers. Polystyrene (PS) and poly(methyl methacrylate) (PMMA) were purchased from PSS Polymer Standards Service GmbH (Mainz, Germany), Polymer Laboratories (now Agilent Inc., Church Stretton, United Kingdom), and Postnova Analytics GmbH (Landsberg, Germany). PS-***b***-PMMA block copolymers were purchased from PSS Polymer Standards Service GmbH (Mainz, Germany). The molecular masses (M_w), hydrodynamic diameters (D_h), translational diffusion coefficients (D), thermal diffusion coefficients (D_T) and Soret coefficients (S_T) of each polymer sample are tabulated in

Table S1 (refer to Supporting Information of article). HPLC grade tetrahydrofuran (THF) was sourced from Honeywell GmbH (Seelze, Germany) and used as received.

3.2.2. Dynamic Light Scattering (DLS)

A DLS detector (Zen 1600, Malvern Instruments, Worcestershire, United Kingdom) equipped with a glass cuvette was used off-line to obtain hydrodynamic diameter data points for each of the samples. Experiments were conducted at 25°C, with a sample concentration of 0.5 $mg.mL^{-1}$ and THF as solvent.

3.2.3. Analytical Separation Techniques and Conditions

Fractionations in the first dimension were performed using a TF2000 thermal FFF instrument (Postnova Analytics GmbH, Landsberg, Germany) consisting of a channel with a tip-to-tip length of 45.6 cm, breath of 2.0 cm, thickness of 127 mm, and a system void volume of 2.1 mL. Constant temperature gradients (ΔT) of 60°C and 80°C were used to achieve fractionation. The temperature of the cold wall was 24.7 ± 0.2 °C and 27.0 ± 0.1 °C, at the respective ΔT. ThFFF temperature gradient and injection were controlled by Postnova TF2000 Software Version 1.0.0.8 (Postnova Analytics GmbH, Landsberg, Germany). The samples were introduced into the channel via a Rheodyne manual injection valve (Thermo Scientific, Waltham, MA, USA) equipped with a 100 µL capillary sample loop. The flow rate for the first dimension was 0.1 mL min^{-1} and was generated by an Agilent 1200 quaternary pump (G1311A, Agilent Technologies, Waldbronn, Germany). THF was used as carrier liquid in the first dimension. The injected sample volume was 100 µL at a concentration of 0.5 $mg.mL^{-1}$. The samples were dissolved in THF.

The subsequently collected fractions from the first dimension separation were transferred using an electronically controlled Valco eight-port switching valve (VICI Valco Instruments, Waterbury, Houston, TX, USA) equipped with two identical 500 µL storage loops. Each 500 µL fraction was collected, which was then comprehensively transferred online to the second-dimension every 5.0 min, the time required to completely fill one of the loops while the previously collected fraction is comprehensively analysed in the second-dimension (SEC) during this time. During injection, the eluent of the first dimension was comprehensively transferred to the SEC column.

In the second dimension, a PSS-SDV linear M High-Speed column, with a 5 µm average particle size, 50 mm x 20 mm i.d. (PSS Polymer Standards Service GmbH, Mainz, Germany) was used. Separation of samples according to hydrodynamic volume was conducted at ambient temperature with THF as

the isocratic mobile phase. A flow rate of 3.0 mL.min^{-1} was maintained by using an Agilent 1260 isocratic pump (G1310B, Agilent Technologies, Waldbronn, Germany).

An Agilent 1200 variable wavelength detector (UV-Vis) (G1314B, Agilent Technologies, Waldbronn, Germany) in series with an Agilent 1260 Infinity evaporative light scattering detector (ELSD), equipped with a large flow nebulizer, were used for detection. The UV/Vis-detector was set to a wavelength of 270 nm. The ELSD was set to an operating temperature of 100°C and detector sensitivity (gain) of 9. For data acquisition as well as controlling of the pumps (quaternary and isocratic) and transfer valve PSS WINGPC-Unity version 8.1 (PSS Polymer Standards Service GmbH, Mainz, Germany) was used. A Postnova PN3120 refractive index detector (Postnova Analytics GmbH, Landsberg, Germany) was used for the one-dimensional analysis.

Analytica Chimica Acta 1107 (2020) 225–232

Contents lists available at ScienceDirect

Analytica Chimica Acta

journal homepage: www.elsevier.com/locate/aca

Two-dimensional fractionation of complex polymers by comprehensive online-coupled thermal field-flow fractionation and size exclusion chromatography

Zanelle Viktor , Harald Pasch *

Department of Chemistry and Polymer Science, University of Stellenbosch, Private Bag X1, 7602, Stellenbosch, South Africa

HIGHLIGHTS

- As a novel analytical approach, ThFFF has been coupled comprehensively and online with SEC.
- The advantages of ThFFF X SEC for the separation of complex polymers such as PS-***b***-PMMA block co-polymers are demonstrated.
- The developed method simultaneously provides molecular information, the thermal and translational diffusion coefficients.

GRAPHICAL ABSTRACT

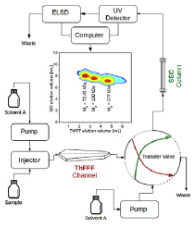

ARTICLE INFO

Article history:
Received 28 November 2019
Received in revised form
8 February 2020
Accepted 15 February 2020
Available online 18 February 2020

Keywords:
Thermal field-flow fractionation
Size exclusion chromatography
Two-dimensional fractionation
Polystyrene-poly(methyl methacrylate) block copolymers

ABSTRACT

Thermal field-flow fractionation (ThFFF) was successfully coupled online to size exclusion chromatography (SEC) in a comprehensive two-dimensional configuration. In the first dimension, fractionation according to chemical composition based on the interplay of thermal and translational diffusion took place in the ThFFF channel. Fractions from the first dimension were comprehensively transferred to the second dimension, SEC, and separated according to hydrodynamic volume which is a function of molar mass. To illustrate the capabilities of this novel two-dimensional fractionation approach, polystyrene-poly (methyl methacrylate) block copolymers were comprehensively fractionated and characterized. Blends of homopolymers, homo- and copolymers, and copolymers with different compositions were fractionated and the effects of experimental conditions, the components' molar masses and compositions were investigated.

The results illustrated the molar mass independence of the thermal diffusion coefficient in ThFFF. Translational diffusion coefficients were quantitatively determined via dynamic light scattering. The study aimed at proving the versatility of the comprehensive online coupling of ThFFF and SEC for the analysis of complex polymers having the ability to provide detailed molecular information (chemical composition and molar mass distribution) as well thermal and translational diffusion information in a single analysis. Finally, the merits of using information-rich detectors are highlighted.

1. Introduction

Complex polymers exhibit molecular compositions with two or more distributions in molecular parameters such as molar mass,

* Corresponding author.
E-mail address: hpasch@sun.ac.za (H. Pasch).

https://doi.org/10.1016/j.aca.2020.02.033
0003-2670/

chemical composition and molecular topology. To address this molecular complexity, over the years two powerful analytical scenarios have emerged, namely (A) the combination of a selective fractionation method with information-rich detectors and (B) the combination of different selective fractionation methods. Both scenarios have been discussed extensively and a large number of applications has been developed [1–3]. Information-rich detectors provide structural information on chromatographic fractions but these fractions are not necessarily homogeneous. For a heterogeneous chromatographic fraction even the most powerful detector can only provide average structural information.

Due to the limitations of one-dimensional fractionation methods, two- and multidimensional fractionation schemes were developed where each single method is selective towards a specific molecular property. Such multidimensional analytical techniques are crucial to obtain information regarding multiple property distributions and the correlation of these distributions preferably in a single analytical analysis [1,4,5].

During multidimensional fractionation, a sample will be subjected to one separation mechanism sensitive to one molecular parameter (e.g. chemical composition), and the subsequently collected fractions will then be subjected to the next separation step (e.g. according to molar mass). Numerous configurations of different separation mechanisms have been combined to obtain valuable information regarding the molecular properties of complex materials [1,2,6,7]. Nearly exclusively, these configurations are based on column chromatographic methods such as liquid interaction chromatography (IC) and size exclusion chromatography (SEC). IC is a well-established technique for the chemical composition separation of complex polymers, where separation is based on the enthalpy-driven (adsorptive) interaction of the analyte with a given stationary phase [1,3,8,9]. SEC is the standard method for molar mass fractionation of polymers. Separation in SEC is entropy-driven and based on molecular size in solution (hydrodynamic volume) in a given solvent and temperature [2,8,9]. The comprehensive coupling of IC and SEC provides dual information on two different molecular parameters, e.g. chemical composition and molar mass that are obtained simultaneously [10].

Another attractive fractionation method for complex polymers, field-flow fractionation (FFF), received much less attention in multidimensional fractionation protocols. FFF is a family of subtechniques that does not use a stationary phase for separation but an empty ribbon-like channel [11,13]. Fractionation is achieved by an external field applied perpendicular to the channel flow, and analytes are fractionated according to different diffusion coefficients that are a function of the molecular composition of the analyte (chemical composition, molar mass, molecular topology) [11,14].

In thermal FFF (ThFFF) the applied field force is obtained by a temperature gradient across the channel between a hot and a cold channel plate. Fractionation is governed by the interplay of the thermal diffusion (D_T) and the translational diffusion (D) coefficients of the analyte molecules [11–14]. The ratio of the two diffusion coefficients is called the Soret coefficient ($S_T = D_T/D$) and is a measure of the retention of a specific analyte molecule.

Due to ThFFF being an open channel-based technique, shear degradation is significantly reduced as compared to column-based fractionations, which provides the capability to characterize complex polymer assemblies such as block copolymers, particles, micelles and aggregates ranging in size from micrometer to nanometer [11,13,15–19]. The physical simplicity, alongside its many experimental advantages (short analysis time, reduced use of solvent, multiple detector capabilities) makes ThFFF an ideal analytical technique to be used in multidimensional configurations [11,13,20].

It is quite surprising that the advanced capabilities of online coupling of column- and channel-based fractionation methods have been investigated so far only for very few cases. The inventor of FFF, Calvin Giddings, was the first to discuss the theoretical possibility of coupling FFF to a chromatographic technique [21]. As a first promising step, van Asten et al. successfully performed the off-line coupling of SEC and ThFFF to fractionate a number of copolymers and polymer blends to study chemical composition as a function of molar mass. They also proposed that this off-line technique could be coupled to flow FFF or hydrodynamic chromatography (HDC) as an alternative to SEC [22]. This was later demonstrated by Venema et al. who used the coupling of ThFFF and HDC to characterize polyisoprene and styrene-acrylonitrile copolymers. HDC was used in the second dimension to characterize the polymer fractions generated by ThFFF according to hydrodynamic volume. The fractions were obtained by 'heart-cutting' and comprised only a small portion of the total samples, thus the fractionation could not be classified as comprehensive [23]. The most recent advancement and (to our knowledge) only truly comprehensive protocol was published by Yohannes et al. who coupled asymmetric field-flow field fractionation (AF4) to a reversed phase LC system to characterize biopolymers such as egg white protein [24].

Despite the advances made over the last decades, the characterization of complex polymers remains a challenge due to the interdependence of the different molecular parameters. In ThFFF, polymers with the same Soret coefficient co-elute regardless of composition and hydrodynamic volume [25–27]. In SEC, analytes with the same hydrodynamic volume co-elute, regardless of chemical composition [9,28]. By coupling ThFFF, which is driven by the translational and thermal diffusion coefficients, with SEC, which is driven by hydrodynamic size, two complementary fractionation methods can be combined that may provide compositional and size information at the same time. It is, therefore, the aim of the present study to explore the experimental conditions that are required for comprehensive online coupling of the two methods. The coupled set-up shall be hyphenated with a UV-detector and an evaporative light scattering detector (ELSD) as two complementary concentration-sensitive detectors. To demonstrate the capabilities of comprehensive online ThFFF x SEC, polystyrene-poly (methyl methacrylate) block copolymers are fractionated and analysed as representative examples.

2. Experimental

2.1. Materials

Samples of homopolymers and block copolymers were used as received from manufacturers. Polystyrene (PS) and poly (methyl methacrylate) (PMMA) were purchased from PSS Polymer Standards Service GmbH (Mainz, Germany), Polymer Laboratories (now Agilent Inc., Church Stretton, United Kingdom), and Postnova Analytics GmbH (Landsberg, Germany). PS-***b***-PMMA block copolymers were purchased from PSS Polymer Standards Service GmbH (Mainz, Germany). The molar masses (M_w), hydrodynamic diameters (D_h), translational diffusion coefficients (D), thermal diffusion coefficients (D_T) and Soret coefficients (S_T) of each polymer sample are tabulated in Table S1 (refer to Supporting Information). HPLC grade tetrahydrofuran (THF) was sourced from Honeywell GmbH (Seelze, Germany) and used as received.

2.2. Dynamic light scattering (DLS)

DLS detector (Zen 1600, Malvern Instruments, Worcestershire, United Kingdom) equipped with a glass cuvette was used off-line to

obtain hydrodynamic diameter data points for each of the samples. Experiments were conducted at 25 °C, with a sample concentration of 0.5 mg mL^{-1} and THF as solvent.

2.3. Separation system and conditions

Fractionations in the first dimension were performed using a TF2000 thermal FFF instrument (Postnova Analytics GmbH, Landsberg, Germany) consisting of a channel with a tip-to-tip length of 45.6 cm, breath of 2.0 cm, thickness of 127 µm, and a void volume of 2.1 mL. Constant temperature gradients (ΔT) of 60 °C and 80 °C were used to achieve fractionation. The temperature of the cold wall was 24.7 ± 0.2 °C and 27.0 ± 0.1 °C, at the respective ΔT. ThFFF temperature gradient and injection were controlled by Postnova TF2000 Software Version 1.0.0.8 (Postnova Analytics GmbH, Landsberg, Germany). The samples were introduced into the channel via a Rheodyne manual injection valve (Thermo Scientific, Waltham, MA, USA) equipped with a 100 µL capillary sample loop. The flow rate for the first dimension was 0.1 mL min^{-1} and was generated by an Agilent 1200 quaternary pump (G1311A, Agilent Technologies, Waldbronn, Germany). THF was used as carrier liquid in the first dimension. The injected sample volume was 100 µL at a concentration of 0.5 mg mL^{-1}. The samples were dissolved in THF.

The subsequently collected fractions from the first dimension separation were transferred using an electronically controlled Valco eight-port switching valve (VICI Valco Instruments, Waterbury, Houston, TX, USA) equipped with two identical 500 µL storage loops. Each 500 µL fraction was collected, which was then comprehensively transferred online to the second-dimension every 5.0 min, the time required to completely fill one of the loops while the previously collected fraction is comprehensively analysed in the second-dimension (SEC) during this time. During injection, the eluate of the first dimension was transferred to the SEC column.

In the second dimension, a PSS-SDV linear M High-Speed column, with a 5 µm average particle size, 50 mm × 20 mm i.d. (PSS Polymer Standards Service GmbH, Mainz, Germany) was used. Separation of samples according to hydrodynamic volume was conducted at ambient temperature with THF as the isocratic mobile phase. A flow rate of 3.0 mL min^{-1} was maintained by using an Agilent 1260 isocratic pump (G1310B, Agilent Technologies, Waldbronn, Germany).

An Agilent 1200 variable wavelength detector (UV/Vis) (G1314B, Agilent Technologies, Waldbronn, Germany) in series with an Agilent 1260 Infinity evaporative light scattering detector (ELSD), equipped with a large flow nebulizer, were used for detection. The UV/Vis-detector was set to a wavelength of 270 nm. The ELSD was set to an operating temperature of 100 °C and detector sensitivity (gain) of 9. For data acquisition as well as controlling of the pumps (quaternary and isocratic) and transfer valve PSS WINGPC-Unity version 8.1 (PSS Polymer Standards Service GmbH, Mainz, Germany) was used. A Postnova PN3120 refractive index detector (Postnova Analytics GmbH, Landsberg, Germany) was used for the one-dimensional analysis. A scheme of the ThFFF x SEC experimental setup is presented in Fig. 1.

3. Results and discussion

3.1. Optimization of experimental parameters

Comprehensive online coupling of two fundamentally different techniques in a multidimensional configuration requires optimization of the experimental conditions used in each separate dimension. Comprehensive analysis, in contrast to off-line and 'heart cut' analysis requires the entirety of the collected fractions

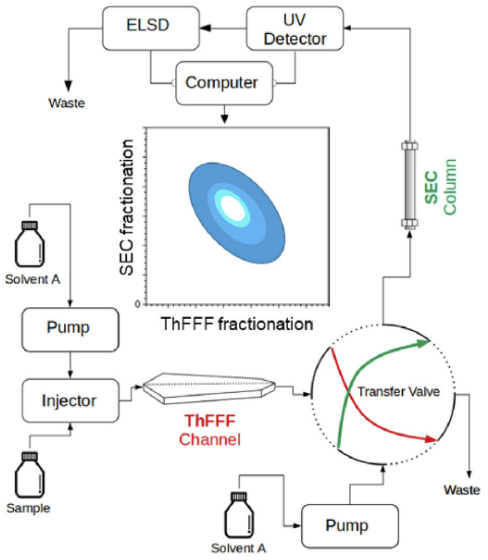

Fig. 1. Schematic presentation of the comprehensive online coupling of ThFFF and SEC.

from the first dimension to be subjected to fractionation in the second dimension. The experimental parameters of each dimension in comprehensive multidimensional analysis are interrelated, meaning the flow rate of the first dimension, the volumetric rate of fraction collection and transfer to the second dimension are dependent on the flow rate of the second dimension. The time required to collect a given fraction from the first dimension is equal to the time required to transfer the fraction and have it fractionated in the second dimension. More details on the optimization of experimental parameters in comprehensive two-dimensional separations can be found in previous publications [2,28].

Thus, the first experimental step was to optimize the analysis time of the first dimension, which in the present case is ThFFF. In ThFFF, analysis time can be adjusted by applying an exponential decay temperature gradient across the channel instead of a constant temperature profile (Fig. 2A). For both cases, bimodal elution profiles were obtained for the block copolymer sample. The limitation of such an optimization step is that the calculation of the thermal diffusion coefficient becomes complex. D_T is generally determined at a constant temperature gradient, i.e at a constant applied force across the channel [27,29]. Once the temperature gradient is decreased over time, solvent parameters that are temperature dependent, such as viscosity and thermal conductivity, change and, subsequently, the applied force on the analytes within the channel also change. Although D_T can be calculated at a constant temperature gradient, it comes at a cost as can be seen in Fig. 2A. Longer analysis time is required for high molar mass polymers and consequently band broadening of peaks is seen. An exponential decay temperature can be used if only separation of the analyte is required and information on chemical composition is not to be obtained from D_T but via information-rich detectors. For this work, D_T was required and thus a constant temperature gradient was used. In a more general consideration, of course a dependency of the translational diffusion coefficient on temperature exists. However, detailed knowledge of this dependency is not required for the studies carried out in this work as separation is governed

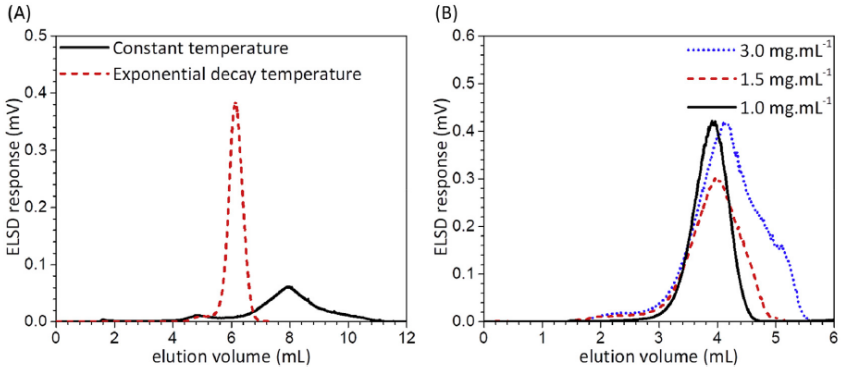

Fig. 2. (**A**) Superimposed fractograms of PS-b-PMMA (407 kg mol^{-1}) analysed at a constant temperature gradient profile of $\Delta T = 60$ °C (**black solid line**) versus an exponential decay temperature program consisting of a constant $\Delta T = 60$ °C for 40 min, an exponentially decay (0.4) over 20 min from 60 °C to 0 °C and kept constant at 0 °C for 15 min (**red dash line**), sample concentrations of 0.5 and 1.0 mg mL^{-1}, respectively.(**B**) Superimposed fractograms of PS (M_p = 130 kg mol^{-1}) at various injected sample concentrations. (For interpretation of the references to colour in this figure legend, the reader is referred to the Web version of this article.)

primarily by the difference in Soret coefficients. In many cases it is practically not possible to mimic the conditions in the channel, especially if working with a low boiling point solvent such as THF. Thus for practical reasons, when the D_h of the polymer in solution is measured by off-line DLS, it is conducted at 25 °C. The measured D_h is used, in turn, to calculate D, which is used in the simplified equation for the calculation of D_T, as provided in the supporting information.

Another approach to optimize analysis time is to work at optimal flow rates. Several studies have reported that separation in ThFFF is not influenced by the flow rate [27,30]. It was, thus, decided that a flow rate of roughly 0.1 mL min^{-1} would be the optimum for the first dimension. This flow rate is sufficiently low to ensure that fractions collected from the first dimension have adequate time to do the SEC separation in the second dimension.

The next challenge to address was the detection limit after the second dimension. Band broadening is amplified during multiple separation steps resulting in reduced local analyte concentrations that might be too low for the given detector to yield a suitable chromatogram. However, sufficiently high detector signals are necessary for the detection of all sample components. In order to mitigate these effects, injected analyte concentrations must be sufficiently high to ensure proper detection and quantification. The injected sample concentration was increased but as can be seen in Fig. 2B, channel overloading can occur as indicated by peak tailing and unexpected bimodality (see e.g. at a concentration of 3 mg mL^{-1}). To eliminate the effects of channel overloading, concentrations of 0.5 mg mL^{-1} for both the homopolymers and block copolymers were used that still provided sufficiently strong detector signals.

Additional experimental parameters that were optimized in the first dimension (ThFFF) were those relating to temperature and the relaxation time. It was found that in instances where the difference in Soret coefficient was small, an increase in temperature improved separation due to a larger difference in the Soret coefficients. Increasing the relaxation time from 2 to 7 min improved the separation as a result of the analytes' molecules being allowed more time to reach individual equilibrium heights along the transverse direction of the temperature gradient. Separation in ThFFF can further be enhanced by the choice of solvent as the thermal diffusion coefficient is dependent on both the chemical composition of the polymer and the solvent. However, a discussion of solvent effects is beyond the scope of this work. A comprehensive discussion regarding optimization of ThFFF experimental parameters can also be found in literature [11,27,30].

3.2. Two-dimensional separation of a PS blend

As the next experimental step, the new two-dimensional ThFFF x SEC was tested with a blend of three PS homopolymers as is shown in Fig. 3. This experiment was simply to prove that the online coupled ThFFF X SEC experimental set-up worked. For this reason, the initial experiment was conducted at a flow rate of 0.08 mL min^{-1} with an exponential decay temperature program in the first dimension as given in Fig. 3. The one-dimensional separation of the blend by ThFFF alone is presented in Fig. 3A.

The contour diagram in Fig. 3B represents the two-dimensional fractionation of the PS blend with ThFFF x SEC. In the contour diagram, the horizontal axis corresponds to the ThFFF fractionation and the vertical axis to the SEC separation. The order of the eluting peaks in ThFFF corresponds to increasing molar masses as is expected. Separation in ThFFF is governed by the D_T/D ratio (Soret coefficient). It has been found that D_T for similar polymers is independent of molar mass for high molar mass samples. Therefore, when polymers of the same structure are fractionated by ThFFF, retention is governed by the change in D which is molar mass dependent [31]. In this case, the fractionation in ThFFF which is a function of the translational diffusion coefficient corresponds well with the separation in SEC being a function of hydrodynamic size which is used as the second dimension. Accordingly, in the second dimension the highest molar mass PS elutes first followed by the samples of lower molar masses.

3.3. Two-dimensional separation of blends of homopolymer and block copolymers

When block copolymers are prepared via sequential controlled radical polymerization, frequently small amounts of the first block are still present in the reaction mixture. The SEC separation of such complex mixtures depends on the relative molar masses of the first block and the block copolymer. Alternatively, such samples can be fractionated by ThFFF where chemical compositions (via D_T) and molar masses (via D) influence the quality of the result. When this type of fractionation is coupled to SEC as a complementary

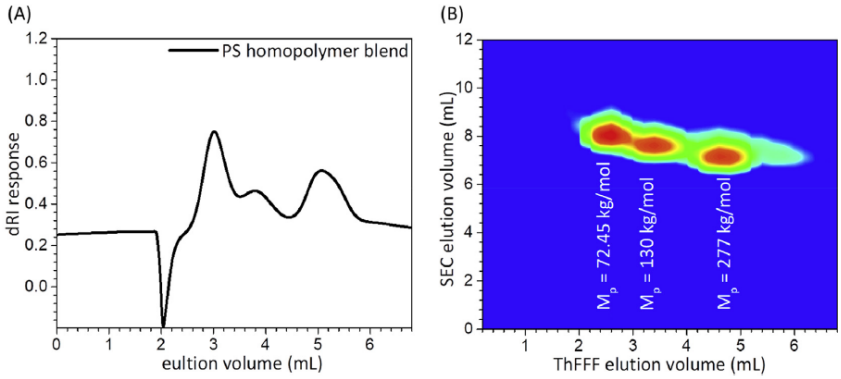

Fig. 3. (**A**) ThFFF fractogram of the one-dimensional analysis of a blend of PS homopolymers under the same experimental conditions as used in ThFFF x SEC. (**B**) ThFFF x SEC contour diagram of PS homopolymer blend. First dimension: flow rate 0.08 mL min^{-1}, cold wall 23.8 °C, temperature gradient 50 °C for 40 min then decreased over 20 min to 0 °C (power decay = 0.4) and kept constant for 15 min. Second dimension: flow rate 4.8 mL min^{-1}, ambient temperature, column SDV High-Speed Linear M, transfer loops 200 µL. Detector ELSD.

technique, the quality of the result can be enhanced due to the synergistic effects of the different fractionation principles.

To investigate the capabilities of ThFFF x SEC for the fractionation of complex polymer mixtures, various blends of either PS or PMMA with PS-***b***-PMMA block copolymers were investigated. THF, a thermodynamically good solvent for both PS and PMMA, was used as the mobile phase in both dimensions. The superimposed ELS-detector fractograms of PS, PS-***b***-PMMA and the corresponding blend are presented in Fig. 4A. A proper separation of the two components is obtained and the concentration of PS can directly be quantified from the ELSD trace. For the quantification of the block copolymer a more complex procedure is required since the ELSD signal intensity depends on the copolymer composition. The molar mass of PS could be determined from S_T which is not the case for the copolymer since S_T in this case depends on molar mass (via D) and composition (via D_T). For the analysis of the molar masses of both components, SEC is used where separation is based on hydrodynamic sizes which can be directly correlated to molar masses. The contour diagram of the blend separation is presented in Fig. 4B. As can be seen, both components can be identified readily in both dimensions.

In the same context, a blend of PMMA and PS-***b***-PMMA was fractionated by ThFFF x SEC. In this case, the components were less perfectly separated in the ThFFF dimension, see Fig. 5A, making it difficult to determine the concentrations and molar masses just by ThFFF. SEC in the second dimension improves the separation and, therefore, the molar mass analysis of the blend components becomes more feasible, see Fig. 5B.

A different (and more powerful) way to quantify the blend components is using dual concentration detection after the two-dimensional fractionation. As has been shown before, ELSD is a suitable universal concentration detector that works irrespective of the chemical composition of the analyte. In contrast, a UV detector can only detect the UV-active chromophores (at a given

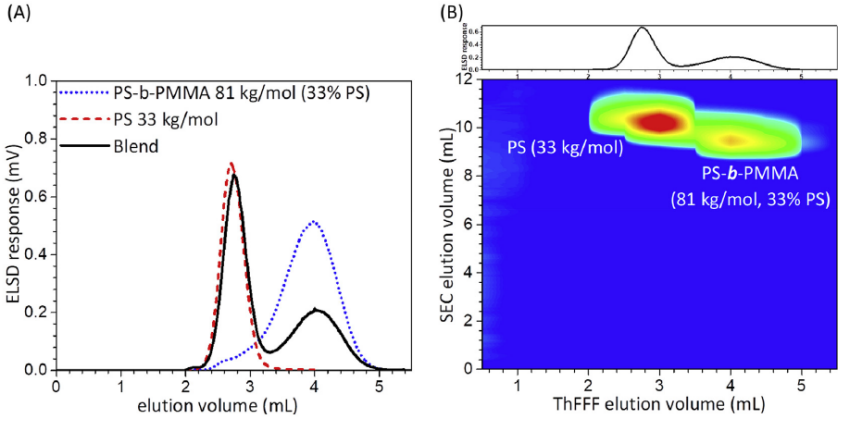

Fig. 4. (A) Superimposed ELSD fractograms of PS (33 kg mol^{-1}), PS-***b***-PMMA (81 kg mol^{-1}, 33% PS) and the corresponding blend. (B) ThFFF x SEC contour diagram of the blend of PS and PS-*b*-PMMA. First dimension: flow rate 0.10 mL min^{-1}, T_c = 24.7 °C, ΔT = 60 °C. Second dimension: flow rate 3.0 mL min^{-1}, ambient temperature, column SDV High-Speed Linear M, transfer loops 500 µL. Detector ELSD.

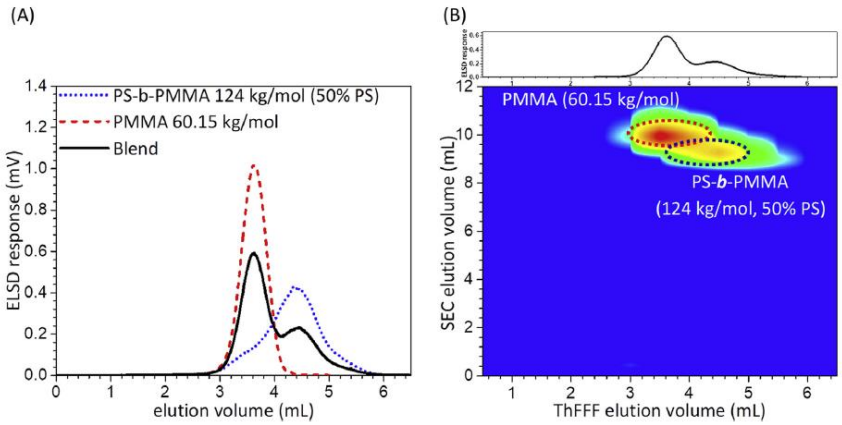

Fig. 5. (**A**) Superimposed ELSD fractograms of PMMA (60.15 kg mol^{-1}), PS-***b***-PMMA (124 kg mol^{-1}, 50% PS) and the corresponding blend. (**B**) ThFFF x SEC contour diagram of the blend of PMMA and PS-***b***-PMMA. Experimental conditions see Fig. 4.

wavelength). In the present case, the ELSD detects PMMA as well as the block copolymer (see Fig. 5) while at a wavelength of 270 nm the UV detector does not detect PMMA which is optically transparent at this wavelength.

The superimposed UV chromatograms of PS-**b**-PMMA and the blend with PMMA shown in Fig. 6A exhibit identical elution profiles that indicate that PMMA is not seen by the UV detector. This is confirmed by the contour diagram in Fig. 6B that only shows the block copolymer. Compared to the contour diagram obtained using ELSD, UV detection allows for the selective detection of only one component of the binary blend. This shows that, although the separation between PMMA and PS-**b**-PMMA is not perfect, the molar mass of the block copolymer can be analysed via selective detection. In this case, the UV detector acts like an information-rich detector. Even more versatile would be the use of an infrared detector that can identify different polymer structures via specific functional groups.

3.4. Two-dimensional separation of block copolymer blends

For the fine-tuning of specific materials' properties it is common not only to combine homopolymers and copolymers but also copolymers of different molar masses and compositions.

To explore the capabilities of the newly developed ThFFF x SEC approach, the following applications address the fractionation of block copolymer blends. In the first application, two block copolymers with distinctively different molar masses and similar compositions are analysed, see Fig. 7. Due to their similar compositions, the block copolymers have nearly identical thermal diffusion coefficients but the Soret coefficients are distinctively different due to the different molar masses.

The perfect separation of the two blend components allows for the precise determination of a number of molecular parameters. SEC in the second dimension provides information on the molar masses of the two block copolymers. From the ThFFF fractionation in the first dimension, the chemical composition of the block

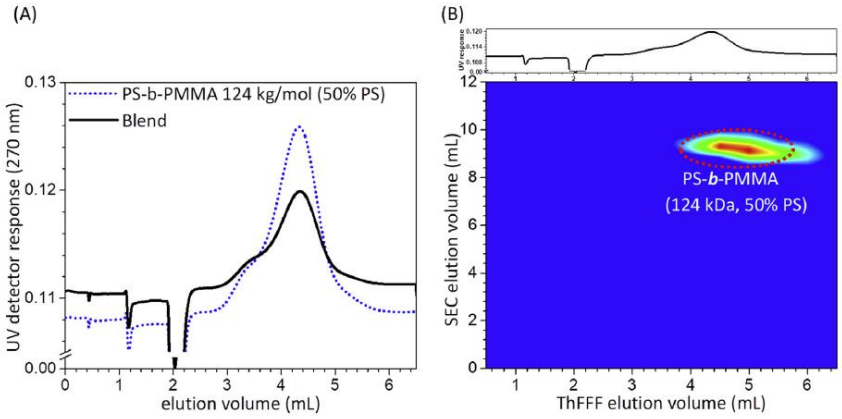

Fig. 6. (**A**) Superimposed UV (270 nm) fractograms of PS-***b***-PMMA (124 kg mol^{-1}, 50% PS) and the blend with PMMA (60.15 kg mol^{-1}). (**B**) ThFFF x SEC contour diagram of the blend of PMMA and PS-***b***-PMMA. Experimental conditions see Fig. 4.

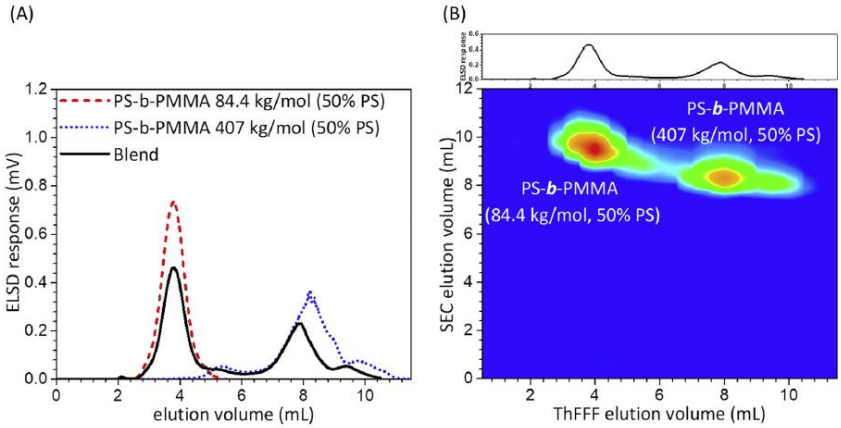

Fig. 7. (A) Superimposed ELSD fractograms of PS-***b***-PMMA (84.4 kg mol^{-1}, 50% PS), PS-***b***-PMMA (407 kg mol^{-1}, 50% PS) and the corresponding blend. (B) ThFFF x SEC contour diagram of the blend of PS-***b***-PMMA (84.4 kg mol^{-1}, 50% PS) and PS-***b***-PMMA (407 kg mol^{-1}, 50% PS). Experimental conditions see Fig. 4.

copolymers can be obtained from D_T while the sizes can be obtained via D.

A different scenario is seen when the molar masses of the block copolymers are similar but the chemical compositions are different. In this case, the fractionation in ThFFF is expected to be mainly driven by differences in D_T. As the molar masses of the blend components were rather low, a ΔT of 80 °C was used to obtain sufficient retention. In general, one has to keep in mind that depending on the fractionation problems, ΔT must be adjusted. However, in addition to achieving sufficient retention, the properties of the carrier liquid (e.g. the boiling point) must be considered.

The two PS-***b***-PMMA samples of similar molar masses (50 and 50.7 kg mol^{-1}, respectively), had compositions of 44 and 83% PS corresponding to D_T of 1.34 ± 0.04 and $0.84 \pm 0.02 \times 10^{-7}$ cm^2 s^{-1} K^{-1}, respectively. The superimposed ELSD fractograms of the block copolymers and the blend are shown in Fig. 8A and the ThFFF x SEC contour diagram is shown in Fig. 8B. From the ThFFF fractogram in the first dimension, a bimodal peak was observed for the blend as expected, based on the difference in D_T which is primarily influenced by the chemical composition of the polymers. D_T of the block copolymers increased with increasing PMMA content as PMMA has a larger D_T in THF compared to PS. This will result in block copolymers with larger D_T values to elute later as retention in ThFFF is governed by the D_T/D ratio. However, due to the fact that the ThFFF elution profile of PS-***b***-PMMA (50.7 kg mol^{-1}, 83% PS) was very broad, the blend also produced a very broad elution profile that made it difficult to identify the two blend components.

In the SEC dimension of the contour diagram, a slight difference in the elution volumes of the blend components was observed. This was expected as the chemical compositions of the polymers are different and as a result they will have different random coil conformations in solution. For an improved fractionation of the blend in the ThFFF dimension it will be necessary to optimize the experimental conditions. One way to obtain better separation is to

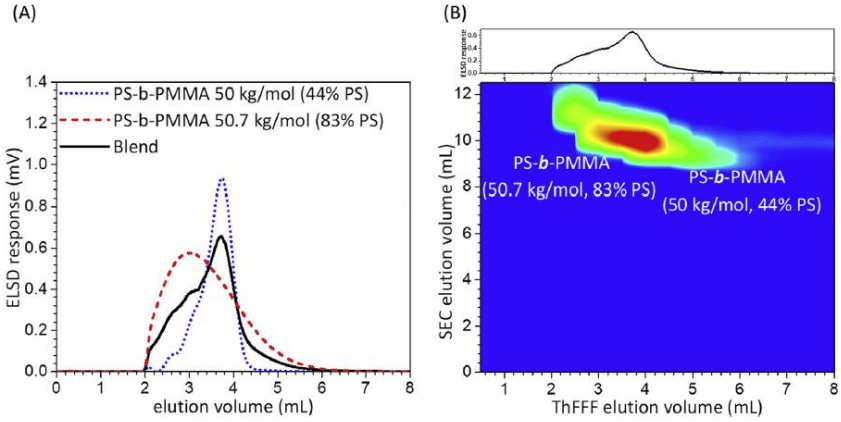

Fig. 8. (**A**) Superimposed ELSD fractograms of PS-***b***-PMMA (50.7 kg mol^{-1}, 83% PS), PS-***b***-PMMA (50 kg mol^{-1}, 44% PS) and the corresponding blend. (**B**) ThFFF x SEC contour diagram of the blend of PS and PS-***b***-PMMA. First dimension: flow rate 0.10 mL min^{-1}, T_c = 27.1 °C, ΔT = 80 °C. Second dimension: flow rate 3.0 mL min^{-1}, ambient temperature, column SDV High-Speed Linear M, transfer loops 500 μL. Detector ELSD.

change the mobile phase e.g. to a solvent that exhibits different thermodynamic qualities for the copolymer blocks.

4. Conclusion

It has been demonstrated that thermal field-flow fractionation and size exclusion chromatography can be coupled online and comprehensively. Both techniques are operating on different fractionation principles and provide complementary information on important molecular parameters. Taking the fractionation of complex polymer blends as examples it was shown that comprehensive online ThFFF x SEC is a useful alternative approach for the separation and characterization of homopolymers, block copolymers, and polymer blends. The applicability and success of this two-dimensional system was demonstrated by the comprehensive characterization of PS-*b*-PMMA block copolymers and respective homopolymers. Investigation and optimization of system parameters such as relaxation time, sample concentration, and applied temperature gradient have been shown to be essential for the successful method development. It was shown that using information-rich detectors such as UV in combination with a concentration detector (ELSD), the depth of information obtained by ThFFF x SEC can be enhanced. In future work, the capabilities of using multidetector systems will be explored in more detail.

Declaration of competing interest

The authors declare that they have no known competing financial interests or personal relationships that could have appeared to influence the work reported in this paper.

Credit authorship contribution statement

Zanelle Viktor: Conceptualization, Methodology, Validation, Formal analysis, Investigation, Resources, Writing - review & editing, Project administration. **Harald Pasch:** Conceptualization, Methodology, Validation, Formal analysis, Investigation, Resources, Writing - review & editing, Project administration.

Declaration of competing interest

The authors declare that they have no known competing financial interests or personal relationships that could have appeared to influence the work reported in this paper.

Acknowledgements

The authors thank Dr. Guilaume Greyling for his guidance and advice and Postnova Analytics GmbH (Landsberg, Germany) for technical support.

Appendix A. Supplementary data

Supplementary data to this article can be found online at https://doi.org/10.1016/j.aca.2020.02.033.

References

[1] H. Pasch, Hyphenated separation techniques for complex polymers, Polym. Chem. 4 (2013) 2628–2650.
[2] H. Pasch, B. Trathnigg, Multidimensional HPLC of Polymers, Springer-Verlag, Heidelberg, Germany, 2013.
[3] H. Pasch, B. Trathnigg, HPLC of Polymers, Springer, Berlin, Germany, 1997.
[4] H. Pasch, M.I. Malik, T. Macko, Recent advances in high-temperature fractionation of polyolefins, Adv. Polym. Sci. 251 (2013) 77–140.
[5] H. Pasch, Advanced fractionation methods for the microstructure analysis of complex polymers, Polym. Adv. Technol. 26 (2015) 771–784.
[6] B.W.J. Pirok, A.F.G. Gargano, P.J. Schoenmakers, Optimizing separations in online comprehensive two-dimensional liquid chromatography, J. Separ. Sci. 41 (2018) 68–98.
[7] B. Trathnigg, S. Abrar, Characterization of complex copolymers by two-dimensional Liquid Chromatography, Procedia Chem 2 (2010) 130–139.
[8] W. Radke, J. Falkenhagen, Liquid interaction chromatography, in: S. Fanali, P.R. Haddad, C.F. Poole, P. Schoenmakers, D. Lloyd (Eds.), Liquid Chromatography, Elsevier, Amsterdam, The Netherlands, 2013, pp. 93–129.
[9] W. Radke, Polymer separations by liquid interaction chromatography: principles – prospects – limitations, J. Chromatogr., A 1335 (2014) 62–79.
[10] P. Schoenmakers, P. Aarnoutse, Multi-dimensional separations of polymers, Anal. Chem. 86 (2014) 6172–6179.
[11] M.E. Schimpf, K. Caldwell, J.C. Giddings, Field-Flow Fractionation Handbook, John Wiley and Sons, New York, USA, 2000.
[12] E.P.C. Mes, W. Th Kok, R. Tijssen, Prediction of polymer thermal diffusion coefficients from polymer-solvent interaction parameters: comparison with thermal field flow fractionation and thermal diffusion forced Rayleigh scattering experiments, Int. J. Polym. Anal. Char. 8 (2003) 133–153.
[13] F.A. Messaud, R.D. Sanderson, J.R. Runyon, T. Otte, H. Pasch, S.K.R. Williams, An overview on field-flow fractionation techniques and their applications in the separation and characterization of polymers, Prog. Polym. Sci. 34 (2009) 351–368.
[14] J.C. Giddings, Field-flow fractionation: analysis of macromolecular, colloidal, and particulate materials, Science 260 (1993) 1456–1465.
[15] S.K.R. Williams, J.R. Runyon, A.A. Ashames, Field-flow fractionation: addressing the nano challenge, Anal. Chem. 83 (2011) 634–642.
[16] C. van Batten, M. Hoyos, M. Martin, Thermal field-flow fractionation of colloidal materials: methylmethacrylate-styrene linear di-block copolymers, Chromatographia 45 (1997) 121–126.
[17] C.A. Ponyik, D.T. Wu, S.K.R. Williams, Separation and composition distribution determination of triblock copolymers by thermal field-flow fractionation, Anal. Bioanal. Chem. 405 (2013) 9033–9040.
[18] G. Greyling, H. Pasch, Characterisation of block copolymer self-assemblies by thermal field-flow fractioantion, Polym. Int. 66 (2017) 745–751.
[19] U.L. Muza, G. Greyling, H. Pasch, Characterization of complex polymer self-assemblies and large aggregates by multidetector thermal field-flow fractionation, Anal. Chem. 89 (2017) 7216–7224.
[20] M.I. Malik, H. Pasch, Field-flow fractionation: new and exciting perspectives in polymer analysis, Prog. Polym. Sci. 63 (2016) 42–85.
[21] J.C. Giddings, Two-dimensional field-flow fractionation, J. Chromatogr. 504 (1990) 247–258.
[22] A.C. van Asten, R.J. van Dam, W. Th Kok, R. Tijssen, H. Poppe, Determination of the compositional heterogeneity of polydisperse polymer samples by the coupling of size-exclusion chromatography and thermal field-flow fractionation, J. Chromatogr., A 703 (1995) 245–263.
[23] E. Venema, P. de Leeuw, J.C. Kraak, H. Poppe, R. Tijssen, Polymer characterization using on-line coupling of thermal field flow fractionation and hydrodynamic chromatography, J. Chromatogr., A 765 (1997) 135–144.
[24] G. Yohannes, S.K. Wiedmer, J. Hiidenhovi, A. Hietanen, T. Hyötyläinen, Comprehensive two-dimensional field-flow fractionation-liquid chromatography in the analysis of large molecules, Anal. Chem. 79 (2007) 3091–3098.
[25] A.C. van Asten, H.F.M. Boelens, W. Th Kok, H. Poppe, P.S. Williams, J.C. Giddings, Temperature dependence of solvent viscosity, solvent thermal conductivity, and soret coefficient in thermal field-flow fractionation, Separ. Sci. Technol. 29 (1994) 513–533.
[26] D. Melucci, C. Contado, I. Mingozzi, M. Hoyos, M. Martin, F. Dondi, Evaluation of the soret coefficient for polystyrene in decalin by means of thermal Field-Flow Fractionation, J. Liq. Chromatogr. Relat. Technol. 23 (2000) 2067–2082.
[27] G. Greyling, H. Pasch, Thermal Field-Flow Fractionation of Polymers, Springer, Heidelberg, Germany, 2019.
[28] I. François, K. Sandra, P. Sandra, Comprehensive liquid chromatography: fundamental aspects and practical considerations – a review, Anal. Chim. Acta 641 (2009) 14–31.
[29] J.J. Gunderson, J.C. Giddings, Chemical composition and molecular-size factors in polymer analysis by thermal field-flow fractionation and size exclusion chromatography, Macromolecules 19 (1986) 2618–2621.
[30] A.C. van Asten, G. Stegeman, W. Th Kok, R. Tjissen, H. Poppe, Separation speed in thermal field flow fractionation, Anal. Chem. 66 (1994) 3073–3080.
[31] M.E. Schimpf, J.C. Giddings, Characterization of thermal diffusion of copolymers in solution by thermal field-flow fractionation, J. Polym. Sci., Part B: Polym. Phys. 28 (1990) 2673–2680.

Supporting Information

Two-dimensional fractionation of complex polymers by comprehensive online-coupled thermal field-flow fractionation and size exclusion chromatography.

Zanelle Viktor, Harald Pasch*

Department of Chemistry and Polymer Science, University of Stellenbosch, Private Bag X1, 7602, Stellenbosch, South Africa, e-mail: hpasch@sun.ac.za

Table S1 Molar masses (M_w), retention times (t_r), hydrodynamic diameters (D_h), translational diffusion coefficients (D), thermal diffusion coefficients (D_T) and Soret coefficients (S_T) for PS, PMMA and PS-***b***-PMMA samples as determined in THF.

Sample	ΔT [°C]	M_w [kg/mol][a]	t_r [min]	D_h [x 10^{-7} cm][b]	D [x 10^{-7} cm^2 s^{-1}][c]	D_T [x 10^{-7} cm^2 s^{-1} K^{-1}][d]	S_T [K^{-1}][e]
PS	60	33	27.1	9.18 ± 0.15	10.44 ± 0.64	1.35 ± 0.08	0.129 ± 0.011
PS	60	62.5	32.5	12.63 ± 0.39	7.58 ± 0.25	1.17 ± 0.04	0.155 ± 0.007
PMMA	60	40.3	31.3	8.84 ± 0.40	10.83 ± 0.24	1.62 ± 0.04	0.149 ± 0.005
PMMA	60	60.15	36.3	12.00 ± 0.34	7.98 ± 0.28	1.38 ± 0.05	0.173 ± 0.009
PS-***b***-PMMA [44:56]	80	50	37.5	9.59 ± 0.31	9.99 ± 0.31	1.34 ± 0.04	0.134 ± 0.006
PS-***b***-PMMA [83:17]	80	50.7	30.3	12.35 ± 0.66	7.76 ± 0.14	0.84 ± 0.02	0.108 ± 0.003
PS-***b***-PMMA [33:67]	60	81	39.8	15.46 ± 0.23	6.20 ± 0.43	1.17 ± 0.08	0.190 ± 0.018
PS-***b***-PMMA [50:50]	60	84.4	37.8	16.86 ± 0.66	5.68 ± 0.14	1.02 ± 0.03	0.180 ± 0.006
PS-***b***-PMMA [50:50]	60	124	44.1	20.54 ± 0.34	4.66 ± 0.28	0.98 ± 0.06	0.210 ± 0.018
PS-***b***-PMMA [50:50]	60	407	82.3	37.16 ± 0.44	2.58 ± 0.22	1.01 ± 0.09	0.392 ± 0.046

a) As provided by manufacturers. (Molar mass provided for PMMA 60.15 kg/mol, corresponds to the M_p value)

b) Determined by DLS (T = 25°C, 1.0 mg of sample dissolved in 2.0 mL of THF).

c) Calculated by the Stokes-Einstein equation: $D = kT/3\pi\eta D_h$, where ***k*** is Boltzmann's constant, T is the temperature, η is the viscosity and D_h is the hydrodynamic diameter.

d) Calculated using: $D_T = 6Dt_r/\Delta T\, t_0$, where t^0 is the void volume, t_r is the retention time of the sample, and ΔT is the temperature difference between the hot and the cold wall.

e) Determined according to equation: $S_T = D_T/D$.

CHAPTER 4

SOLUTION BEHAVIOUR OF SYNDIOTACTIC- AND ISOTACTIC POLY(METHYL METHACRYLATE) AS INVESTIGATED BY VARIABLE TEMPERATURE ASYMMETRIC FLOW FIELD-FLOW FRACTIONATION.

(manuscript to be submitted to Anal. Chim. Acta)

4.1. Introduction

Size exclusion chromatography (SEC) is one of the standard methods used for the molecular mass analysis of complex polymers and is classified as a relative method. This means that with the aid of a suitable calibration procedure of the columns the molecular mass and molecular mass distributions can be determined [1-5]. Alternatively, mass-sensitive detectors (multiangle light scattering or viscometer) can be coupled to SEC to acquire molecular mass distribution information. The separation in SEC takes place on a stationary phase based on micrometer-sized particles with a given pore size distribution and in a mobile phase that is a thermodynamically good solvent for the analyte. Accordingly, the analyte is assumed to adopt a random coil conformation based on its interactions with the given solvent at a specific temperature and will thus have different hydrodynamic sizes in solution as a function of molecular mass [1-5]. Separation in SEC is based on the distribution of the analyte molecules between the stationary phase and the mobile phase. The interactions that the analyte molecules have with the stationary phase, which depends on the conformational changes (hydrodynamic size) the analyte experiences when penetrating the pores, is the primary separation mechanism in SEC [1-5]. In effect this means that analyte molecules having the same hydrodynamic size in solution will elute from the column at the same time, regardless of chemical composition. The hydrodynamic size of an analyte in a given solution is a function of the polymer chain length (i.e. degree of polymerization), chemical composition and molecular topology (due to branching or differences in microstructure such as tacticity) [1, 4-6]. In the case where the molecular masses of the analytes are similar, a separation is only obtained if the analyte has a different hydrodynamic size in solution due to differences in chemical composition or molecular topology. As the resolution in SEC is inherently low, the differences in hydrodynamic size of different molecular topology polymers with similar degrees of polymerization is not sufficient for separation [1, 4, 5].

An alternative to column-based analytical techniques is field-flow fractionation (FFF). FFF is an empty channel-based analytical fractionation technique in which an external force field is applied perpendicular to the parabolic channel flow velocity profile to achieve separation. The separation mechanism of FFF is based on the type of applied force and the interaction of the analyte molecules with the given applied force [7-9]. Due to the empty channel configuration of FFF it has the ability to separate polymer molecules and particles that range from nanometer to micrometer in size. Two of the leading sub-techniques in the family of FFF are thermal field-flow fractionation (ThFFF) and asymmetrical flow field-flow fractionation (AsFlFFF) [8-11, 13, 14]. In ThFFF the applied field force is a temperature gradient which is generated between an upper hot channel wall and a lower cold

channel wall [7, 12]. Separation in ThFFF is governed by the Soret coefficient (S_T), which is determined by the interplay of thermal diffusion and normal diffusion. ThFFF is capable of separating analyte molecules based on molecular mass and/or chemical composition. In the case of molecular mass separation of the analytes with the same chemical structure, the S_T ratio is predominantly governed by the normal diffusion coefficient (D) of the analyte molecules [7, 12]. For the chemical composition based separation of the analyte molecules, the changes in the thermal diffusion coefficient (D_T) of the analyte are the main contributing factor to achieve separation. In ThFFF, analytes with the same Soret coefficient co-elute regardless of composition and hydrodynamic size [7, 12].

AsFlFFF is considered to be a complementary fractionation technique to SEC for molecular mass characterization of complex polymers. AsFlFFF consists of a solid impermeable upper channel wall and a semi-permeable frit at the lower channel wall on top of which an ultrafiltration membrane is placed. The applied force in AsFlFFF is known as the cross flow, which is generated through the semi-permeable frit, when a single channel inlet flow is divided into the axial parabolic flow and the cross flow [7, 10, 13, 14]. Solvent (carrier liquid) molecules can pass through the ultrafiltration membrane when the cross flow is applied, however, the molecular mass cut-off limit of the membrane is specifically chosen to prevent the loss of analyte molecules and thus stay within the channel volume. Different from SEC, AsFlFFF retention and the subsequent separation is governed by the differences in diffusion coefficients (D) [7, 10, 13, 14]. Therefore, based on the interaction that the analyte molecules have with the cross-flow and their respective diffusion coefficients, analyte molecules will be retained to different degrees, and as such separation can be achieved in AsFlFFF. D is a function of hydrodynamic size, which correlates to the primary molecular parameters (chemical composition, degree of polymerization and molecular topology). Additionally, hydrodynamic size (d_h) is influenced by the thermodynamic quality of the solvent and temperature as expressed by the Stokes-Einstein equation ($\frac{D = kT}{3\pi\eta d_h}$).

Similar to SEC, AsFlFFF can elucidate the molecular mass and molecular mass distribution of a polymeric sample with the aid of suitable mass-sensitive detectors. As D decreases with increasing hydrodynamic size, the elution order in AsFlFFF is from the smallest hydrodynamic size to the largest hydrodynamic size, opposite to that of SEC. AsFlFFF has been employed in the characterization of complex polymers with regard to molecular mass and structural parameters [7, 10, 13-16]. Therefore, as the separation in AsFlFFF is predominantly governed by D, it can potentially be capable of separating polymers that differ with regard to tacticity through the use of solvents of different thermodynamic qualities and viscosities at various channel temperatures. Greyling *et al.* have shown

that channel-based fractionation techniques are capable of microstructure-based separation. In multiple studies conducted by Greyling *et al*., various isomers of poly(methyl methacrylate) (PMMA), polyisoprene (PI), polybutadiene (PB), and poly(butyl methacrylate) (BuMA) were separated, based on their difference in tacticity and demonstrated that ThFFF was thus sensitive to the topology and chemical composition of a polymer [17-19].

The present study aims at using AsFlFFF to separate poly(methyl methacrylate) (PMMA) homopolymers of similar molecular masses and different tacticities. As separation in AsFlFFF is based on the difference in D, which is a function of the hydrodynamic size of the analyte in solution, the objective of the study was to investigate the solution behaviour of syndiotactic PMMA, atactic PMMA and isotactic PMMA in solvents with different thermodynamic properties. Lastly, the influence of solvent quality and channel temperature on the separation of the different tacticity PMMA samples was to be investigated.

4.2. Experimental

4.2.1. Materials

Samples of poly(methyl methacrylate) (PMMA) were used as received from manufacturers. Syndiotactic PMMA (*s*-PMMA), atactic PMMA (*a*-PMMA) and isotactic PMMA (*i*-PMMA) were purchased from Polymer Source Inc. (Montreal, Canada). HPLC grade tetrahydrofuran (THF) (Honeywell GmbH, Seelze, Germany), chloroform ($CHCl_3$) (Sigma-Aldrich, Steinheim, Germany) and acetonitrile (ACN) (Sigma-Aldrich, Saint-Quentin-Fallavier, France) were used as received. The molecular masses, dispersities (Đ) and tacticity contents of the polymer samples are tabulated in **Table 4.1**.

4.2.2. Dynamic Light Scattering (DLS)

A DLS instrument (Zen 1600, Malvern Instruments, Worcestershire, United Kingdom) equipped with a quartz SUPRASIL flow cell (Hellma Analytics) to acquire the size of each sample in the different carrier liquids was used. Experiments were conducted at 25°C and the temperature was increased in 5°C increments to 55°C. The size of each PMMA sample was also determined off-line with the aid of the DLS instrument for sample concentration of 5.0 $mg.mL^{-1}$ with ACN as solvent. A glass cuvette was used for the off-line analysis and experiments were conducted at temperatures ranging from 25°C to 55°C.

4.2.3. Separation Systems and Conditions

Fractionations were performed using a AF2000 asymmetric-flow FFF instrument (Postnova Analytics GmbH, Landsberg, Germany) coupled with a multiangle laser light scattering (MALLS) detector (PN3609), differential refractive index (dRI) detector (PN3150) and DLS detector (Zen 1600, Malvern Instruments, Worcestershire, United Kingdom). The AsFlFFF instrument consisted of an autosampler (PN5300), a tip-pump (PN1122), a focus-pump (PN1122), a cross-flow pump and a channel oven. The channel consisted of a regenerated cellulose membrane with an average molecular mass cut-off of 10 $kg.mol^{-1}$ and a spacer with a thickness of 350 µm. The void volume of the system was determined to be 4.4 mL (8.8 min) in THF and 4.1 mL (8.2 min) in ACN. Samples were introduced into the channel via an autosampler equipped with a 100 µL capillary sample loop at a flow rate of 0.2 $mL\ min^{-1}$ for a period of 6 min. The injection time includes the focusing time for the samples and both were controlled by Postnova NovaFFF AF2000 Software Version 2.1.0.5 (Postnova Analytics GmbH, Landsberg, Germany). The cross flow was kept constant at 4.5 $mL.min^{-1}$ and the focus flow was automatically adjusted to 4.8 $mL\ min^{-1}$ during the injection and focussing step to maintain a detector flow rate of 0.5 $mL\ min^{-1}$. After the sample was injected, the focus flow rate was decreased to 0.0 $mL\ min^{-1}$ in 1 min, also known as the transition step. Thereafter, the cross flow was maintained at 4.5 $mL.min^{-1}$ for 4 min followed by the cross flow being linearly decreased to 2.0 $mL.min^{-1}$ in 4 min and then decreased linearly to 0.0 $mL.min^{-1}$ in 7 min and kept constant for 15 min. The injected sample volume was 50 µL at a concentration of 5.0 $mg\ mL^{-1}$ using THF, ACN and $CHCl_3$ as the dissolution solvent, which were used as carrier liquid, respectively.

SEC analysis was performed on a Waters system. The instrument was equipped with a Waters 717plus autosampler, Waters 600E system controller and Waters 610 fluid unit. A Waters 2414 refractive index detector was used for detection. The column oven temperature was kept at 30 °C and 100 µL of 2.0 $mg.mL^{-1}$ sample in THF (HPLC grade, BHT stabilised) was injected into the column set that consisted of PLgel 5µm Mixed-C columns (300 × 8.0 mm i.d.) connected in series with a PLgel 5µm guard column. A flow rate of 1.0 $mL{\cdot}min^{-1}$ was used for analysis. The system was calibrated using narrow dispersed polystyrene standards ranging from 800 to 2 x 106 $g{\cdot}mol^{-1}$. Data acquisition and processing were done on Breeze software.

4.3. Results and Discussion

Syndiotactic-, atactic- and isotactic poly(methyl methacrylate) were selected as representative samples with different tacticities for this study. The molecular information as provided by the manufacturers is reported in **Table 4.1**.

Table 4.1 Molecular masses and tacticity contents of the PMMA homopolymers.

	M_n (kg.mol^{-1})	M_w (kg.mol^{-1})	Đ	Syndiotactic content (mol %)[a]	Atactic content (mol %)[a]	Isotactic content (mol %)[a]
s-PMMA	131	142	1.06	80.7	18.5	0.8
a-PMMA	139	151	1.09	56.5	39	4.5
i-PMMA	135	150	1.10	5.5	1.9	92.6

(a) The tacticity content of each sample was previously determined by ^{1}H NMR [17]

The selected PMMA samples are comparable with regard to molecular mass. However, having similar molecular masses does not necessarily mean that the samples have similar hydrodynamic diameters in solution. The hydrodynamic diameter of a sample in solution is a function of molecular topology, the thermodynamic quality of the solvent, the viscosity of the solvent and the analysis temperature [17-21]. Therefore, similar polymers with different tacticities may adopt different random coil conformations depending on the solvent and temperature used for characterization. As the solvent can potentially have an influence on the retention behaviour of an analyte molecule, solvents of different thermodynamic qualities were selected to investigate the effect of solvent quality and channel temperature on the resolution. The solvents that were selected included THF (thermodynamically good solvent for PMMA), ACN (a theta solvent for PMMA) and $CHCl_3$ (thermodynamically good and non-complexing solvent for PMMA) [22].

4.3.1. SEC analysis in tetrahydrofuran

In the first set of experiments, *s*-PMMA, *a*-PMMA and *i*-PMMA were analysed by SEC with THF as the mobile phase (**Fig. 4.1**). The PMMA samples eluted within a narrow retention band, with the difference in retention between the *s*-PMMA and *i*-PMMA, being 0.33 min (0.33 mL). It is of interest to note that *a*-PMMA having the highest nominal molecular mass (M_n = 139 kg.mol^{-1}) does not elute first but between the lower molecular mass *i*-PMMA (M_n = 135 kg.mol^{-1}) and *s*-PMMA (M_n = 131 kg.mol^{-1}). This indicates that the tacticity of the PMMA samples affects the hydrodynamic diameter.

Therefore, the retention behaviour of the PMMA samples is assumed to be a function of both tacticity and molecular mass.

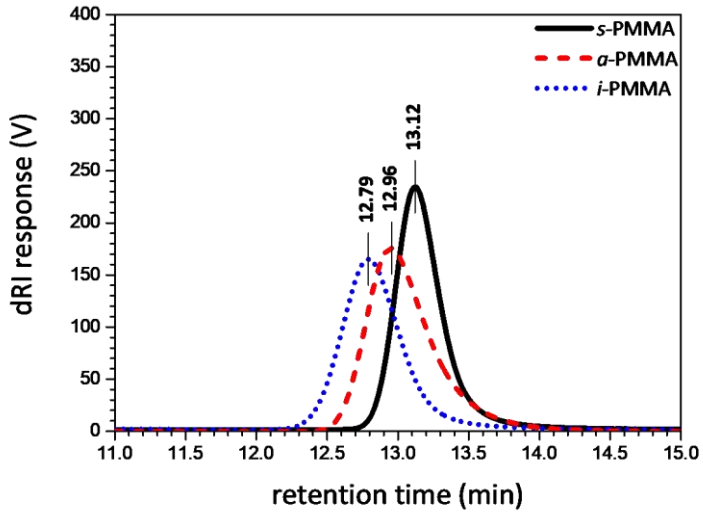

Figure 4.1 Enlarged superimposed dRI elugrams of *s*-PMMA, *a*-PMMA and *i*-PMMA as analysed by SEC with THF as mobile phase at a flow rate of 1.0 mL.min^{-1} and a column temperature of 30°C (refer to **Fig. S1** in the supporting information for the complete superimposed dRI elugrams).

4.3.2. AsFlFFF analysis

s-PMMA, *a*-PMMA and *i*-PMMA were characterised by AsFlFFF with THF, $CHCl_3$ and ACN as the carrier liquids, respectively. The same AsFlFFF experimental conditions were used for all three carrier liquids (refer to supporting information, **Fig. S2**, for the AsFlFFF separation method used). The differences in retention times for *s*-PMMA, *a*-PMMA and *i*-PMMA in the various carrier liquids are tabulated in **Table 4.2**.

Table 4.2 Retention times of *s*-PMMA, *a*-PMMA and *i*-PMMA in the various solvents.

	t_R (min)		
	ACN (0.34 cP, 25°C)	THF (0.46 cP, 25°C)	$CHCl_3$ (0.53 cP, 25°C)
s-PMMA	14.98	16.86	18.04
a-PMMA	16.32	17.79	19.26
i-PMMA	17.93	18.64	20.07

In agreement with the SEC results, *a*-PMMA eluted between *s*-PMMA and *i*-PMMA. The diffusion coefficient (D) is the driving force for retention and the resultant separation achieved in AsFlFFF and is associated with the hydrodynamic diameter of the analyte molecules in a given solvent. AsFlFFF separates in the direction of decreasing diffusion coefficients that correspond to increasing hydrodynamic diameters. The elution order observed in the AsFlFFF fractogram confirms the SEC results. The difference in retention between *s*-PMMA and *i*-PMMA was more significant in the AsFlFFF analysis of the samples compared to the SEC analysis. The difference in retention time was 1.78 min (0.89 mL) in THF as shown in **Fig. 4.2 (a)**.

Similar to THF, $CHCl_3$ is a thermodynamically good solvent for PMMA. Even though $CHCl_3$ and THF are comparable with regard to viscosity, $CHCl_3$ retained the PMMA samples to a higher degree in comparison to THF. As a result, the difference in retention between *s*-PMMA and *i*-PMMA was slightly larger in $CHCl_3$ compared to THF, with the difference being 2.03 min (1.02 mL) (**Fig. 4.2 (b)**). $CHCl_3$ is classified as a non-complexing solvent for PMMA, which mitigates the effects of stereocomplex formation in PMMA. Therefore, a blend of a 1:1 mixture of *s*-PMMA and *i*-PMMA could be analysed in $CHCl_3$ and as shown in **Fig. 4.3 (a)**, a bimodal peak distribution was obtained. The peak maximum for the first eluting peak of the blend was at 18.36 min (9.18 mL), which corresponds well to the retention time of the individual *s*-PMMA, 18.04 min (9.02 mL), analysed under the same experimental conditions. For the second eluting peak of the blend, the peak maximum was at 19.87 min (9.94 mL), similar to that of the individual *i*-PMMA, 20.07 min (10.04 mL)**.** The separation between *s*-PMMA and *i*-PMMA in a 1:1 blend could be improved by adding an additional step to the separation method, as illustrated in **Fig. 4.3 (b)**.

In contrast to the thermodynamically good solvents THF and $CHCl_3$, CAN which is a theta solvent and a strong stereocomplexing solvent for PMMA, was evaluated as a carrier liquid. Being a theta solvent for PMMA in effect means that the polymer-solvent and polymer-polymer interactions are balanced, thus forming unperturbed (ideal) PMMA chains. It would, therefore, be expected that *s*-PMMA and *i*-PMMA would exhibit different hydrodynamic diameters in ACN, which would lead to a difference in retention behaviour. **Fig. 4.2 (c)** shows the superimposed MALLS fractograms of the different PMMA samples in ACN, from which it can be seen that a significant difference of 2.95 min (1.48 mL) in retention time between *s*-PMMA and *i*-PMMA was observed at 25°C. The difference in retention time between *s*-PMMA and *i*-PMMA increased in the theta solvent compared to the thermodynamically good solvents, showing that the thermodynamic quality of the carrier liquid does indeed influence retention behaviour in AsFlFFF.

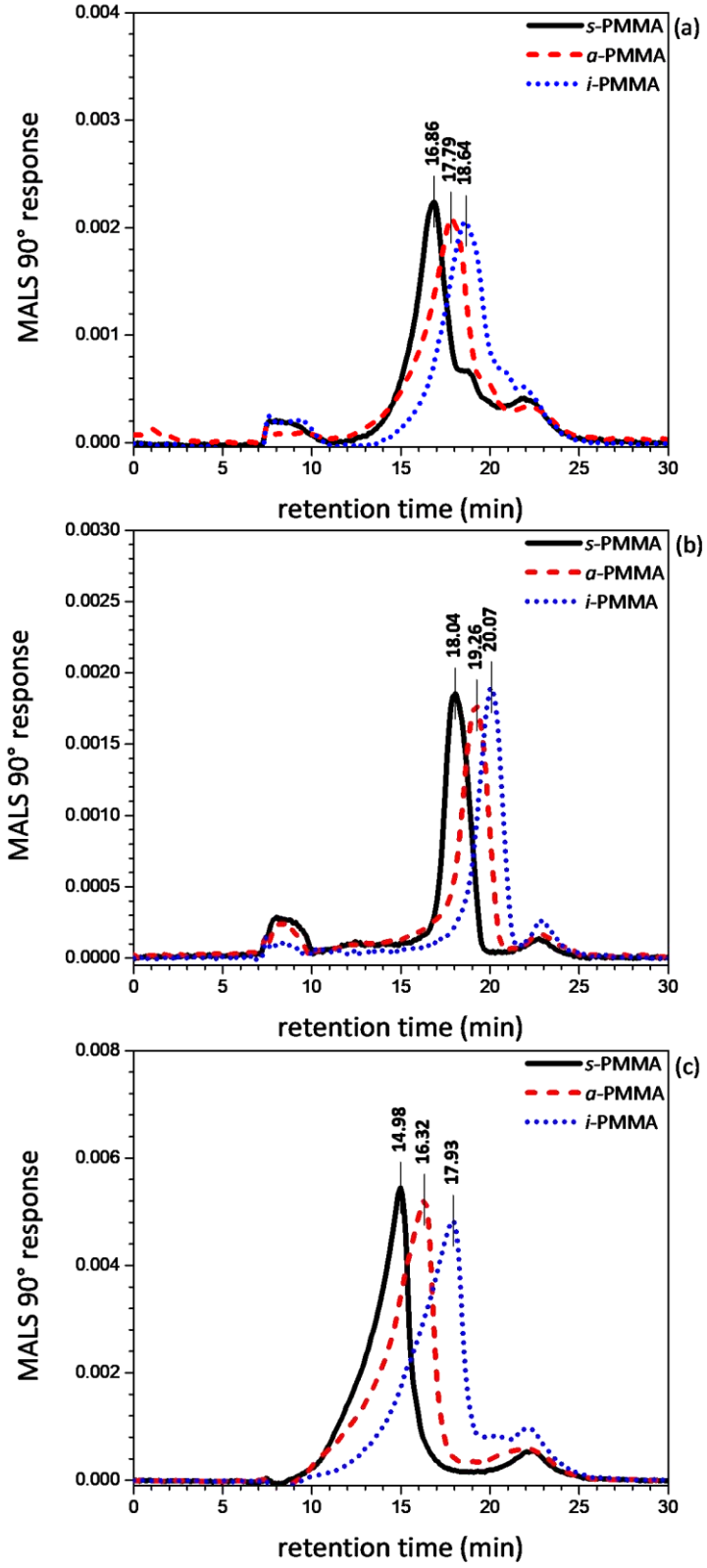

Figure 4.2 Superimposed MALLS fractograms of *s*-PMMA, *a*-PMMA and *i*-PMMA in **(a)** THF, **(b)** $CHCl_3$ and **(c)** ACN analysed by AsFlFFF at a channel temperature of 25°C (see supporting information, **Fig. S3**, for the corresponding dRI fractograms).

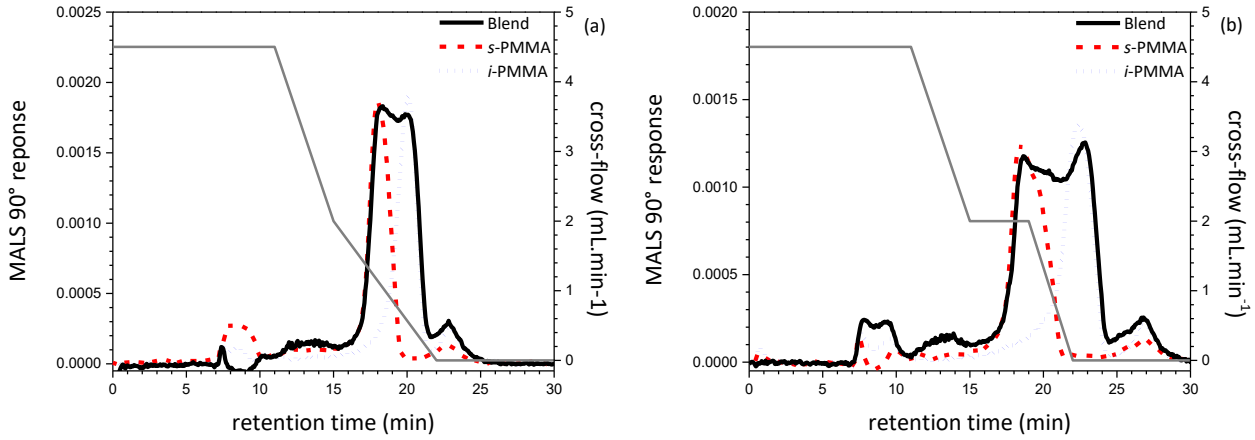

Figure 4.3 Superimposed MALLS fractograms of a blend of *s*-PMMA and *i*-PMMA analysed in $CHCl_3$ as carrier liquid, with a channel temperature of 25°C. Note that different cross-flow protocols were used in (a) and (b).

4.3.3. The effect of channel temperature on retention behaviour

After establishing that the type of carrier liquid has an influence on retention behaviour in AsFlFFF, the influence of the channel temperature was investigated. For the variable temperature study, ACN and THF were used as carrier liquids. The PMMA samples were analysed at an initial channel temperature of 25°C, from which the temperature was increased in 5°C increments to 55°C. It is expected that the thermodynamically good solvent (THF) should show minimal temperature dependent changes with regard to retention whereas temperature dependence is expected for the theta solvent (ACN) as the theta solvent will become more or less of a thermodynamically good solvent for PMMA depending on the theta solvent characteristics. However, whether this temperature dependence can be exploited by AsFlFFF to yield a difference in retention behaviour was to be investigated.

Starting with THF as carrier liquid, *s*-PMMA, *a*-PMMA and i-PMMA were analysed at various channel temperatures to investigate the retention behaviour of these samples as a function of temperature as shown in **Fig. 4.4 (a)**. For the MALLS- and dRI fractograms of the PMMA samples analysed at varying channel temperatures in THF, see supporting information, **Fig. S4** and **Fig. S5**. To present the retention behaviour of the PMMA samples, the difference between *s*-PMMA and *i*-PMMA as a function of temperature is illustrated in **Fig. 4.4 (b)**. The difference in retention between *s*-PMMA and *i*-PMMA remained fairly constant as the channel temperature increased. However, a maximum difference in retention was observed at 35°C, while the smallest difference in retention between *s*-PMMA and *i*-PMMA was noticed at 55°C.

For a quantitative evaluation of the effect of tacticity on size in solution, DLS was coupled online with AsFlFFF in a combined instrumental set-up. The z-average diameter obtained for the PMMA samples analysed in THF at various channel temperatures are shown in **Fig. 4.5**. From the plot provided in **Fig. 4.5**, it was observed that at 35°C, the size of *s*-PMMA in solution was 20.85 ± 0.35 nm, corresponding to its most collapsed coil conformation within the temperature range. In contrast to this, *i*-PMMA was at its most expanded conformation at 35°C, with a size of 27.83 ± 0.15 nm. It would, therefore, be expected that i-PMMA is retained to a larger extent as the diffusion coefficient decreases with increase in polymer size and that *s*-PMMA, being less retained, will elute faster from the channel. This is in agreement with the retention behaviour trend observed in **Fig. 4.4 (b)**, where the maximum difference between *s*-PMMA and *i*-PMMA in THF was observed. The z-average diameter (d.nm) determined for each PMMA sample by online DLS was superimposed with the PMMA tacticity MALLS fractograms acquired in THF and are provided in the supporting information (**Fig. S6 – Fig.S12**).

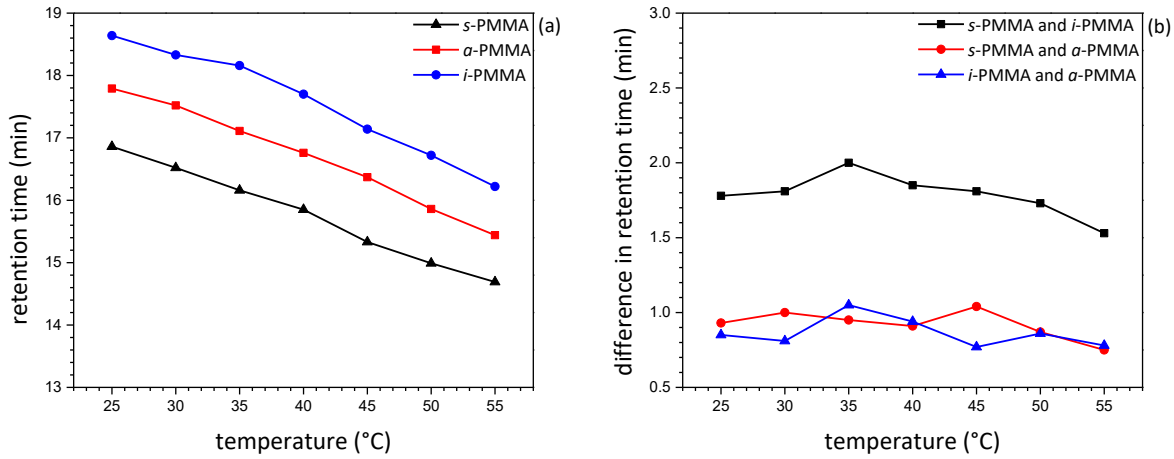

Figure 4.4 Plots of **(a)** the retention time as a function of temperature for *s*-PMMA, *a*-PMMA and *i*-PMMA and **(b)** the difference between *s*-PMMA and *i*-PMMA as a function of temperature in THF.

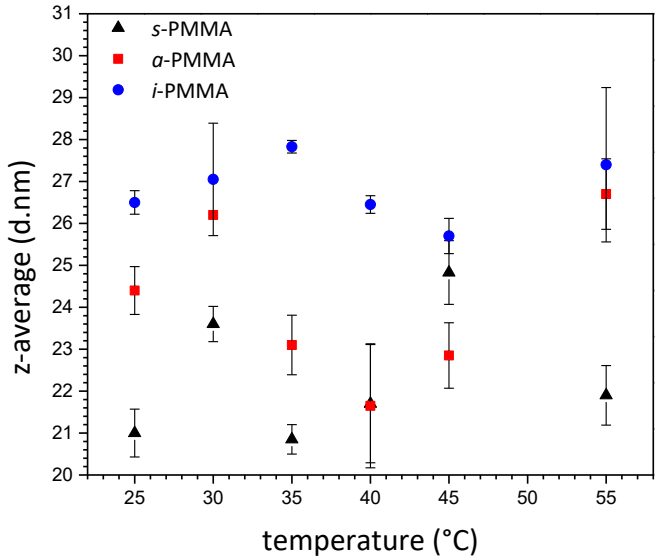

Figure 4.5 The z-average diameter (d.nm) acquired for individual *s*-PMMA, *a*-PMMA and *i*-PMMA as analysed in THF at various channel temperatures by coupling DLS with AsFlFFF.

Literature has reported several theta temperatures for PMMA in ACN i.e. 27.6°C, 33°C, 44°C and 45°C [23-26]. In each of the reported findings, the PMMA samples studied were different with regard to topology e.g. conventional PMMA, atactic PMMA or isotactic PMMA. The random coil conformation that a polymer chain adopts in solution is influenced by not only the thermodynamic quality of the solvent and temperature, but also by the molecular topology of the polymer. Hence, it would be expected that PMMA that differs in tacticity, could have a unique theta temperature in ACN, as the polymer-solvent interactions or polymer-polymer interactions will be different based on the type of tacticity as well as the tacticity content of the polymer. As such, the retention behaviours of *s*-PMMA, *a*-PMMA and *i*-PMMA at various channel temperatures that were either close to and/or at the reported theta temperature for PMMA in ACN were studied.

The retention of the PMMA samples as a function of temperature as well as the retention behaviour (i.e. the difference between the *s*-PMMA and *i*-PMMA retention) of the PMMA samples as a function of time are presented in **Fig. 4.6 (a)** and **Fig. 4.6 (b)**, respectively. The MALLS- and dRI fractograms for the PMMA samples analysed at varying channel temperatures in ACN are provided in the supporting information, **Fig. S13** and **Fig. S14**.

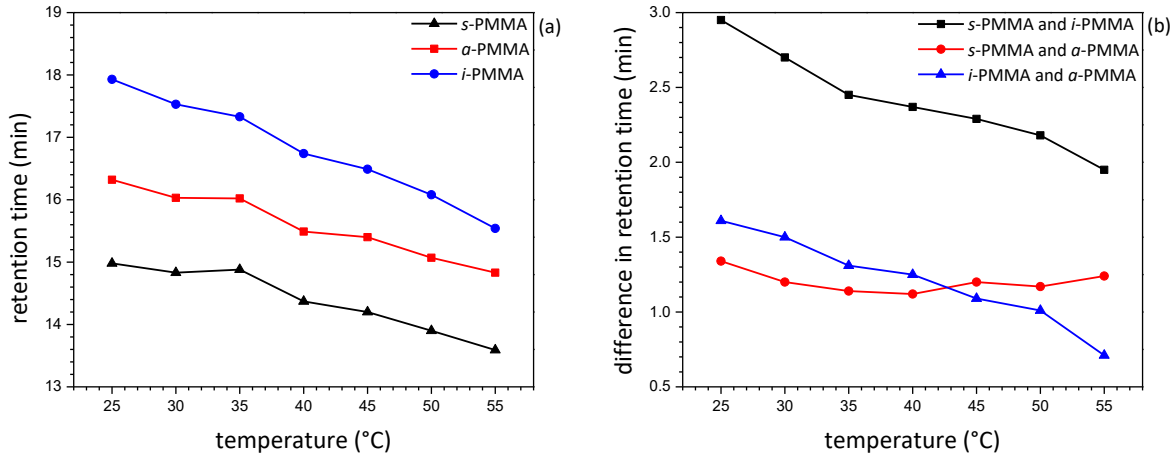

Figure 4.6 Plots of **(a)** the retention time as a function of temperature for *s*-PMMA, *a*-PMMA and *i*-PMMA and **(b)** the difference between *s*-PMMA and *i*-PMMA as a function of temperature in ACN.

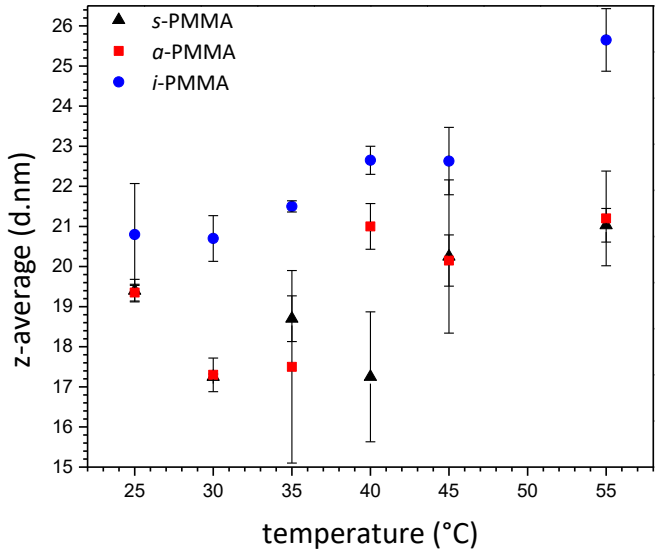

Figure 4.7 The z-average diameter (d.nm) acquired for the individual *s*-PMMA, *a*-PMMA and *i*-PMMA as analysed in ACN at various channel temperatures by coupling DLS with AsFlFFF.

The difference in retention between *s*-PMMA and *i*-PMMA in ACN continuously decreased as the channel temperature increased. From the plot provided in **Fig. 4.7**, it was observed that the increase in size for *i*-PMMA with an increase in temperature was more significant as compared to *s*-PMMA and *a*-PMMA. Krause *et al.* reported that the theta temperature for isotactic PMMA in acetonitrile was 27.6°C [23]. For temperatures above the theta temperature, the solvent becomes more thermodynamically favourable and as a result, the random coil conformation of the polymer chain will expand to allow for more favourable polymer-solvent interactions to occur. As such, *i*-PMMA is

more expanded in the theta solvent than the *s*-PMMA and *a*-PMMA. The z-average diameter (d.nm) determined for each PMMA sample by online DLS was superimposed with each of its individual MALLS fractograms obtained in ACN and is shown in **Fig. S15 – Fig. S21** in the supporting information. The off-line DLS conducted for the PMMA samples in ACN at varying temperatures for a sample concentration of 5.0 mg.mL^{-1}, are given in **Fig. S22** in the supporting information.

An additional parameter to consider in order to fully explain the different retention behaviour of *s*-PMMA and *i*-PMMA is their difference in persistence length. The random coil conformation dimensions are a function of the persistence length (Kuhn segment length) which (among other parameters) is determined by tacticity. The Kuhn length provides information on the short scale interactions and the stiffness of the polymer chain. The larger the Kuhn length value, the more rigid the polymer chain is. In the case of *s*-PMMA and *i*-PMMA, the Kuhn length is 0.41 nm and 0.47 nm, respectively. This, therefore, means that *i*-PMMA is more rigid than *s*-PMMA, which will coil more strongly than the extended *i*-PMMA [17, 27-29]. It is thus theorized that due to their different Kuhn lengths (or backbone flexibility), s-PMMA and *i*-PMMA adopt differently sized coil conformations under the shear forces in the channel. This backbone flexibility difference is enhanced in a theta solvent and thus not observed in THF.

4.4. Conclusion

The capability of AsFlFFF to separate PMMA samples that are different in tacticity and similar in molecular mass has been demonstrated. It was established that the thermodynamic quality of the solvent does influence the degree to which the PMMA samples are retained within the channel and that by using a theta solvent (ACN) as carrier liquid, the most favourable separation condition can be achieved. In addition, it was shown that by using a non-stereocomplexing solvent for PMMA, such as $CHCl_3$, the resolution of the peaks and fractionation selectivity could be improved as a blend of *s*-PMMA and *i*-PMMA was separated. The retention behaviour of *s*-PMMA, *a*-PMMA and *i*-PMMA showed minimal temperature dependency in the thermodynamically good solvent, THF. However, it was found that the maximum difference in retention between *s*-PMMA and *i*-PMMA, when analysed in THF, can be achieved at 35°C. In contrast to the thermodynamically good solvent, the difference in retention between the *s*-PMMA and *i*-PMMA in ACN decreases with an increase in the channel temperature and thus showed that temperature does indeed have an influence on the retention behaviour of s-PMMA and i-PMMA. This was observed, in particular, for *i*-PMMA, where the change in size with increase in temperature was the most significant of all the PMMA samples.

References

[1] W. Radke, Polymer separations by liquid interaction chromatography: Principles – prospects – limitations. J. Chromatogr. A. 1335 (2014) 62-79.

[2] I. Teraoka, Calibration of retention volume in size exclusion chromatography by hydrodynamic radius. Macromolecules. 37:17 (2004) 6632-6639.

[3] D. Cho, I. Park, T. Chang, K. Ute, I-i. Fukuda, T. Kitayama, Tacticity effect on size exclusion chromatography retention of stereo-regular poly(ethyl methacrylate). Macromolecules. 35:15 (2002) 6067-6069.

[4] Chi-San Wu, ed. Handbook Of Size Exclusion Chromatography And Related Techniques: Revised And Expanded, Marcel Dekker, Inc., New York, 2003.

[5] A.M. Striegel, J.J. Kirkland, W.W. Yau, D.D. Bly, Modern Size Exclusion Chromatography. Practice of Gel Permeation and Gel Filtration Chromatography, Wiley, New York, 2009.

[6] H. Pasch, B. Trathnigg, HPLC of Polymers, Springer: Berlin, Germany, 1999.

[7] M.E. Schimpf, K. Caldwell, J.C. Giddings, Field-Flow Fractionation Handbook, John Wiley and Sons: New York, USA, 2000.

[8] F.A. Messaud, R.D. Sanderson, J.R. Runyon, T. Otte, H. Pasch, S.K.R. Williams, An overview on field-flow fractionation techniques and their applications in the separation and characterization of polymers, Prog. Polym. Sci. 34 (2009) 351–368.

[9] M.I. Malik, H. Pasch, Field-flow fractionation: New and exciting perspectives in polymer analysis, Prog. Polym. Sci. 63 (2016) 42–85.

[10] K.-G. Wahlund, Flow field-flow fractionation: Critical overview, J. Chromatogr. A, 1287 (2013) 97-112

[11] T. Kowalkowski, B. Buszewski, C. Cantado, F. Dondi, Field-flow fractionation: theory, techniques, applications and the challenges, Crit. Rev. Anal. Chem., 36 (2006), 129-135

[12] G. Greyling, H. Pasch, Thermal Field-Flow Fractionation of Polymers, Springer: Heidelberg, Germany, 2019.

[13] G. Yohannes, M. Jussila, K. Hartonen, M.-L., Riekkola, Asymmetrical flow field-flow fractionation technique for separation and characterization of biopolymers and bioparticles, J. Chromatogr. A. 1218 (2011) 4104-4116

[14] W. Fraunhofer, G. Winter, The Use of Assymetrical Flow Field-Flow Fractionation in Pharmaceutics and Biopharmaceutics, Eur. J. Pharm. Biopharm. 58, 369 (2004).

[15] M. Baalousha, B. Stolpe, J.R. Lead, Flow field-flow fractionation for the analysis and characterization of natural colloids and manufactured nanoparticles in environmental systems: A critical review, J. Chromatogr. A. 1218 (2011) 4078-4103

[16] J. Ehrhart, A.-F. Mingotaud, F. Violleau, Asymmetrical flow field-flow fractionation with multi-angle light scattering and quasi elastic light scattering for characterization of poly(ethyleneglycol-b-ε-caprolactone) block copolymer self-assemblies used as drug carriers for photodynamic therapy. J. Chromatogr. A. 1218:27 (2011) 4249–4256.

[17] G. Greyling, H. Pasch, Tacticity separation of poly(methyl methacrylate) by multidetector thermal field-flow fractionation. Anal. Chem. 87 (2015) 3011–3018.

[18] G. Greyling, H. Pasch, Multidetector thermal field-flow fractionation as a novel tool for the microstructure separation of polyisoprene and polybutadiene. Macromol. Rapid. Commun. 35 (2014) 1846–1851.

[19] G. Greyling, H. Pasch, Fractionation of poly(butyl methacrylate) by molecular topology using multidetector thermal field-flow fractionation. Macromol. Rapid. Commun. 36 (2015) 2143–2148.

[20] P.J. Flory, Statistical Mechanics of Chain Molecules, John Wiley & Sons, .New York, 1969.

[21] Y. Gnanou, M. Fontanille, Organic and Physical Chemistry of Polymers. Hoboken, N.J.:Wiley-Interscience, 2008.

[22] G. Wypych (Ed.), Handbook of Solvents, ChemTec Publishing: Toronto-New York, 2001

[23] S. Krause, E. Cohn-Ginsberg, Dilution solution properties of tactic poly-(methyl methacrylates). II. Isotactic fractions in a theta solvent. Polym. 3 (1969) 1479-1481.

[24] K. Mahmood, A. Saeed, M. Siddiq, B. Mohammad, Light scattering studies of poly(methyl methacrylate) (PMMA) in different solvents. J. Chem. Soc. Pak. 27:1 (2005).

[25] Y. Tamai, T. Konishi, Y. Einaga, M. Fujii, H. Yamakawa, Mean-square radius of gyration of oligo- and poly(methyl methacrylate)s in dilute solutions. Macromolecules. 23 (1990) 4067-4075.

[26] M. Doğan, A. Kuntman, Study on conformational transition phenomena of poly(methyl methacrylate) in acetonitrile near theta conditions. Polym. Int. 49 (2000) 1648-1652.

[27] B. Wunderlich, Thermal Analysis of Polymeric Materials; Springer-Verlag: Heidelberg, Germany, 2005.

[28] J.M.G. Cowie, I.J. McEwen, Influence of microstructure on the upper and lower critical solution temperatures of poly (methyl methacrylate) solutions. J. Chem. Soc., Faraday Trans. 1. 72 (1976) 526-533.

[29] U.M. Apel, R. Hentschke, J. Helfrich, Molecular dynamics simulation of syndio- and isotactic poly (methyl methacrylate) in benzene. Macromolecules 28 (1995) 1778-1785.

Supporting Information

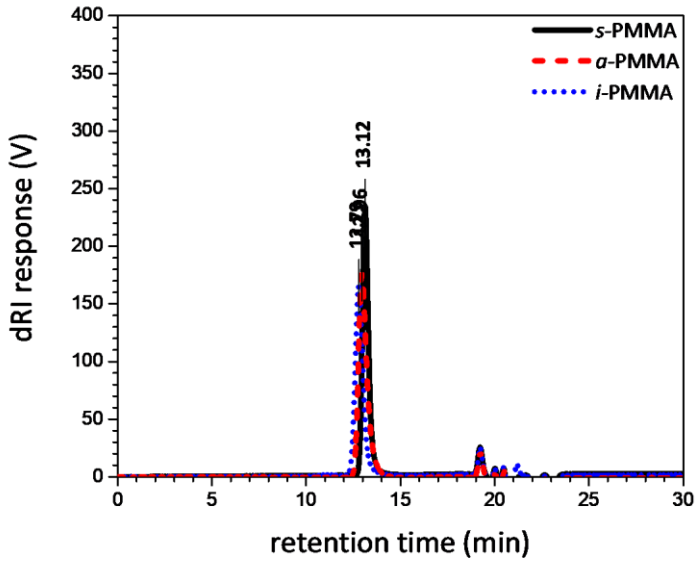

Figure S1 Superimposed dRI elugrams of *s*-PMMA, *a*-PMMA and *i*-PMMA analysed by SEC with THF as mobile phase at a flow rate of 1.0 ml.min^{-1} and the column temperature set to 30°C.

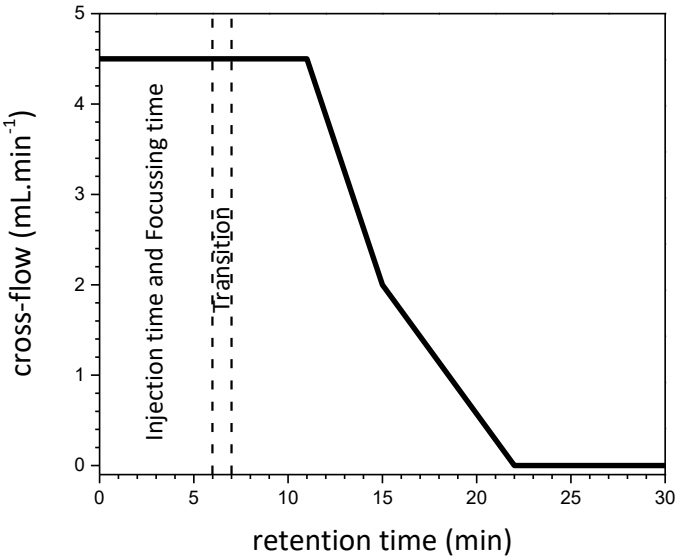

Figure S2 Cross-flow profile used for the analysis of *s*-PMMA, *a*-PMMA and *i*-PMMA in THF, $CHCl_3$ and ACN as carrier liquids at variable AsFlFFF channel temperatures.

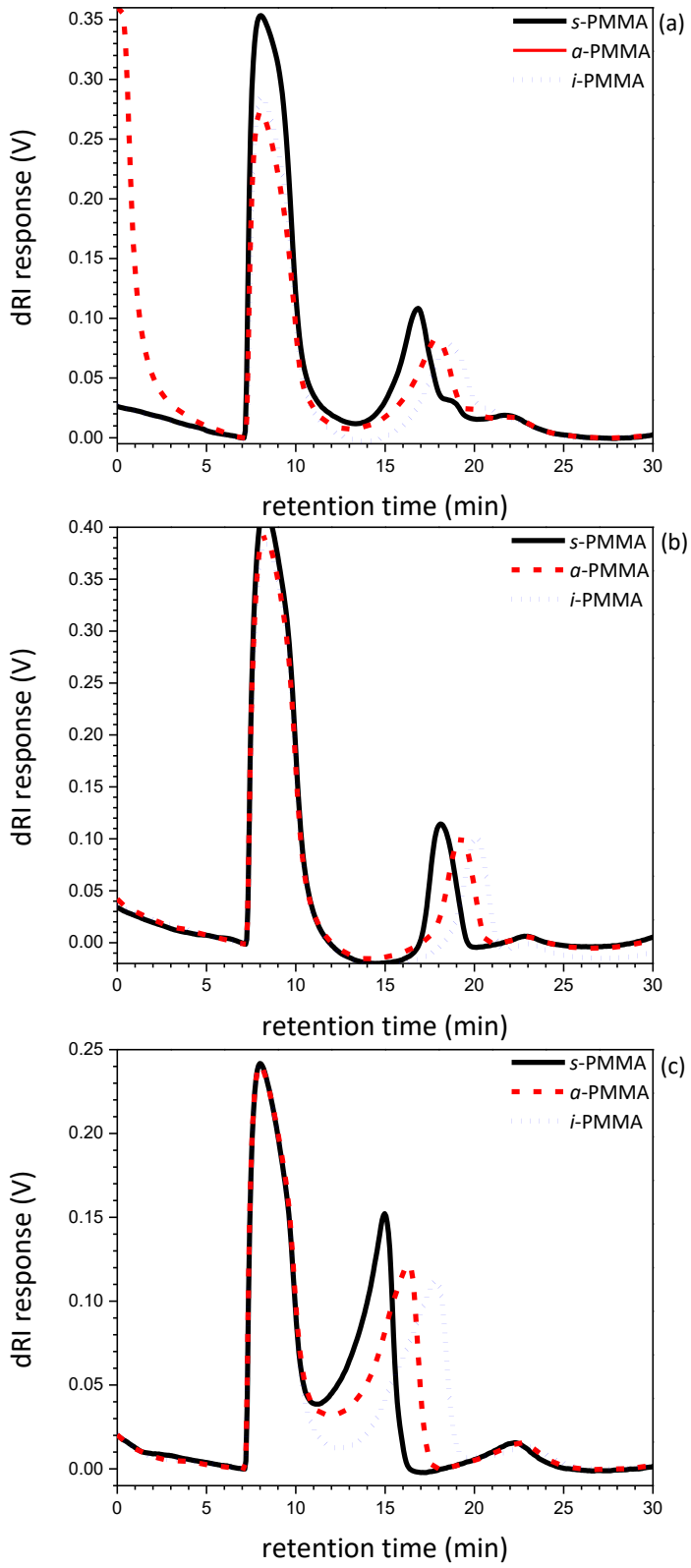

Figure S3 Superimposed dRI fractograms of *s*-PMMA, *a*-PMMA and *i*-PMMA in **(a)** THF, **(b)** $CHCl_3$ and **(c)** ACN analysed by AsFlFFF at a channel temperature of 25°C.

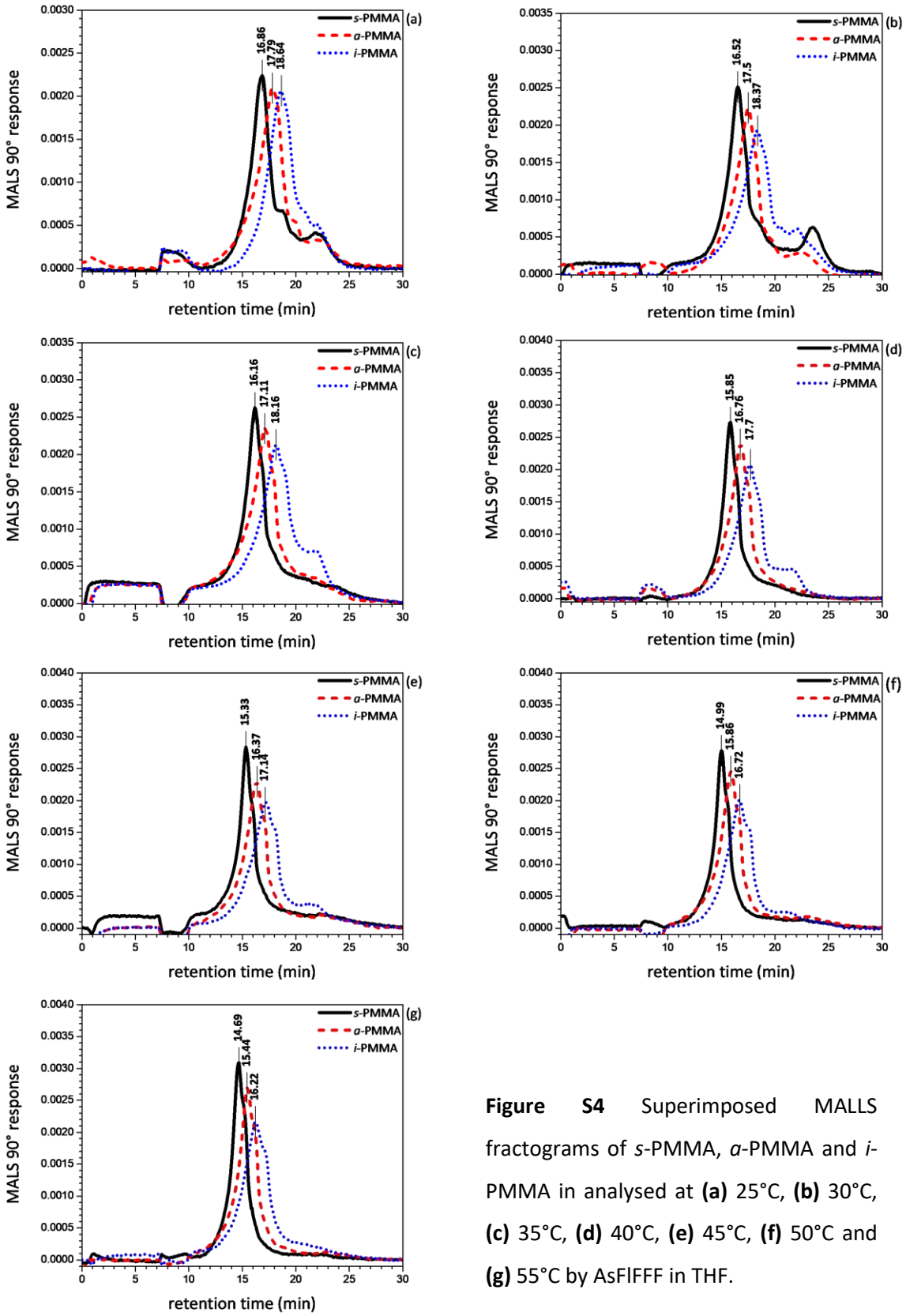

Figure S4 Superimposed MALLS fractograms of *s*-PMMA, *a*-PMMA and *i*-PMMA in analysed at **(a)** 25°C, **(b)** 30°C, **(c)** 35°C, **(d)** 40°C, **(e)** 45°C, **(f)** 50°C and **(g)** 55°C by AsFlFFF in THF.

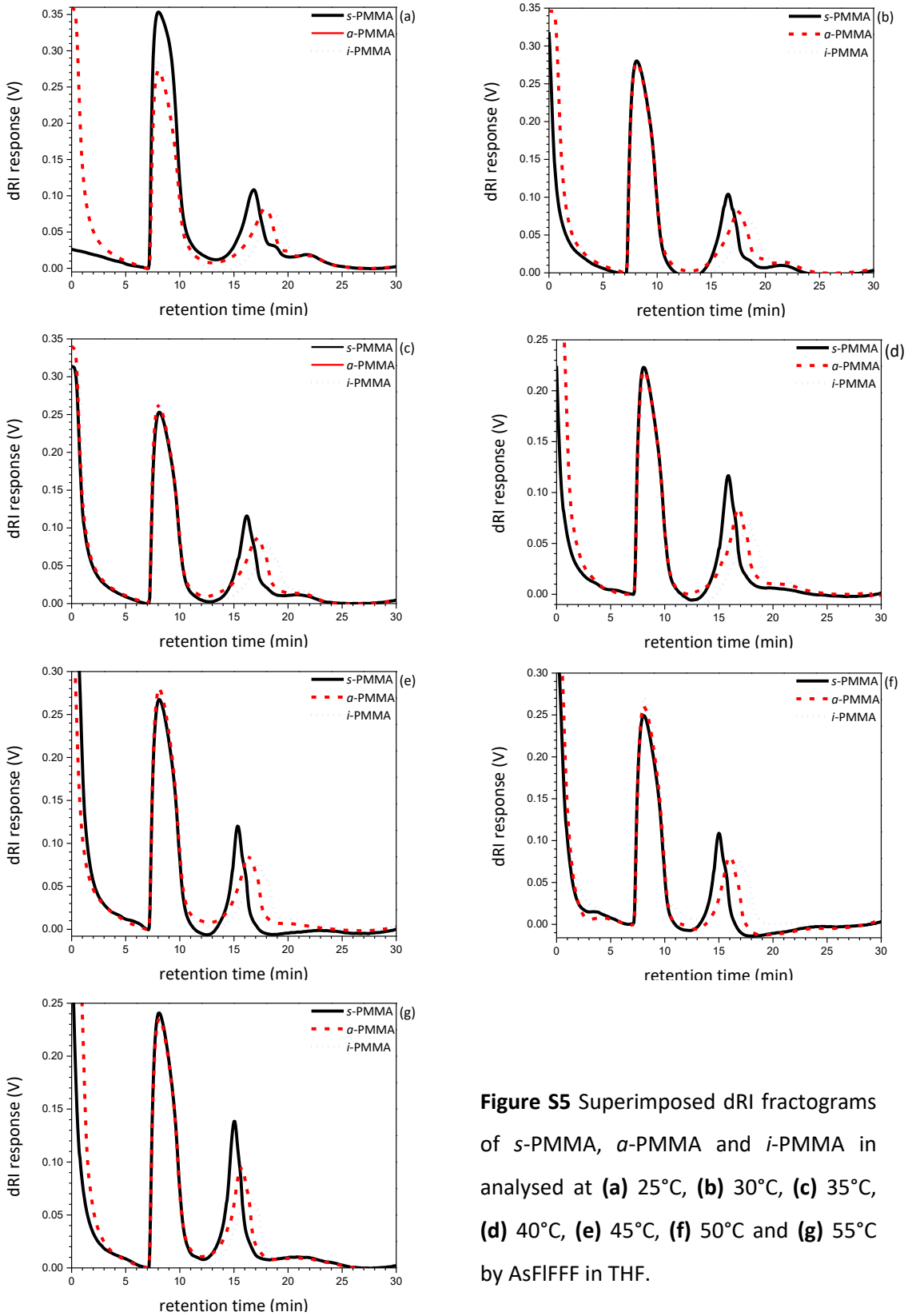

Figure S5 Superimposed dRI fractograms of *s*-PMMA, *a*-PMMA and *i*-PMMA in analysed at **(a)** 25°C, **(b)** 30°C, **(c)** 35°C, **(d)** 40°C, **(e)** 45°C, **(f)** 50°C and **(g)** 55°C by AsFlFFF in THF.

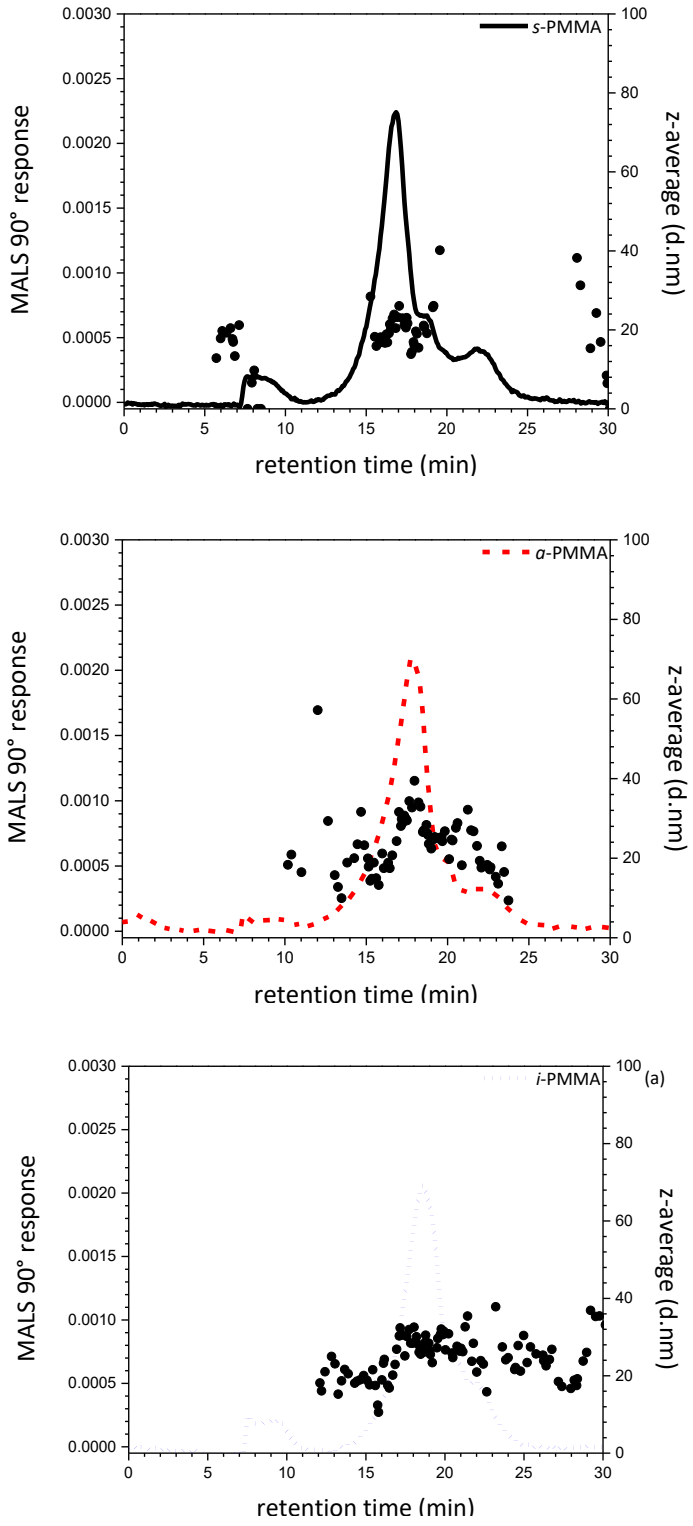

Figure S6 Superimposed z-average diameters (d.nm) determined for each PMMA sample by online DLS with the PMMA tacticity MALLS fractograms at 25°C as analysed by AsFlFFF with THF as carrier liquid.

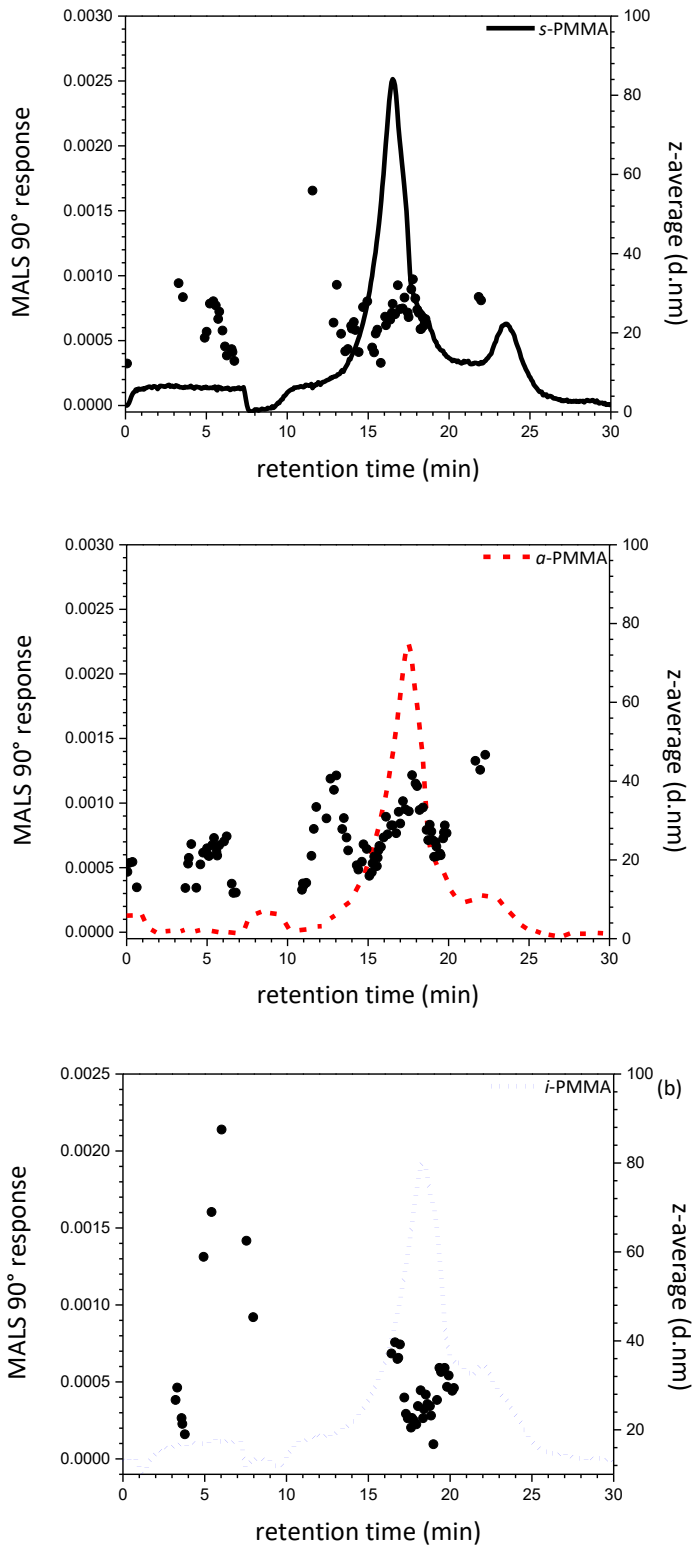

Figure S7 Superimposed z-average diameters (d.nm) determined for each PMMA sample by online DLS with the PMMA tacticity MALLS fractograms at 30°C as analysed by AsFlFFF with THF as carrier liquid.

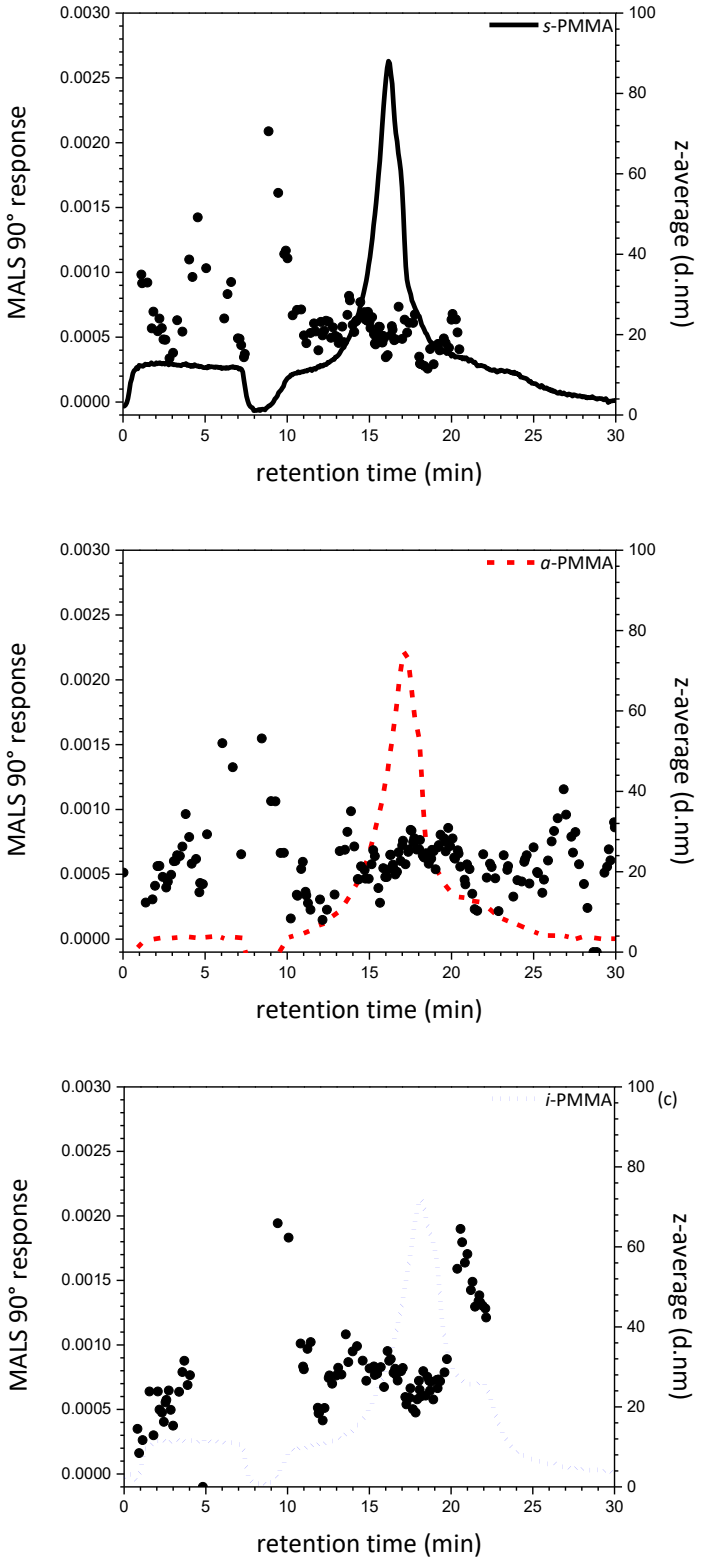

Figure S8 Superimposed z-average diameters (d.nm) determined for each PMMA sample by online DLS with the PMMA tacticity MALLS fractograms at 35°C as analysed by AsFlFFF with THF as carrier liquid.

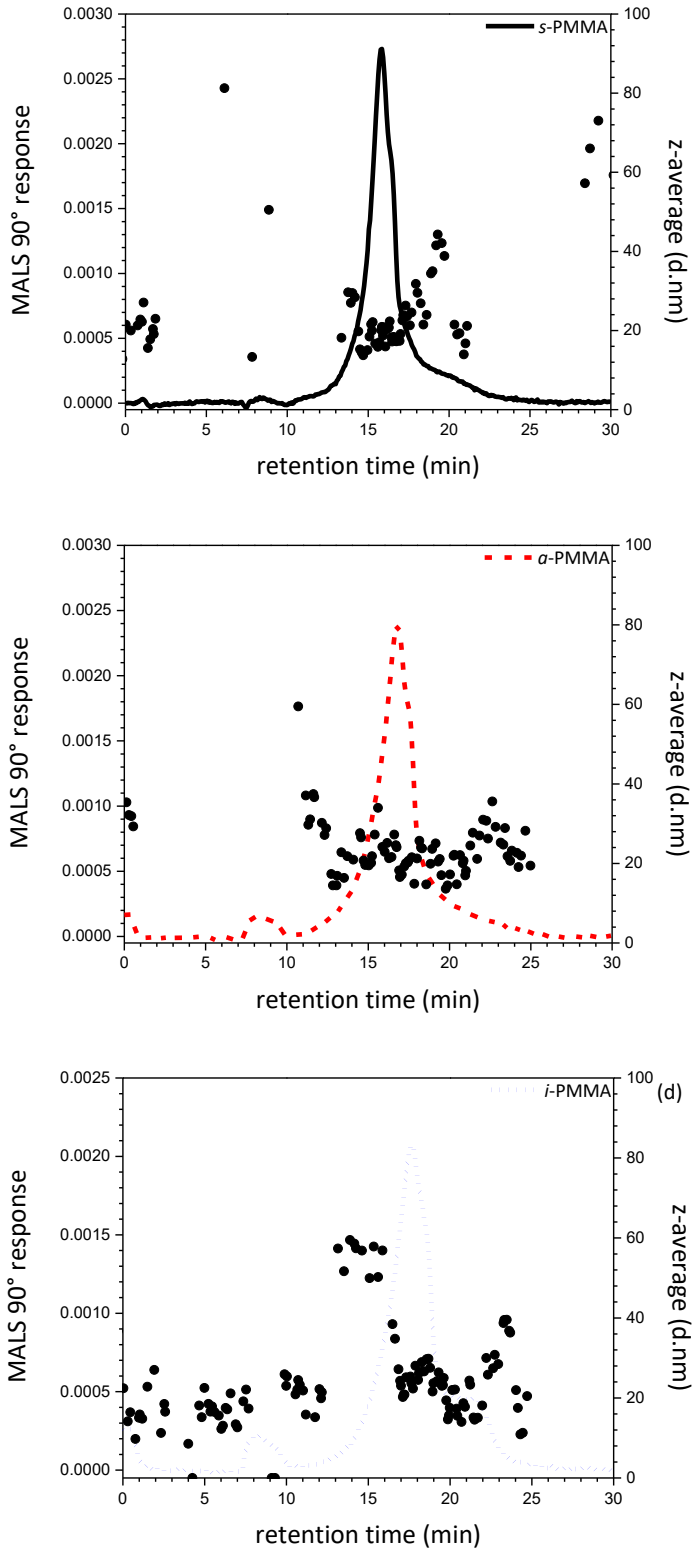

Figure S9 Superimposed z-average diameters (d.nm) determined for each PMMA sample by online DLS with the PMMA tacticity MALLS fractograms at 40°C as analysed by AsFlFFF with THF as carrier liquid.

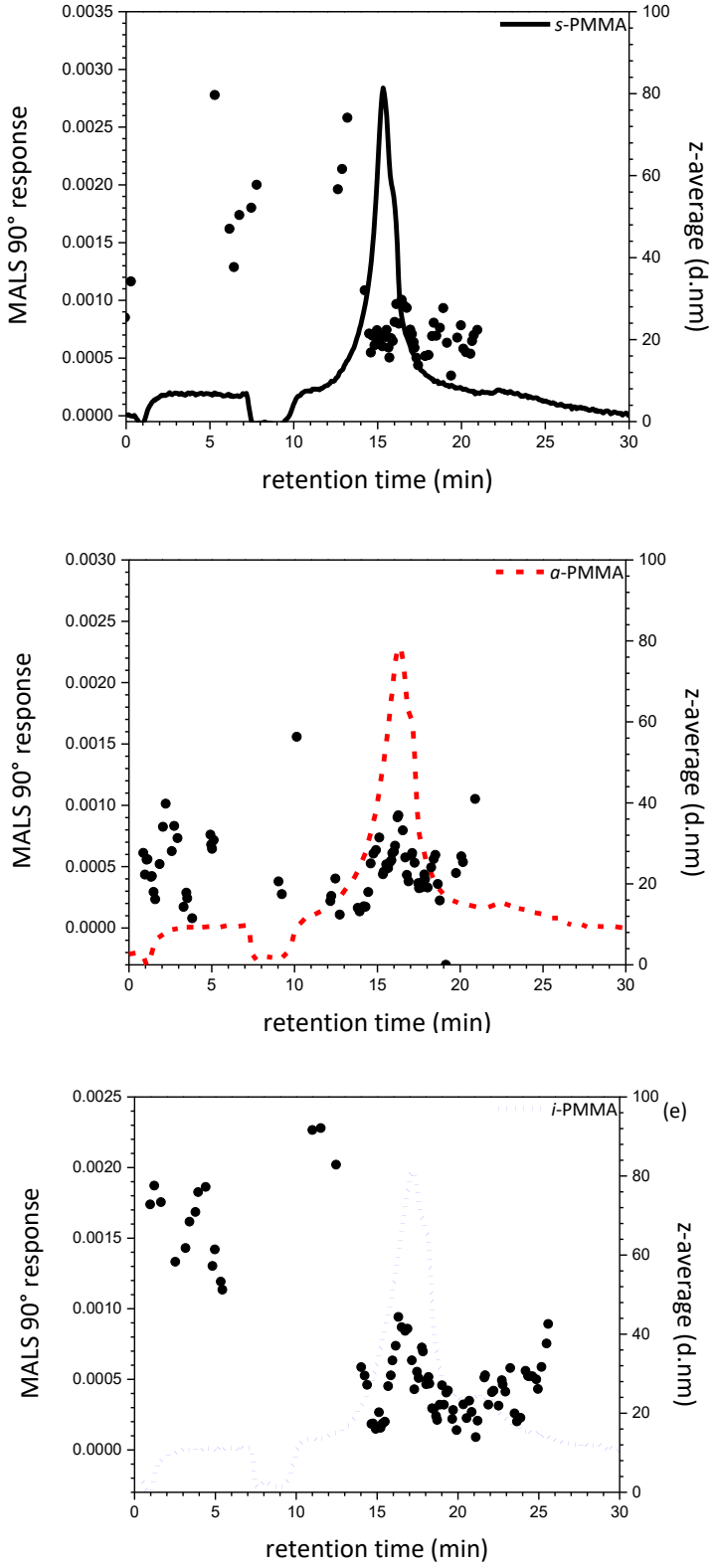

Figure S10 Superimposed z-average diameters (d.nm) determined for each PMMA sample by online DLS with the PMMA tacticity MALLS fractograms at 45°C as analysed by AsFlFFF with THF as carrier liquid.

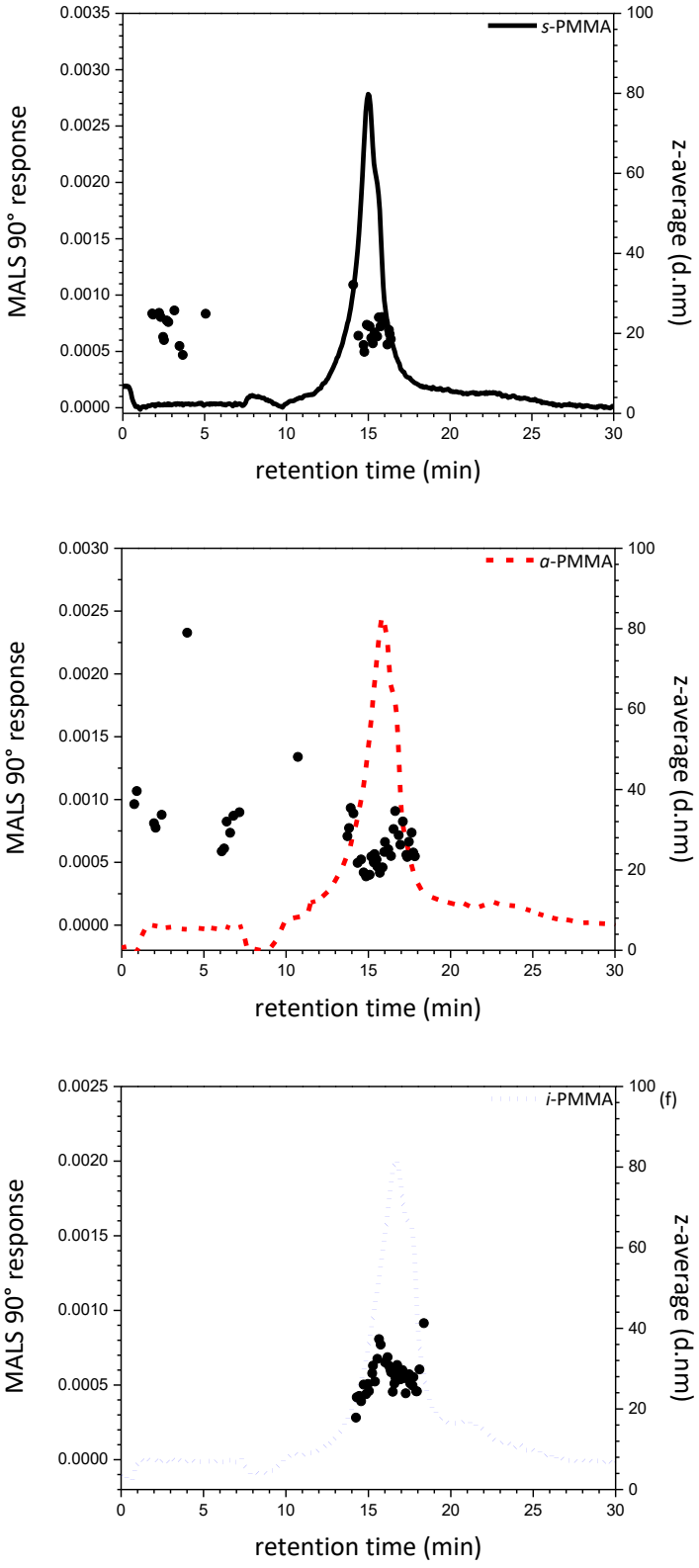

Figure S11 Superimposed z-average diameters (d.nm) determined for each PMMA sample by online DLS with the PMMA tacticity MALLS fractograms at 50°C as analysed by AsFlFFF with THF as carrier liquid.

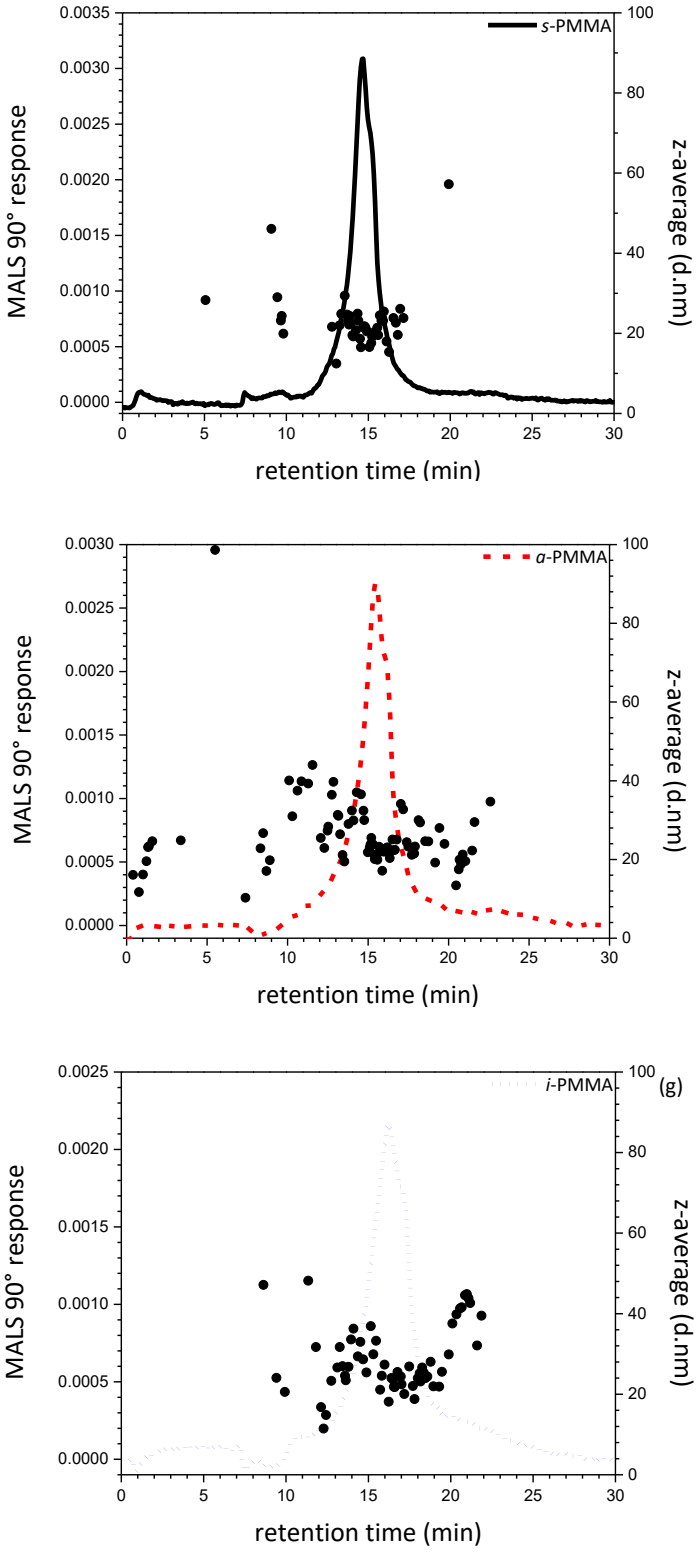

Figure S12 Superimposed z-average diameters (d.nm) determined for each PMMA sample by online DLS with the PMMA tacticity MALLS fractograms at 55°C as analysed by AsFlFFF with THF as carrier liquid.

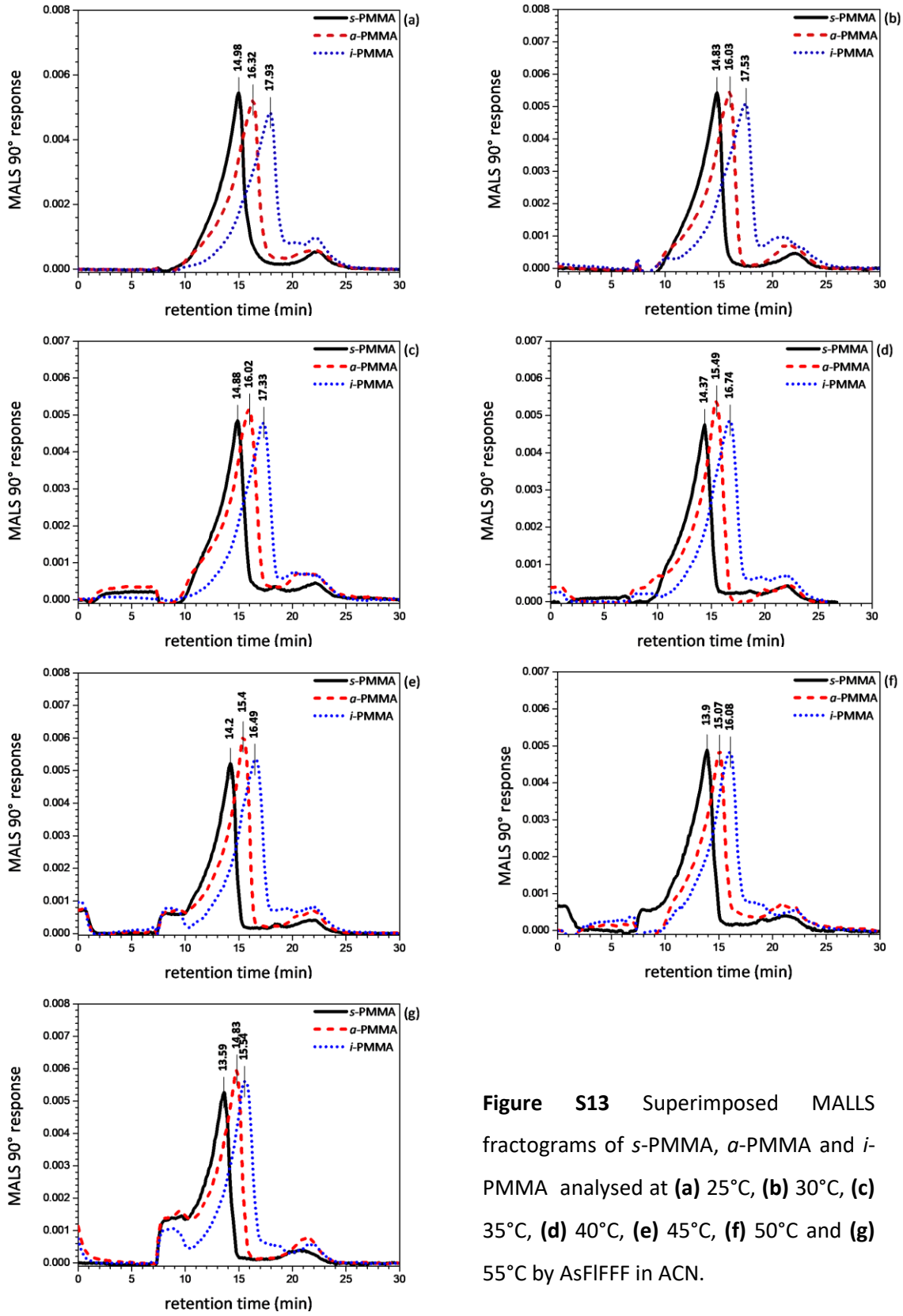

Figure S13 Superimposed MALLS fractograms of *s*-PMMA, *a*-PMMA and *i*-PMMA analysed at **(a)** 25°C, **(b)** 30°C, **(c)** 35°C, **(d)** 40°C, **(e)** 45°C, **(f)** 50°C and **(g)** 55°C by AsFlFFF in ACN.

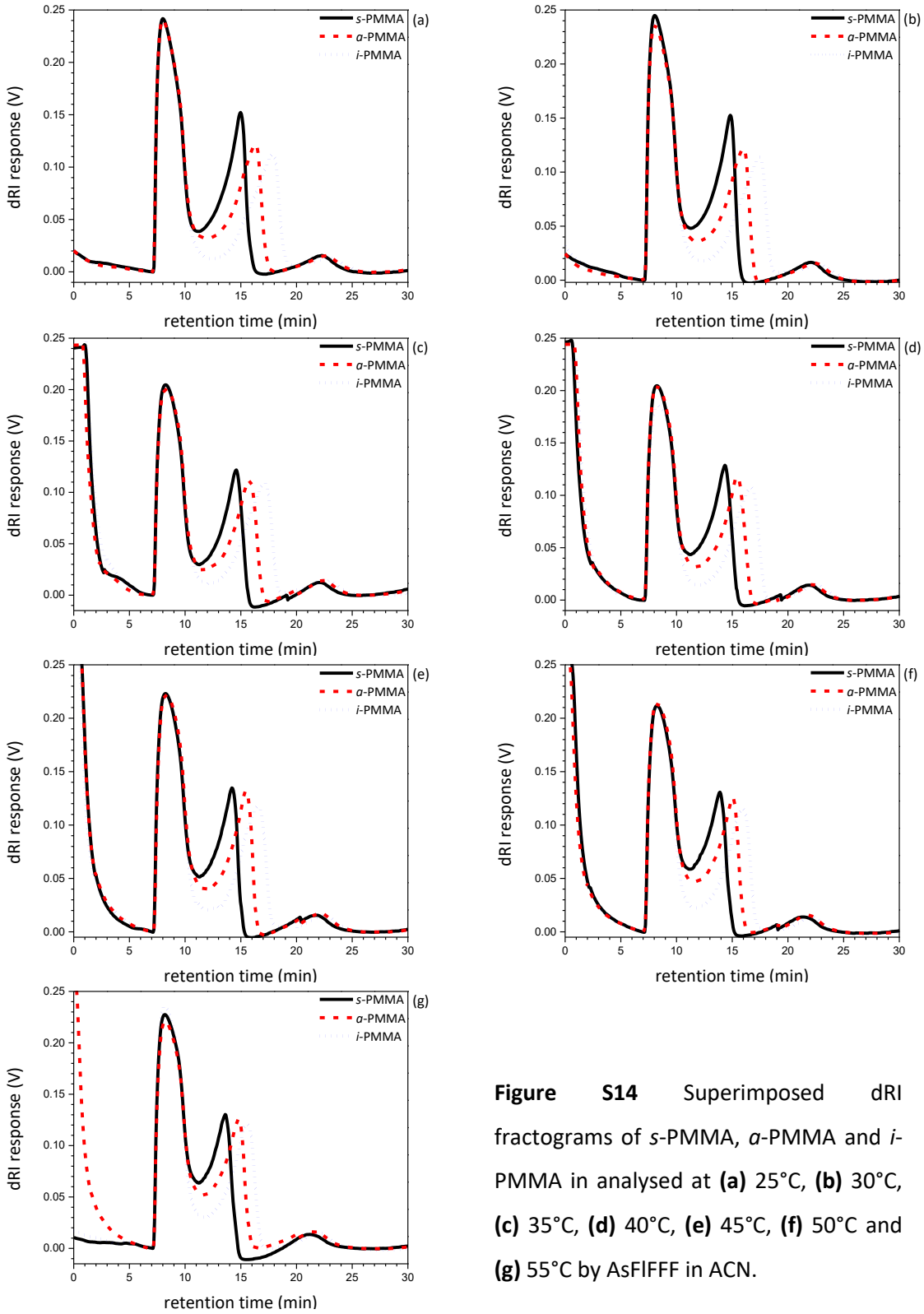

Figure S14 Superimposed dRI fractograms of *s*-PMMA, *a*-PMMA and *i*-PMMA in analysed at **(a)** 25°C, **(b)** 30°C, **(c)** 35°C, **(d)** 40°C, **(e)** 45°C, **(f)** 50°C and **(g)** 55°C by AsFlFFF in ACN.

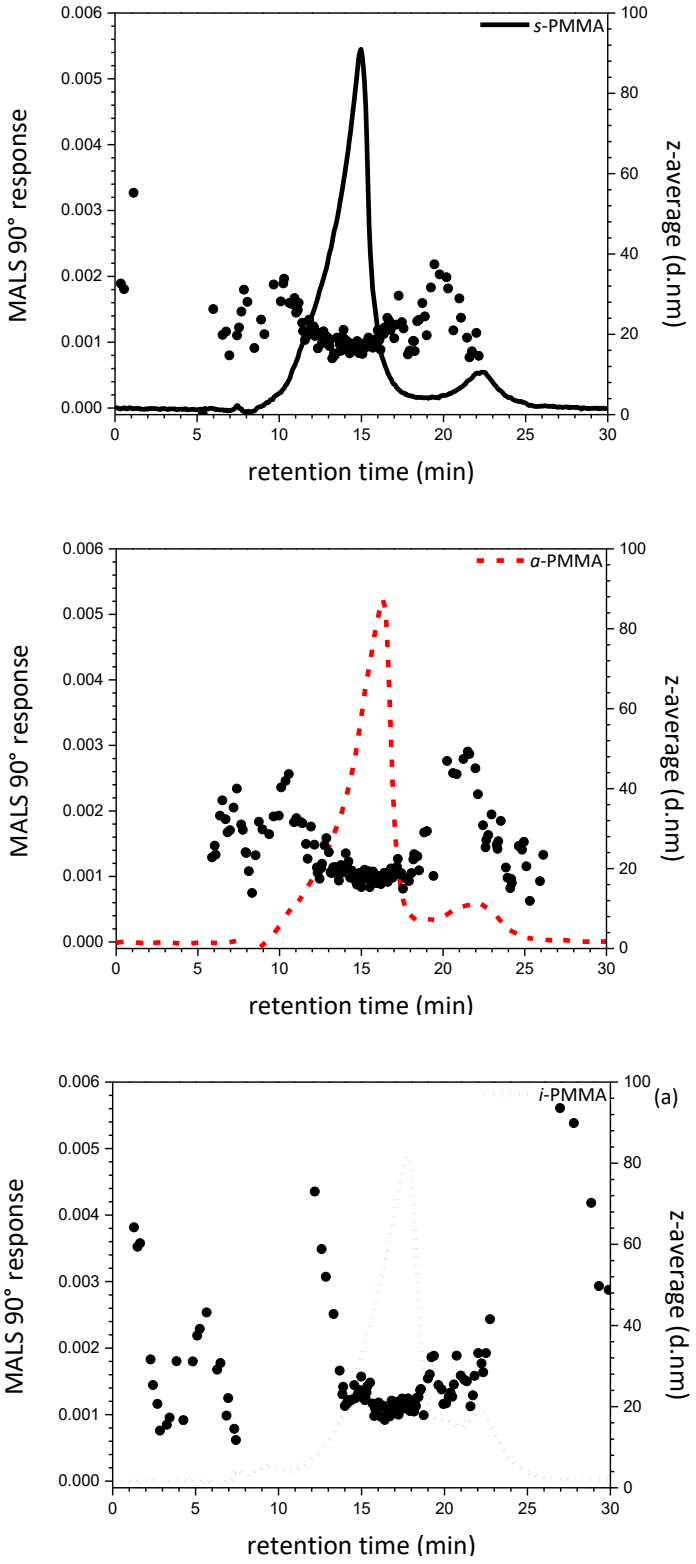

Figure S15 Superimposed z-average diameters (d.nm) determined for each PMMA sample by online DLS with the PMMA tacticity MALLS fractograms at 25°C as analysed by AsFlFFF with ACN as carrier liquid.

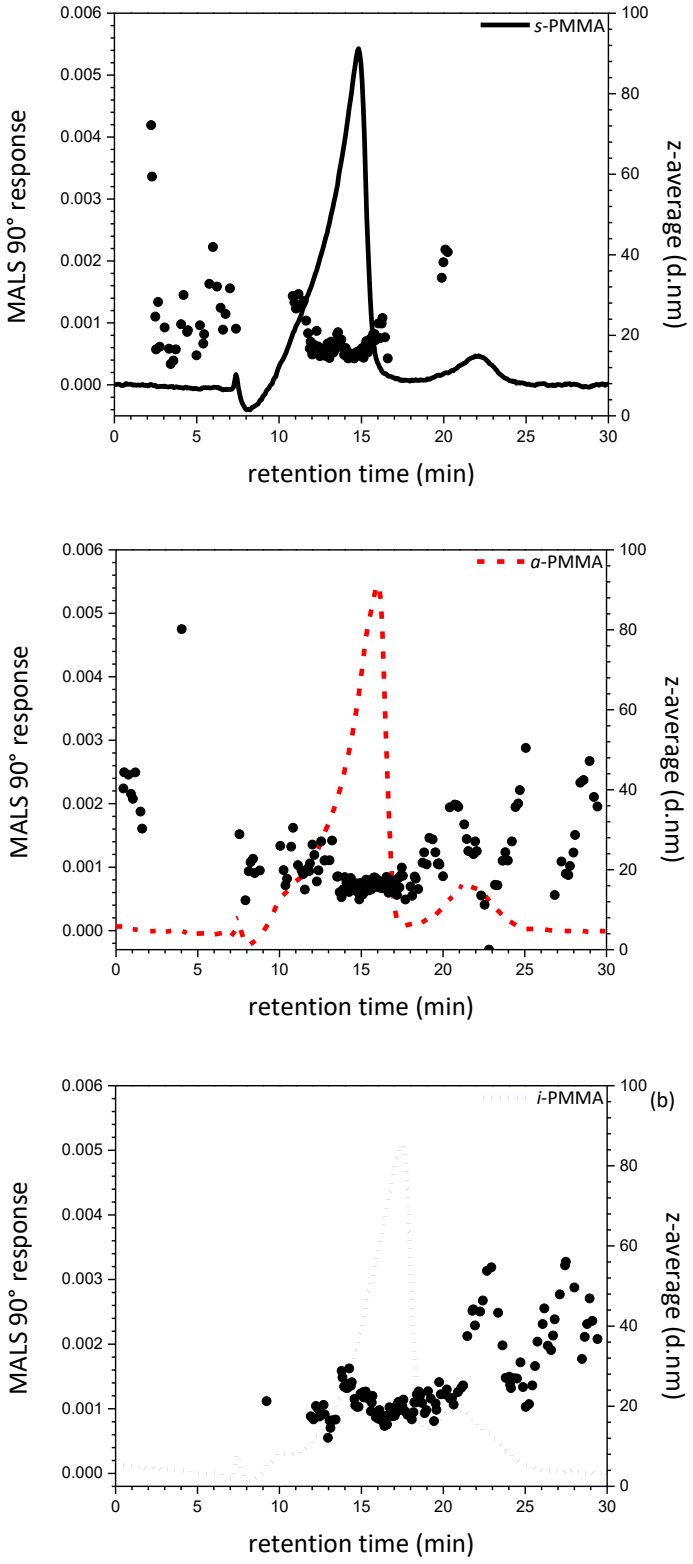

Figure S16 Superimposed z-average diameters (d.nm) determined for each PMMA sample by online DLS with the PMMA tacticity MALLS fractograms at 30°C as analysed by AsFlFFF with ACN as carrier liquid.

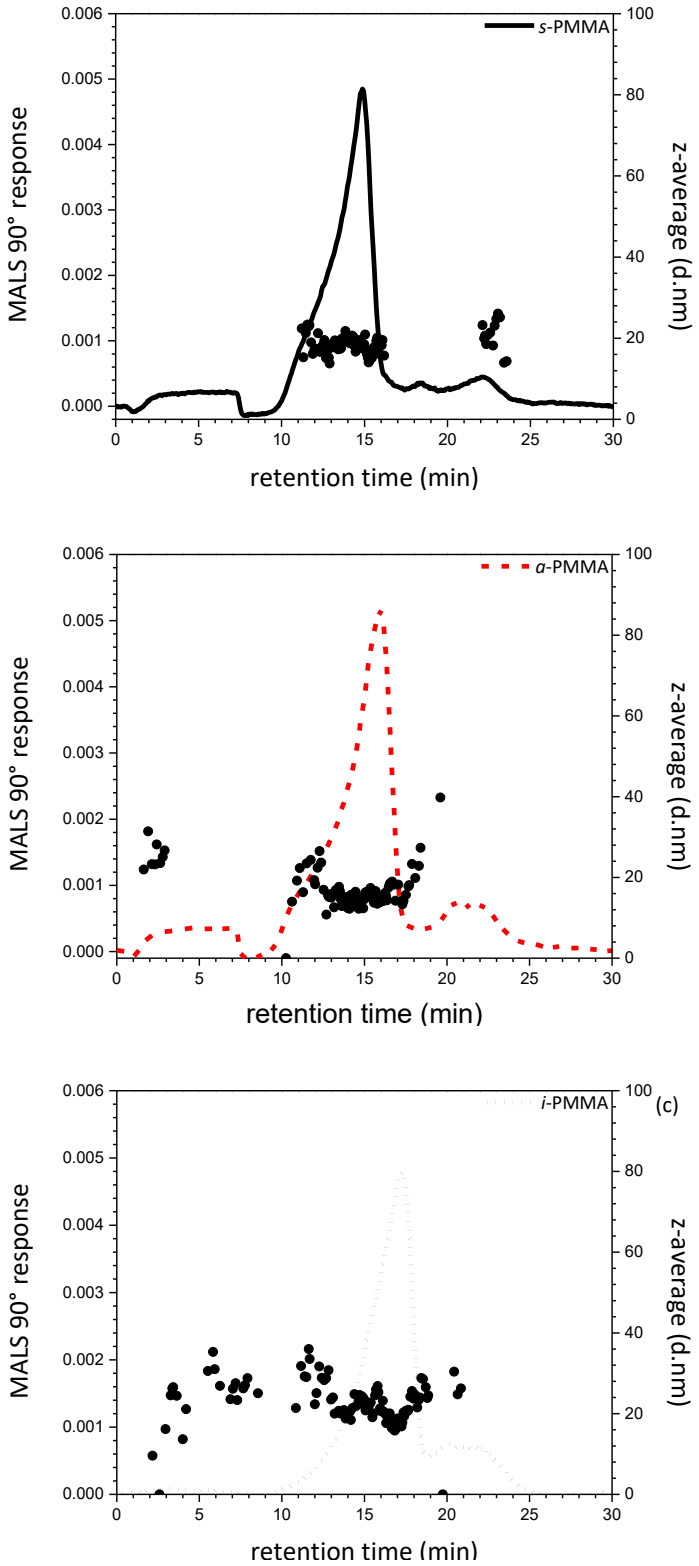

Figure S17 Superimposed z-average diameters (d.nm) determined for each PMMA sample by online DLS with the PMMA tacticity MALLS fractograms at 35°C as analysed by AsFlFFF with ACN as carrier liquid.

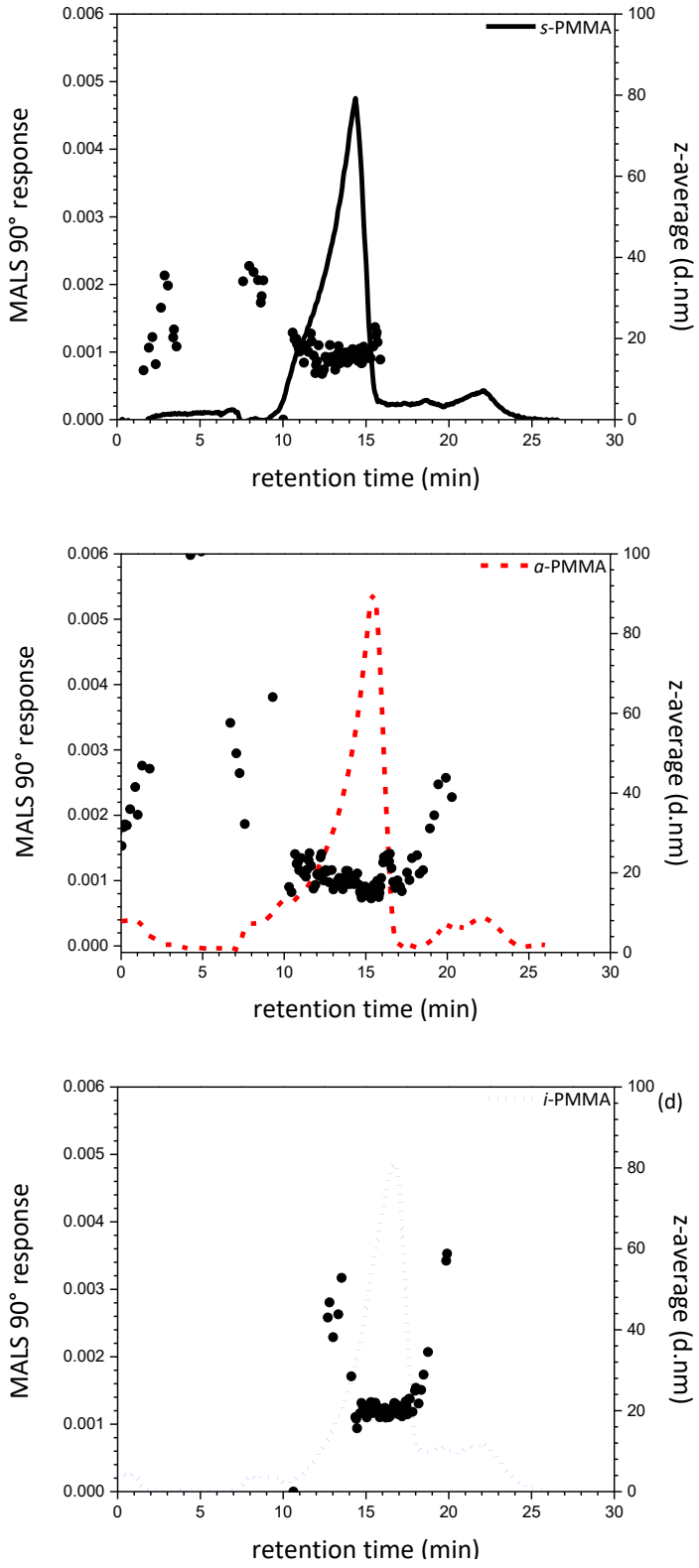

Figure S18 Superimposed z-average diameters (d.nm) determined for each PMMA sample by online DLS with the PMMA tacticity MALLS fractograms at 40°C as analysed by AsFlFFF with ACN as carrier liquid.

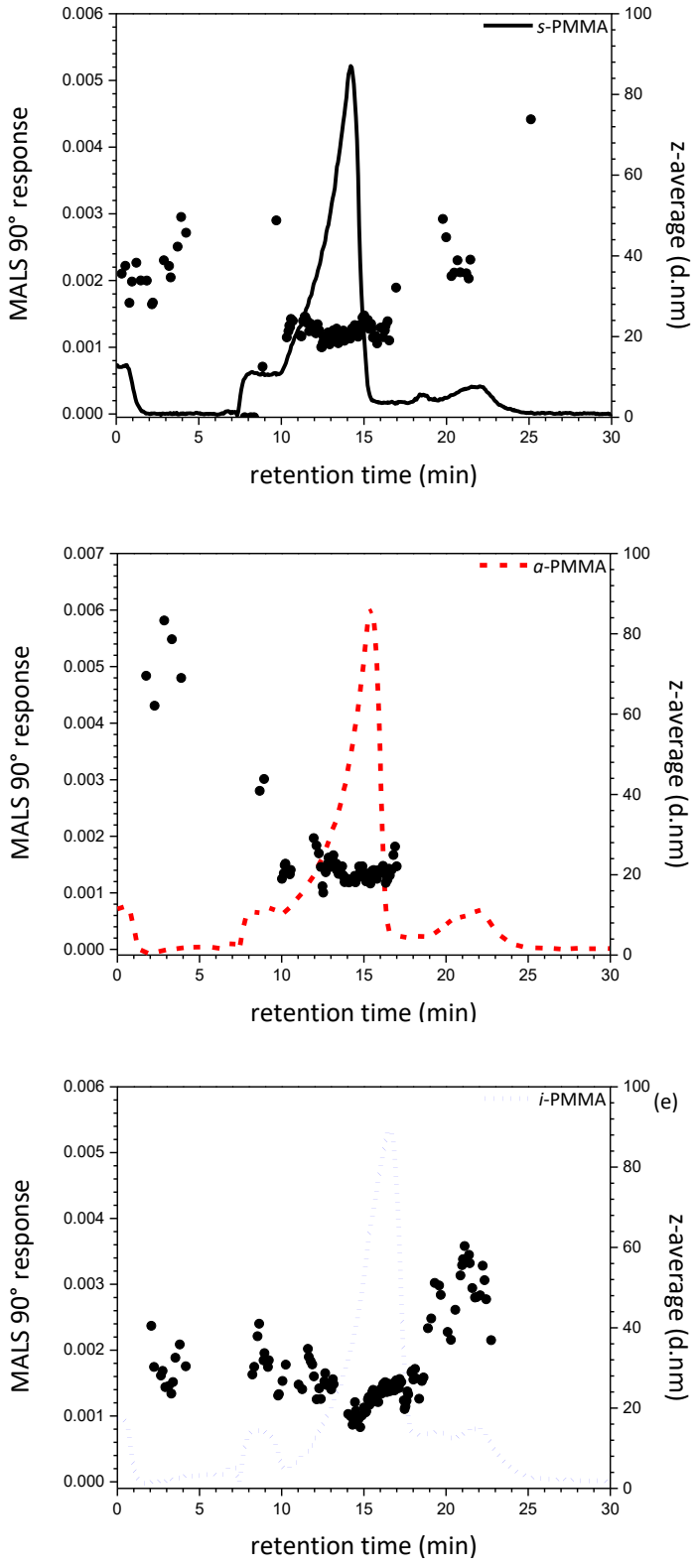

Figure S19 Superimposed z-average diameters (d.nm) determined for each PMMA sample by online DLS with the PMMA tacticity MALLS fractograms at 45°C as analysed by AsFlFFF with ACN as carrier liquid.

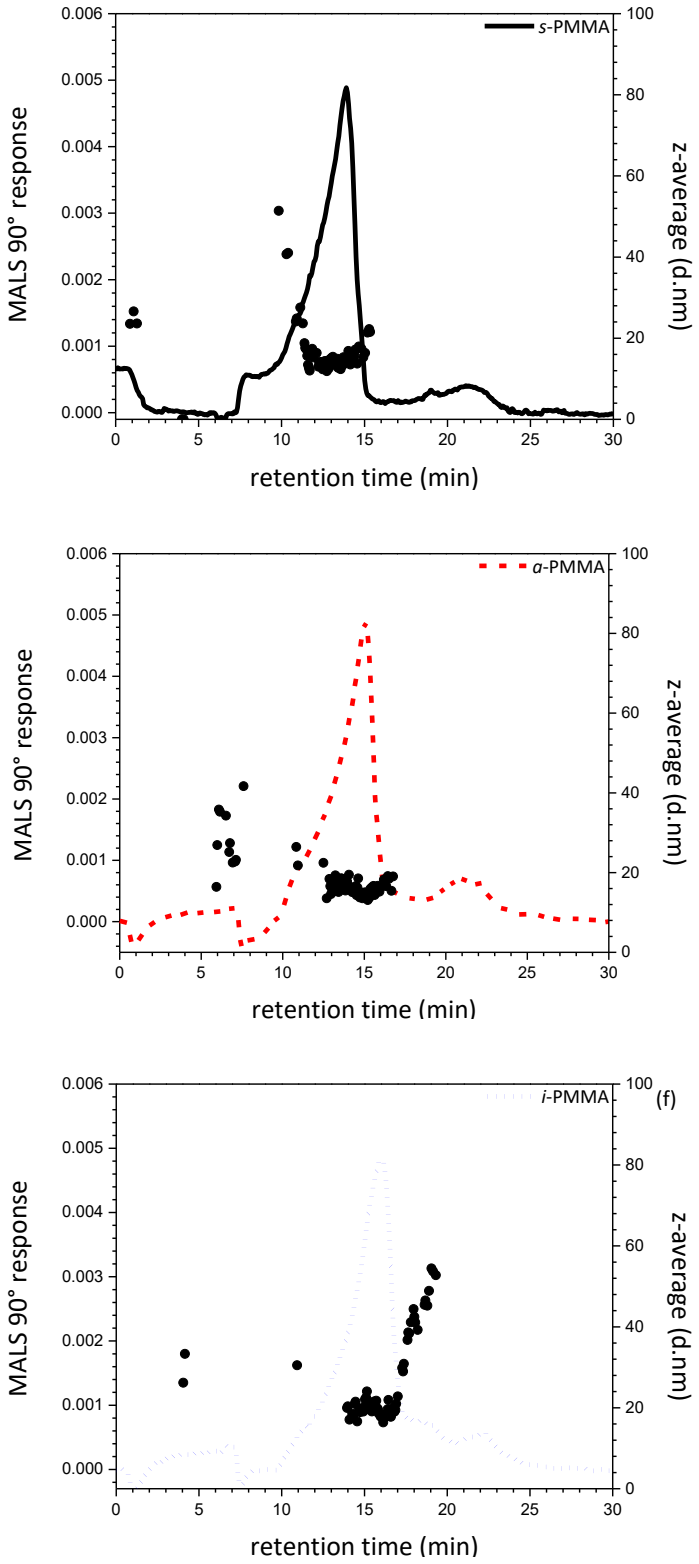

Figure S20 Superimposed z-average diameters (d.nm) determined for each PMMA sample by online DLS with the PMMA tacticity MALLS fractograms at 50°C as analysed by AsFlFFF with ACN as carrier liquid.

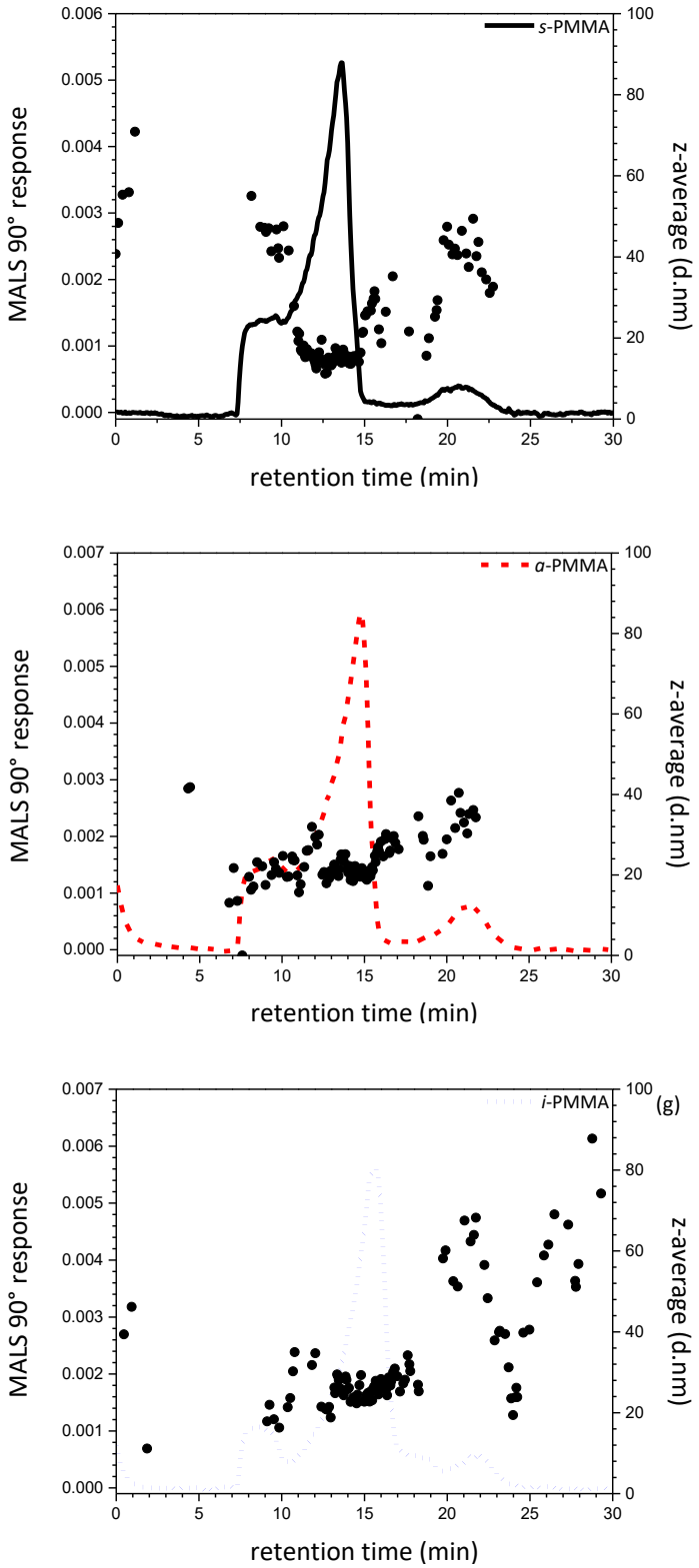

Figure S21 Superimposed z-average diameters (d.nm) determined for each PMMA sample by online DLS with the PMMA tacticity MALLS fractograms at 55°C as analysed by AsFlFFF with ACN as carrier liquid.

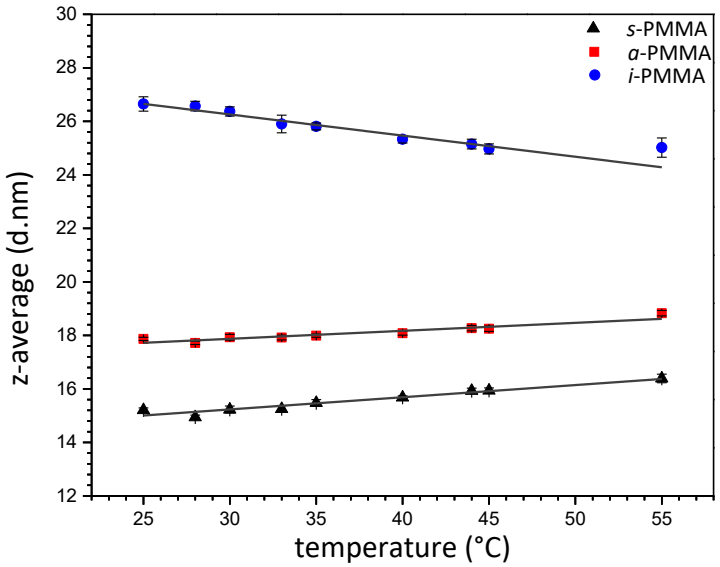

Figure S22 The size of each PMMA sample as a function of temperature as determined off-line with the aid of a DLS instrument. The sample concentration was 5.0 mg.mL^{-1} and ACN was used as solvent.

CHAPTER 5

CONCLUSIONS AND FUTURE WORK

5.1. Conclusions

The focus of this research was to demonstrate the versatility and separation power of field-flow fractionation (FFF) as an analytical technique for the characterization of complex polymers. The objective was achieved by (1) illustrating that thermal field-flow fractionation (ThFFF) could be coupled in an online comprehensive multidimensional configuration with size exclusion chromatography (SEC) and (2) by demonstrating that asymmetric flow field-flow fractionation (AsFlFFF) is a powerful analytical tool that, by careful selection of experimental parameters and conditions, enables the separation various isomers of PMMA.

One of the main aims of the research was to develop a comprehensive online multidimensional protocol for the coupling of ThFFF, a channel-based technique and SEC, a column-based technique. ThFFF was used in the first dimension, where the driving force for separation was the Soret coefficient (S_T), which is based on the interaction of thermal diffusion with the normal (translational) diffusion. SEC was used in the second dimension and separation in SEC is governed by the difference in the hydrodynamic diameter of the analyte molecules. In order to couple the two fundamentally different techniques, optimization of the experimental conditions was required for each separation dimension as they are interrelated. For the optimization of the various experimental parameters, blends of poly(styrene) and poly(methyl methacrylate) homopolymers were used. Experimental conditions optimized and investigated, included the type of temperature gradient method applied, flow rate, sample concentration and temperature, as well as relaxation time. In ThFFF, different temperature gradient profiles can be applied across the channel to achieve separation. In the case of a power decay temperature gradient profile, it was found that even though it decreased the analysis time in the first dimension, information and calculation of the thermal diffusion coefficient (D_T) becomes complex due to the continuous change in temperature. As such, in order to obtain D_T, which correlates to the chemical composition, a constant temperature gradient was applied across the channel. The detection limit after the second dimension was also an important experimental parameter that needed to be addressed. Due to multiple separation steps, the local analyte concentration can be too low for a given detector to yield a suitable chromatogram. However, it was observed that at high sample concentration (1.5 $mg.mL^{-1}$ or higher) channel overloading occurred and bimodality was observed in the eluting peaks. It was found that a low sample concentration of 0.5 $mg.mL^{-1}$ could be used without the occurrence of channel overloading. In addition, a universal concentration detector, ELSD, was used in the second dimension as it turned out to be the most suitable and sensitive detector.

Once the optimized experimental parameters were established for the multidimensional protocol, the objective was to illustrate and validate the capabilities of the ThFFF X SEC technique. This was achieved by separating and characterizing various blends of poly(styrene)-***b***-poly(methyl methacrylate) (PS-***b***-PMMA) block copolymers as well as blends of PS-***b***-PMMA with PS and PMMA homopolymers. THF was used as the carrier liquid in both dimensions as it is a thermodynamically good solvent for both PS and PMMA. It was demonstrated that a blend of PS homopolymer and PS-***b***-PMMA could be separated into its two components and that not only could the PS content be quantified from the ELSD trace, but the molecular mass of PS could be determined from S_T. In the case of the block copolymer, the quantification thereof was more complex as the signal from the ELSD depends on the concentration of the sample and may be sensitive to the copolymer composition. This was a similar case for the molecular mass characterization of the block copolymer, as S_T could not be used to determine the molecular mass of the copolymer. S_T in this case depends on molecular mass (via D) and composition (via D_T). However, with SEC used in the second dimension, the molecular mass of both components could be determined as SEC is based on the hydrodynamic sizes. The benefit of using SEC in the second dimension was thus illustrated. A second blend, consisting of PMMA and PS-***b***-PMMA, could not be sufficiently separated in ThFFF. However, separation was improved in the second dimension, SEC, and the blend could be characterized with regard to molecular mass with the aid of a dual concentration detection method that was hyphenated to the ThFFF X SEC set-up. The dual concentration detection method proved to be beneficial for the quantitative analysis of the PMMA/PS-***b***-PMMA blend. PMMA is optically transparent at the set wavelength of 270 nm of the UV-detector; hence only the copolymer (containing styrene units) was detected, which allowed for selective detection. Thus, even though insufficient separation was achieved between PMMA and PS-***b***-PMMA, it was possible to analyse the copolymer with regard to its molecular mass and enhance the information obtained with the aid of selective detection.

The second aim presented in this dissertation was to use asymmetric flow field-flow fractionation (AsFlFFF) for the microstructure-based separation of polymers with different tacticities. To achieve this, the solution behaviour of syndiotactic- (*s*-PMMA), atactic- (*a*-PMMA) and isotactic (*i*-PMMA) poly(methyl methacrylate) of similar molecular masses in solvents with different thermodynamic properties was investigated. In addition to developing a separation method, the effects of the solvent quality and channel temperature on the separation were investigated. The sensitivity of AsFlFFF was illustrated, as PMMA samples with different tacticities but similar molecular masses had different retention times within the channel. It was concluded that the thermodynamic quality of the carrier liquid can have a significant influence on the retention behaviour of polymers in AsFlFFF. It

was shown that the separation of *s*-PMMA and *i*-PMMA can be improved by using a theta solvent (acetonitrile) as the carrier liquid instead of thermodynamically good solvents such as tetrahydrofuran (THF) and chloroform ($CHCl_3$). In addition, it was found that by using a non-stereocomplexing solvent for PMMA, such as chloroform, a blend of *s*-PMMA and *i*-PMMA could be separated. Lastly, it was established that the channel temperature at which the experiments were conducted, had an influence on the retention behaviour of the PMMA samples. For THF as carrier liquid it was noticed that the maximum difference in retention between *s*-PMMA and *i*-PMMA, can be achieved at a channel temperature of 35°C. In the case of ACN being the carrier liquid, it was observed that the retention behaviour of *i*-PMMA was significantly more influenced by a change in temperature compared to *s*-PMMA and *a*-PMMA.

5.2. Future work

The coupled technique, ThFFF X SEC, has been shown to be a useful alternative approach for the characterization of homopolymers, block copolymers and the blends thereof. Both AsFlFFF and ThFFF are capable of characterizing self-assemblies e.g. micelles and vesicles in terms of size, molecular mass, chemical composition and their corresponding distributions [1, 2, 3-5]. SEC has also been used to separate and characterize micelles. However, during the SEC analysis of micelles, they can be trapped in the column or adsorption onto the stationary phase and micelles dissociation in the column can occur. [6, 7] In SEC, analytes with the same hydrodynamic diameter will co-elute, regardless of their chemical composition.

In recent years, mixed micelles have attracted interest, due to their potential application in the biomedical field. Mixed micelles consist of two or more block copolymer and/or homopolymer structures or nanoparticles encapsulated within the micelle. Block copolymers self-assemble into various nanostructures based on a number of factors, which include (1) ratios of the blocks of the block copolymer, (2) solubility of the blocks in selective solvents, (3) concentration, (4) temperature and (5) pH of the solution. Micelles are, therefore, multiply distributed in molecular properties such as aggregation number, size, molecular mass, morphology, and core-corona composition. As the distributed properties greatly influence the application of micelles, an advanced analytical separation approach is required to obtain information regarding the various molecular distributions present within micelles [8-10].

Thus, with the aid of coupling ThFFF (driven by the normal and thermal diffusion coefficients) comprehensively online with SEC (driven by the difference in hydrodynamic diameter), the two complementary separation methods can potentially be used to separate micelles according to

chemical composition, while simultaneously determining size, and molecular mass distribution. In addition, with the aid of SEC, the experiment can potentially provide insight into the formation of mixed micelles and quantify the distribution of different block copolymers within the mixed micelles.

In additional future work, the coupling of ThFFF in an online comprehensive multidimensional configuration can be explored in more detail. A complementary column-based method to that of SEC are monolithic silica columns. The coupling of ThFFF with a monolithic column as the second dimension can have many experimental advantages over the use of a SEC column. The use of monolithic columns as a stand-alone analytical method as well as the application thereof in a multidimensional configuration for the characterization of complex polymers, have been reported [11-13]. Monolithic columns have a high surface area as they consist of a continuous porous rod structure consisting of a network of mesopores, making monolithic columns ideally suited for the characterization of high molecular mass polymers [11-13]. In addition, it has been shown that minimal shear degradation occurs in monolithic columns. One of the main advantages of monolithic columns is that they can operate at high flow rates, while peak capacity is maintained [11-13]. As a result, faster analysis times would be possible as compared to long analysis times associated with the ThFFF X SEC protocol. Therefore, monolithic columns would be an ideally suited analytical approach to be used in a multidimensional configuration with ThFFF.

References

[1] G. Greyling, H. Pasch, Characterisation of block copolymer self-assemblies by thermal field-flow fractionation, Polym. Int. 66 (2017) 745–751.

[2] U.L. Muza, G. Greyling, H. Pasch, Characterization of complex polymer self-assemblies and large aggregates by multidetector thermal field-flow fractionation, Anal. Chem. 89 (2017) 7216–7224.

[3] U.L. Muza, G. Greyling, H. Pasch, Core microstructure, morphology and chain arrangement of block copolymer self-assemblies as investigated by thermal field-flow fractionation. J. Chromatogr. A. 1562 (2018) 87–95.

[4] G. Greyling, H. Pasch, Multidetector thermal field-flow fractionation as a unique tool for the tacticity-based separation of poly(methyl methacrylate)-polystyrene block copolymer micelles. J. Chromatogr. A. 1414 (2015) 163–172.

[5] G. Greyling, H. Pasch, Multidetector thermal field-flow fractionation: a unique tool for monitoring the structure and dynamics of block copolymer micelles. Macromolecules. 49 (2016) 1882–1889.

[6] J.-F. Gohy, in Block Copolym. II (Ed.: V. Abetz), Springer-Verlag, Berlin/Heidelberg, (2005). 65–136.

[7] Z. Grubišić-Gallot, Y. Gallot, J. Sedláček, Study of polystyrene-*block*-poly(methyl methacrylate) micelles by size exclusion chromatography/low-angle laser light scattering, 1. Influence of copolymer concentration and flow rate. J. Liq. Chromatogr. 18:12 (1995) 2291–2307.

[8] A. Blanazs, S. P. Armes, A. J. Ryan, Self-assembled block copolymer aggregates: from micelles to vesicles and their biological applications. Macromol. Rapid Commun. 30 (2009) 267–277.

[9] A.B. Ebrahim Attia, Z.Y. Ong, J. L. Hedrick, P. P. Lee, P. L. R. Ee, P. T. Hammond, Y.-Y. Yang, Mixed micelles self-assembled from block copolymers for drug delivery. Curr. Opin. Colloid Interface Sci. 16:3 (2011) 182–194.

[10] J. Ehrhart, A.-F. Mingotaud, F. Violleau, Asymmetrical flow field-flow fractionation with multi-angle light scattering and quasi elastic light scattering for characterization of poly(ethylene glycol-b-ε-caprolactone) block copolymer self-assemblies used as drug carriers for photodynamic therapy. J. Chromatogr. A. 1218:27 (2011) 4249–4256.

[11] P. Jandera, T. Hájek, M. Staňková, Monolithic and core–shell columns in comprehensive two-dimensional HPLC: a review. Anal. Bioanal. Chem. 407 (2015) 139–151.

[12] S. Miller, Separations in a monolith, Anal.Chem. 76 (2004) 99A–101A.

[13] G. Guiochon, Monolithic columns in high-performance liquid chromatography. J. Chromatogr. A. 1168 (2007) 101–168. .